

## Review on “Vertical profiling of aerosol hygroscopic properties in the planetary boundary layer during the PEGASOS campaigns”

We would like to thank the referees for their detailed and constructive comments, which helped us to improve our manuscript. Our answers to the comments are given below in **blue letters**, while the referee comments are given in black italics. Additionally, we added the changes we made in the revised manuscript in **blue bold** letters.

### Reply to Referee #1:

*Overview: Hygroscopic trends are presented from measurements within the evolving boundary layer in the Po Valley, Italy, and in the fully mixed layer in the Netherlands during the PEGASOS 2012 campaigns. Results from the Po Valley conform to expectation – that newly evolving boundary layer aerosol comprises hygroscopic aerosol with a large nitrate fraction contributed by nighttime HNO<sub>3</sub> chemistry and cool temperatures. Nitrate fraction decreases as temperatures increase (volatilization) and photochemistry takes place (presumably adding SOA), resulting in suppressed hygroscopicity. It is noteworthy that the hygroscopicity of aerosol in the fully mixed layer is similar to that in the aged residual layer. The hygroscopic fraction of aerosol sampled in the Netherlands was high, though no composition data are presented to offer an explanation. In general, the data presented here are limited (one sampling day for each location), but the text contains excessive detail and should be edited for length. Correlations between hygroscopicity and composition are sparingly presented, and should be expanded. Nonetheless, the detailed probing of an evolving mixed layer (for the Po Valley site) is a unique dataset and worthy of publication. I recommend that the presentation of AMS data be integrated with hygroscopicity results, and that AMS data be more fully utilized in explaining hygroscopicity trends from the Po Valley, while decreasing the detail of the hygroscopic results sections. The paper is recommended for publication after revisions and additions.*

We rewrote and restructured sections 4 and 2.3 to make the discussion clearer and more compact (see answers below for more details) as well as the abstract and the conclusion. In particular, we put more emphasis on connecting hygroscopicity and chemical composition data, whenever the latter are available (see section 4). We also decided to exclude data from the Monte Cimone mountain site in Italy and shortened the discussion on possible contributors to the non-hygroscopic mode.

### General recommendations:

- 1) *Overall the paper would benefit from significant compression. As written, the text contains excessive detail and is much longer than necessary. Data from the Netherlands seem somewhat out of place, and the absence of AMS data limits their value. The authors might consider focusing solely on presenting the Po Valley flight in detail, as there is enough presented there to stand on its own – especially once the authors expand the discussion of aerosol composition and utilize more AMS data to explain hygroscopicity trends.*

As mentioned above, we shortened the paper. However, we kept the data from the Netherlands in the paper to show the contrast to the results from Italy. Even though we do not have airborne AMS data available for this flight, the AMS ground measurements are presented and are valuable to complement the WHOPS results.

- 2) *The connections made between composition and hygroscopicity are rather limited. Presumably you have a wealth of data available from the HR-AMS, including things like the organic oxidation state. What is the average O:C ratio for organics in the residual layer, compared with*

*the new mixed layer, for example? The paper would benefit a great deal from expanding the connections between hygroscopicity and composition. On a related note, hygroscopicity results (e.g. 4.1.1, 4.1.2, 4.1.3) are unnecessarily and awkwardly divorced from composition results (e.g. AMS, MAAP, etc). The paper would benefit greatly from co-presentation of hygroscopicity and composition data so that the reader can more naturally make connections between the two, without waiting until the “closure” section.*

We added O:C ratio values for the three different layers and the corresponding organic  $\kappa$  values obtained by applying the parametrization from Duplissy et al. (2011). These organic  $\kappa$  values differ only slightly from the overall mean value of 0.11 that we had previously used. Nevertheless, we adapted all results using the actual O:C ratio measured in a certain layer as input for the  $\kappa$  and closure calculations.

**Revised text: Page 9459; lines: 6-10:**

The  $\kappa$  values for the organics were inferred from the measured O:C ratio using the relationship between O:C and  $\kappa$  value reported in Duplissy et al. (2011) for organics in atmospheric aerosols in three different environments.

**Added text: Page: 9469; line: 8:**

The O:C ratio inferred from the HR-ToF-AMS measurement (using the method presented by Aiken et al., 2007) was found to differ slightly between the three layers with values of  $0.45 \pm 0.03$ ,  $0.55 \pm 0.03$  and  $0.50 \pm 0.05$  for the newly forming ML, the RL and the fully developed ML, respectively. The corresponding  $\kappa$  values were estimated to be 0.09, 0.14 and 0.12 in the newly forming ML, the RL and the fully developed ML, respectively (see Sect. 3 for more details on the method to estimate the  $\kappa$  value). The mean O:C ratio of the organics measured at the SPC ground site was  $0.60 \pm 0.03$ , which translates to a kappa value of 0.17.

**Revised text: Page: 9473; lines: 24-25:**

The O:C ratio of the organic matter measured by the AMS was  $0.48 \pm 0.02$ . The corresponding  $\kappa$  value of the organic matter is estimated to be 0.11 (Sect. 3). The measured composition of PM<sub>1</sub> (Fig. 12) as a whole translates to an average  $\kappa$  value of 0.28 (Eq. 5). This agrees within uncertainty with the WHOPS-derived  $\kappa$  value of 0.25 in the lowermost flight level at 100 m AGL (see Table 3).

- 3) *The Zeppelin was only operated on one day with low wind speeds, low cloud coverage, and clear skies. I would expect this combination of conditions to be most ideal for formation of an aged residual layer, and that this enhanced residual layer would have a disproportionate impact on the fully mixed layer by midday. It should be mentioned that these results are therefore not generally applicable to the Po Valley and Netherlands, but instead likely represent a maximum impact of residual layer on mixed layer aerosol.*

Indeed, the presented flight days show only one possible scenario for summertime conditions in the Po Valley or the Netherlands. When looking at the Po Valley for example, the measurement day - 20 June 2012, was certainly hotter ( $27.5^\circ\text{C}$ ) than the average for this period of the year ( $22.1 \pm 3.1^\circ\text{C}$  for June in San Pietro Capofiume, reference period: 1961 - 2005). However, the climate is changing rapidly in this region of the world, with a positive trend in temperatures of  $0.60^\circ\text{C}$  per decade in summertime.

Therefore, the measurements during PEGASOS cannot be considered representative for the late XX century climatology of the Po Valley, but can be more representative of what the climate is becoming. [source of the climatological data: ARPA Emilia-Romagna]. Such conditions favour strong vertical mixing and the residual layers' entrainment.

The representability of the results for the flight above Cabauw in the Netherlands is discussed in Sect. 4.2.4, where the results are compared against existing literature data.

- 4) *Hygroscopicity results (e.g. 4.1.1, 4.1.2, 4.1.3) are quite long and excessively detailed. Stick to the main points, let the figures do the talking, and try to condense these sections substantially.*

We shortened these sections for the revised manuscript.

- 5) *Does the WHOPS instrument adjust refractive index once particles have been humidified? Uptake of water ( $RI=1.33$ ) lowers overall RI, meaning comparatively less light scattering for the same size particle. This would lead to systematic underestimation of GF, and introduce discrepancies between HTDMA and WHOPS. It would be worth doing a sensitivity study to see how much an error of 0.2 in RI would impact your GF and kappa calculations – just to put HTDMA/WHOPS discrepancies into perspective.*

**Revised text: Page: 9454; line: 23:**

**The index of refraction of the grown particles gradually approaches the index of refraction of pure water ( $m_{H_2O}=1.333$ ) with increasing hygroscopic growth factor. This effect is accounted for in our data analysis approach as detailed in Rosati et al. (2015).**

- 6) *Specific comments/questions:  
Throughout: "Data" is plural. "Datum" is singular. Use "data are" instead of "data is".  
Throughout - especially in Abstract: report data with  $\pm$  standard deviation.*

Grammatical errors were corrected. Standard deviations have been added in the abstract and main text where appropriate.

- 7) *p. 9460 line 26: With significant industrial sources in the Po Valley, I'd expect to see plumes of fresh, non-hygroscopic aerosol like this.*

In Section 4.1.2 we argue that the non-hygroscopic particles are unlikely to originate from combustion sources. The true nature of these particles – dust, tar balls or biological particles – remains speculative.

**Revised text: Page 9460; line: 26:**

**An exception is the measurement taken at around 12:45 LT and 100 m AGL, when the mean  $\kappa$  was considerably lower due to a strongly increased fraction of non-hygroscopic particles (see Fig. 6) likely originating from a local source.**

- 8) *p. 9461 line 9: replace "spread" with "variability"*

We changed this in the revised manuscript.

- 9) *p. 9462 line 14-16: I disagree with this conclusion. The significant changes in hygroscopicity at lower altitudes are likely primarily caused by the change in nitrate mixing state. Nitrate fraction is enhanced at low temperatures in shallow boundary layers in the morning, owing to nighttime  $HNO_3$  chemistry. Nitrate fraction drops significantly during the day due to volatilization of ammonium nitrate – the result of both increased temperatures and dilution with the deepened*

*mixed layer. While an enhancement in externally-mixed hygroscopic growth might indicate strong local influence, a general decrease in hygroscopicity doesn't necessarily.*

We agree with this conclusion and changed the text as follows:

**Revised text: Page: 9462; line: 14-16:**

**This can be explained by the differing chemical composition of the particles in these layers, with a very strong nitrate fraction in the new ML which decreases in the fully developed ML.**

**Revised text: Page: 9468; line: 15-20:**

**During IHP1/2 a clear difference between the mass fractions in the new ML with a high nitrate fraction of 20–22% (Fig. 8a and c) and the RL with a nitrate contribution of only 5% (Fig. 8e) were observed. This increased nitrate fraction in the new ML can be explained by the accumulation of nitrate species overnight at low temperatures, which are formed in the nocturnal surface layer and are then entrained into the new ML after sunrise. The nitrate drop in the fully developed ML is due to volatilization of nitrate species as a result of both, increased temperature and dilution.**

*10) p. 9463 line 26-29: BC in heavily anthropogenically-influenced areas is almost entirely coated with secondary material. For example, results from the SP2 and ATOFMS in the Los Angeles Basin indicated that the vast majority of rBC was coated – even at short photochemical ages (<1h). See Metcalf et al., 2012 and Hersey et al., 2013 (JGR-Atmospheres). So it's highly conceivable that you may have observed coated BC particles here. Nothing to really change here, but I think you're on the right track in considering coated BC.*

We added the proposed citations to the revised manuscript.

*11) p. 9464 line 15 to 9465 line 5: My concern with investing in a long discussion of mineral dust and biological material is that you have no composition data to back it up. Unless you can support these possibilities with very strong presentation of HYSPLIT back-trajectories that suggest dust influence or something like seasonal pollen count data to support biological material, any suggestion that they contribute to the non-hygroscopic fraction is tenuous (and certainly doesn't belong in the abstract - p. 9447 line 23).*

We shortened this discussion and clarified that these are only possible contributors. We also deleted the sentence from the abstract.

*12) One other strong possibility is that hydrophobic SOA coatings may inhibit hygroscopic growth within the WHOPS instrument, resulting in an overestimation of the non-hygroscopic fraction and overall underestimation in apparent GF and kappa. I'm guessing that the humidification time constant in the instrument is on the order of a few seconds, while equilibrium with water vapor for coated particles can take minutes or hours. See Shiraiwa et al., 2011 (Proceedings of the National Academy of Sciences 108 (27), 11003-11008) and Koop et al., 2011 (Physical Chemistry Chemical Physics 13 (43), 19238-19255) for more discussion.*

The residence time of the particles in the humidification system of the WHOPS is approximately 20 s (details on the humidification system are presented in Rosati et al., 2015a). The study by Sjogren et al. (2007) shows that 10-20s are sufficient to reach a stable hygroscopic growth factor for most investigated examples, while >40 s were needed for some extreme systems. Therefore, we think that 20 s should be sufficient for most aerosol particles to reach their equilibrium growth factor including complete deliquescence.

**Revised text: Page: 9454; line: 3:**

**Alternatively, the size-selected dry particles are humidified before being directed to the WELAS to measure the wet optical response (residence time at the high RH ~ 20 s).**

*13) p. 9466 line 6-8: This might support the dust option. I see that the characteristic humidification time in the HTDMA is longer than in the WHOPS (line17-29). It may be that particles are exposed to elevated RH for longer in the HTDMA, causing some of those coated, diffusion-limited particles to come closer into equilibrium with water vapor in the HTDMA than in the WHOPS. It's worth checking. These diffusion inhibition issues are always something that should be considered with SOA and aged, coated particles, and in your case might counteract some of the ammonium nitrate volatilization issues.*

There has been a misunderstanding in this paragraph. What we meant is that the humidification time in the WHOPS is longer than in the HTDMA, however, the time in the dry section of the WHOPS is shorter compared to the HTDMA. Therefore, losses of ammonium nitrate in the WHOPS should be smaller as particles have less time to evaporate.

We changed the text in the revised manuscript as follows:

**Revised text: Page: 9466; line: 17-24:**

**Gysel et al. (2007) provided strong evidence for ammonium nitrate artifacts in the dry part of the HTDMA measurement, which resulted in underestimated hygroscopic GFs. The HTDMA employed in SPC featured smaller residence times in the range between 10-15s, which should minimize nitrate evaporation losses, however, they can still not be fully excluded. GF measurements done with the WHOPS are most likely less susceptible to ammonium nitrate evaporation, as the residence time in the dry part of the instrument is shorter due to higher flow rates.**

*14) p. 9466 line 28-29: possibly, but I think the physical arguments from humidification and ammonium nitrate volatilization are bigger issues here.*

We included additional supporting arguments for the other hypothesis.

**Revised text: Page: 9466; line: 26-28:**

**Another possible reason could be that the particles at the ground (measured in the surface layer) and at 100 m AGL were not exactly the same due to e.g. direct influences by local emissions. This hypothesis is also supported by measurements of the particles' optical properties on this flight day, presented in Rosati et al. (2015b). A comparison of the scattering and extinction coefficients between the airborne and ground based measurements, shown in Fig. 4 and 8 in the stated paper, respectively, also illustrate differences between the two altitudes, which are independent on the hygroscopicity measurements and associated artifacts.**

Rosati, B., Herrmann, E., Bucci, S., Fierli, F., Cairo, F., Gysel, M., Tillmann, R., Größ, J., Gobbi, G. P., Di Liberto, L., Di Donfrancesco, G., Wiedensohler, A., Weingartner, E., Virtanen, A., Mentel, T. F., and Baltensperger, U.: Comparison of vertical aerosol extinction coefficients from in-situ and LIDAR measurements, Atmos. Chem. Phys. Discuss., 15, 18609-18651, doi:10.5194/acpd-15-18609-2015, 2015b.

*15) p. 9472 line 6: double negative; change "neither/nor" to "either/or"*

We changed this in the revised manuscript.

16) p. 9473 lines 7-8: *or water-uptake-inhibited, coated particles*

We consider it unlikely that hygroscopic growth is fully inhibited on a 20 s time-scale (see comment above).

## Reply to Referee #2:

### General comments:

*The manuscript presents a case study of aerosol properties in the atmospheric boundary layer measured from an airborne platform in two places for one day in each location. Suite of instruments on-board of the airship allowed measurement of hygroscopicity and chemical composition including estimate of equivalent black carbon mass concentration. The flights were performed in the vicinity of ground sites equipped to provide similar measurements. The authors discuss measured hygroscopic properties of 500 nm aerosols, results of composition-hygroscopicity closure studies as well as intercomparison with ground sites. It should be noted that experimental data on hygroscopic properties of ambient aerosols are scarce, especially for the larger (few hundred nanometres) aerosols in the atmospheric boundary layer. Undoubtedly, the results of this work could be published in ACP, however only after the manuscript has undergone appropriate revision.*

*The manuscript needs to be re-arranged to separate description of the instrumentation and methods from the results and conclusions; it seems to be burdened with trivial statements and unsupported speculations, which should be avoided. Technical aspects of the current work may be presented in the Supplement to keep the main manuscript concise and focused. The authors are advised to secure help from a professional editor to improve readability of the manuscript.*

We rewrote and restructured sections 4 and 2.3 to make the discussion clearer and more compact (see answers below for more details) as well as the abstract and the conclusion. We also decided to exclude data from the Monte Cimone mountain site in Italy and shortened the discussion on possible contributors to the non-hygroscopic mode. The detailed changes are presented below.

### Specific comments:

- 1) *Please use generally accepted abbreviation for altitude in meters above ground: m a. g. l. or m AGL.*

We changed all occurrences of **m a. g. l.** to **m AGL**.

- 2) *PP 9447-9448, Abstract: The abstract needs major revision to better reflect actual work done and substantiated conclusions reached; currently a reader gets an impression of much broader experimental data basis for the claimed conclusions. Also, it would be advisable to be more scrupulous in descriptions, for example “flown just after sunrise” looks like an exaggeration for the flight started 3 hours after sunrise.*

We adapted the abstract to be more precise.

- 3) *P 9448, L 17: References to entire IPCC reports are not practical; please site the specific reference(s) in the IPCC 2013.*

As we refer to chapter 7 (Clouds and Aerosols) in the IPCC 2013 we changed the reference to: [Boucher, O., D. Randall, P. Artaxo, C. Bretherton, G. Feingold, P. Forster, V.-M. Kerminen, Y. Kondo, H. Liao, U. Lohmann, P. Rasch, S.K. Satheesh, S. Sherwood, B. Stevens and X.Y. Zhang, 2013: Clouds and Aerosols. In: Climate Change 2013: The Physical Science Basis. Contribution of Working Group I to the Fifth Assessment Report of the Intergovernmental Panel on Climate Change \[Stocker, T.F., D. Qin, G.-K. Plattner, M. Tignor, S.K. Allen, J. Boschung, A. Nauels, Y. Xia, V. Bex and P.M. Midgley \(eds.\)\]. Cambridge University Press, Cambridge, United Kingdom and New York, NY, USA.](#)

- 4) *P 9450, L 12-14: There is at least one instrument for size resolved hygroscopicity measurements that was built and deployed earlier than DASH-SP, see: Hegg, D. A.,*

Covert, D. S., Jonsson, H., and Covert, P. A., 2007: An instrument for measuring size-resolved hygroscopicity at both sub- and super-micron sizes, *Aerosol Sci. Technol.*, 41, 873–883.

**Revised text: Page: 9450; line: 12-14:**

The first instrument built for this special task is the aerosol hydration spectrometer (AHS; Hegg et al., 2007). The setup comprises two optical instruments, one to get a dry optical and the other one a humidified optical response. However, the measurement is performed for a polydisperse size distribution rather than investigating the hygroscopic properties of aerosol particles with one specific diameter. The differential aerosol sizing and hygroscopicity spectrometer probe (DASH-SP; Sorooshian et al., 2008) on the other hand, is constructed using a combination ...

- 5) P 9452, L 5-13: Please describe state variables measurement (temperature, humidity, wind speed, etc.) that has been made on board of the airship; including type of sensors, time response, averaging, etc.

We propose to present details on instrumentation together with mean values of the potential temperature and relative humidity, as requested in comment 19, in the supplementary material (please see response to comment 19 for more details).

- 6) Please provide a short description of inlets for the WHOPS, AMS, and aethalometer. Are they isokinetic? Any estimates of transmission efficiency?

We included a short description of the inlets for each instrument.

**Revised text: Page: 9455-9456; line: 28; 1:**

The particles were sampled through a 1500 mm long tube (4 mm ID), ending about 200 mm below the bottom hatch of the Zeppelin. A constant pressure inlet, consisting of an orifice that is pumped with variable flow and installed between the aerosol inlet and the AMS, was used to regulate the downstream pressure to 800 hPa independent of upstream pressure. This ensured constant sampling conditions for the AMS. Within the AMS, the particles pass a critical orifice and an aerodynamic lens, which focuses particles of sizes between 100 and 700 nm into a narrow beam.

**Revised text: Page: 9453; line: 24:**

Briefly, particles are collected through an isokinetic inlet developed for an average flight velocity of 50 kmh<sup>-1</sup> before they reach the WHOPS. Then they are dried...

**Revised text: Page: 9457; line: 1:**

The aerosol was collected through the same isokinetic inlet and sampling line as for the WHOPS.

- 7) P 9453, L 4-7 and 17-18: Please elaborate how the mixing layer depth was retrieved from the ceilometer data. Automated algorithms to retrieve atmospheric boundary layer height from ground based remote sensing measurements (lidar, sodar, ceilometer, radar wind profiler, etc.) are notoriously unreliable. Since the mixing layer depth is one of the key parameters in interpretation of the results, its retrieval procedure should be presented. Is there any radiosonde data from SPC meteo station or Hague Airport available for flight days? Radiosonde derived mixing layer depth could provide useful "hints" for interpretation of ceilometer data.

Radiosonde data is available for the two measurement days, however, during the time of the flight only one launch was performed and consequently, only one data point is available from these measurements. Therefore, we decided to use the continuous measurements from remote sensing instruments. Additionally, we added a new figure to the supplement, illustrating height profiles of the potential temperature ( $\Theta$ ) as measured on board the Zeppelin (see answer to comment 18 below).

**Added text: Page: 9453; line: 6:**

Retrieval of the estimated mixing layer height is performed by operating on a graphical interface presenting the maximum gradient points in the signal daily plot. In this way, the operator solves the ambiguities related to multiple relative maxima often present in the ceilometer signal (e.g., Angelini et al., 2009). The typical imprecision due to the operator's choice amounts to 3 pixels, i.e.  $\pm 45$  m.

- 8) *PP 9453-9455, Section 2.3.1: The description of how the WHOPS works is not complete; please describe "wet" part. Also see comments to PP 9461-9465 and PP 9465 L 24-26.*

**Revised text: Page: 9453-9454; lines: 21-25; 1-7:**

On the Zeppelin the WHOPS was used to determine hygroscopic GF. All instrument specifications, as well as associated calibration and data analysis procedures, are presented in detail in Rosati et al. (2015). Briefly, particles are collected through an isokinetic inlet developed for an average flight velocity of  $50 \text{ kmh}^{-1}$  before they reach the WHOPS. They are then dried ( $\text{RH} < 10\%$ ) and size selected in a differential mobility analyzer (DMA). In a next step, the dry particles are guided directly to a WELAS 2300 optical particle spectrometer (WELAS; Palas GmbH, Karlsruhe, Germany) to measure the dry optical response. Alternatively, the size-selected dry particles are humidified before being directed to the WELAS to measure the wet optical response (residence time at the high RH  $\sim 20$  s). Multiply charged particles appear as a distinctly separated mode in the optical size distribution measured by the WELAS and are discarded from the further data analysis. Hygroscopicity measurements are typically performed at  $\text{RH} = 95\%$ , where the uncertainty in the humidity measurement is estimated to be  $\pm 2\%$ . Since the RH to which particles were exposed to varied only between  $\sim 94-96\%$  during both flight days, no further RH corrections were applied to the results.

- 9) *P 9453, L 24-25: What is "dry" RH? Was it controlled/measured in any way?*

The dry conditions were always characterized by  $\text{RH} < 10\%$ . This RH was continuously monitored throughout all measurements. The revised section 2.3.1 includes now these details (see also response above to comment 8).

- 10) *P 9454, L 3-8: Please provide short description of measuring protocol (timing, averaging, size change and wet/dry sequences, etc.) for the WHOPS operation.*

**Added text: Page: 9454; line: 8:**

Particles with a dry mobility diameter of 300 nm or 500 nm were alternately probed during 250 s per size, whereof 150 s were used for the wet-mode and 100 s for the dry-mode. The results were averaged for each flight segment (probed layer) at a constant flight altitude. This ensured that each GF-PDF shown in Figs. 5, 7, 12 and 15 is based on more than 90 detected particles.

11) P 9454, L 16-19: Any DMA has a well-known artefact of “double sized, double charged” particles – any corrections for this artefact implemented in the WHOPS procedure?

**Added text: Page: 9454:**

**Multiply charged particles appear as a distinctly separated mode in the optical size distribution measured by the WELAS and are discarded from the further data analysis.**

12) P 9454, L 21-25: For absorbing aerosols the real part of the refraction index found via the presented technique is biased low; so, strictly speaking, this retrieved parameter is not the real part of refraction index.

Indeed, the effective index of refraction that we retrieve is not just the real part of the index of refraction but also dependent on the absorbing properties of the analysed particles. Therefore, we use the term “effective” and propose to clarify the definition as follows:

**The term “effective index of refraction” has been clarified:**

**The qualifier “effective” is used because the true index of refraction is slightly different due to simplifications such as assuming an imaginary part of zero, spherical particles and a homogeneously internally mixed aerosol (see Rosati et al., 2015, for more details).**

13) P 9454, L 26 - PP 9455, L 11: This paragraph belongs to the Results and Discussion section. Figure 2 does not show “the temporal variability”. Please try to correct the “effective” index of refraction for absorbing nature of the aerosols in both locations when comparing to other measurements of the refractive index.

Figure 2 illustrates the temporal variability of the effective index of refraction shown as the distribution of the values found throughout the campaign. We moved Fig. 2 to the supplement. The results for the effective index of refraction are now only briefly mentioned in the main text as they are for the most part only of technical interest for the data analysis approach. The comparison of the observed effective index of refraction to literature data has been deleted as it does not exactly reflect the true real part of the index of refraction. With that it becomes obsolete to correct the effective index of refraction for the absorbing nature of the aerosol, which would have required plenty of assumptions too.

14) P9455, L 12-23: Please provide short description of measuring protocol (timing, averaging) used on ground site HTDMA's.

**Revised text: Page: 9455; lines: 12-14:**

**The SPC site was equipped with a hygroscopicity tandem differential mobility analyzer (HTDMA; see e.g. Swietlicki et al., 2008) in order to determine the hygroscopic properties of particles with 4 different dry diameters between 35 and 200 nm. Each scan to record a GF-PDF at a fixed dry size lasted 500 s in total, thus providing a time resolution of 1.8 measurements per hour for each dry size.**

15) P 9456, L 28 - PP 9457, L 6: Please provide short description of measuring protocol (timing, averaging) for AE42 aethalometer.

**Added text: Page: 9457; line: 1:**

**eBC concentrations were logged with a time resolution of 2 min and averaged for the time needed to probe a certain layer.**

16) P 9458, L 8: Looks like unfinished sentence?

**Revised text: Page: 9458; line: 8-10:**

For a composition-hygroscopicity closure, the  $\kappa$  values derived from the GF measurements (WHOPS) are compared to those derived from the chemical composition measurements (AMS and aethalometer).

17) P 9459, L 18-19: Please provide a short description of the flight pattern (linear, box, spiral or ramp ascend/descend, etc.) and a distance from the ground site during measurements, if in excess of a few kilometres.

**Revised text: Page: 9459; line: 17-18:**

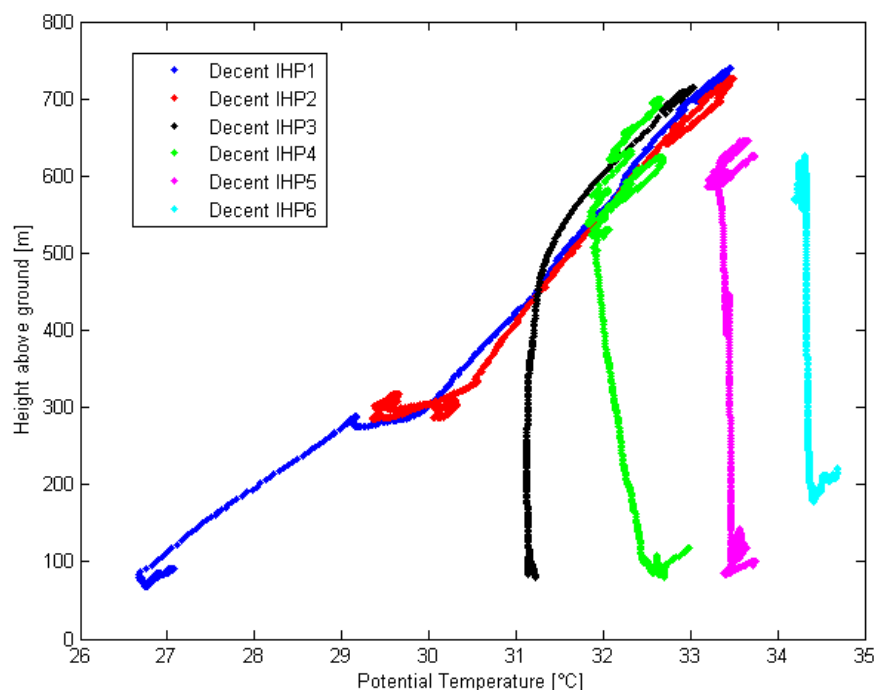
The vertical flight pattern performed on the 20 June 2012 is shown in Fig. 3 and was obtained by flying spirals at selected constant heights and straight ascends and descends. During this day vertical profiles were measured within 5 kilometres horizontal distance from the SPC site ...

18) P 9459, L 23-25: Figure 3 shows time trace of  $T_h$  and RH, rather than vertical profile. It might be beneficial to present vertical profiles of  $T_h$  and RH measured on descent (minimal influence of the airship body?) to help the readers get another (independent) pattern of the mixing layer depth evolution (see also comment P 9453, L 4-7 and 17-18).

**Revised text: Page: 9459; line: 24-25:**

Figure 3 depicts the temporal evolution of potential temperature ( $\Theta$ ) and RH observed during the flight at different altitudes. The shaded area denotes the estimated mixing layer height provided by Ceilometer-Lidar data.

We propose to include the following figure illustrating height profiles of the potential temperature ( $\Theta$ ) to the supplementary material.



### Supplement:

Height profiles of the potential temperature ( $\Theta$ ) during the flight on 20 June 2012 in the Po Valley are presented for all height profiles IHP1-6 using only data from the Zeppelin descents. These data provide an independent measure of the mixing layer height, showing that only during IHP1 and 2 a clear layering of the PBL is visible with a mixing layer height of approximately 300 m AGL.

19) PP 9460 - 9461: Section 4.1.1 needs to be revised. It is not clear why IHP3 has been excluded from discussion – it seems to be in line with general pattern of growing ML. It might be beneficial to present values for all flight legs separately in Table 2; please include also averaging time, mean RH and  $T_h$  (or  $T$ ) for each leg. It would be interesting to see GF (corrected to 95%) measured at the ground site for each leg as well.

We revised the explanation on why IHP3 and IHP4 were excluded from most figures and discussion (see revised text). Averaged values of potential temperature and RH for each probed layer at a constant level are included in a new table in the supplement. The SPC-GFs corrected to RH=95% for each profile are now included in the revised Table 2, as presented below (response to comment 20).

### Revised text: Page: 9460; line: 23-25:

After ~11:00 LT a second set of profiles was performed. To study particles in the fully developed ML the results from IHP5/6 (~12:30–14:00 LT) are considered, while IHP3 and IHP4 are excluded as the ML had not reached its maximum height and could, therefore, be influenced by the RL or the entrainment zone between the layers.

### Supplement Table 1:

	<i>Altitude</i>	<i>Layer</i>	<i>Zeppelin</i>	<i>Zeppelin</i>
			$\Theta$ [ $^{\circ}\text{C}$ ]	RH [%]
IHP1/2	100 m	New ML	26.0 ( $\pm 0.6$ )	60.1 ( $\pm 2.0$ )
	700 m	RL	33.0 ( $\pm 0.9$ )	39.4 ( $\pm 3.1$ )
IHP5/6	100 m	Fully developed ML	33.4 ( $\pm 0.6$ )	31.5 ( $\pm 3.1$ )
	700 m	Fully developed ML	33.6 ( $\pm 0.5$ )	36.5 ( $\pm 4.2$ )

Mean potential temperature ( $\Theta$ ) and relative humidity (RH) during IHP1/2 and IHP5/6 with respective standard deviations representing the temporal variability. Results are presented for two different altitudes, 100 m and 700 m AGL. Measurements of the temperature (Pt100-Sensor; OMEGA; 15s time respond), RH (HMP45-Sensor; Vaisala; 15s time respond), height above ground, wind-speed and direction (all three retrieved by measurement of the pressure using sensors #239 and #270; Setra) were continuously recorded on board the airship. All of these measurements were logged with a 100 Hz frequency and finally averaged over 10 data points.

20) The “upper” leg of IHP4 seems to be “odd” in sense that airship altitude was not kept constant, at the same time the airship was in the vicinity of the ML top; it is quite possible that part of the leg was within the ML or the entrainment layer. For this reason, IHP4 should not be classified/averaged as flown in “fully developed ML” here and in subsequent sections of the manuscript.

After a thorough analysis, we decided not to include IHP4 for the calculations of the fully developed ML as indeed it cannot be clearly classified as part of this layer. Consequently, we adapted Fig. 5, 7, 8 and 9 and all instances in the manuscript where the fully developed ML is defined. Also, the mean values

of the GF and  $\kappa$  in the fully developed ML were recalculated including only IHP5 and 6. However, we want to note here, that the differences are minimal.

Adapted Table 2:

	Altitude		Zeppelin- WHOPS	Zeppelin- WHOPS	Zeppelin- AMS + Aethalometer
			GF(95%)	$K_{WHOPS}$	$K_{chem}$
Size			500 nm	500 nm	PM1
IHP1/2	100 m	New ML	1.88 ( $\pm 0.19$ )	0.34 ( $\pm 0.12$ )	0.26 ( $\pm 0.06$ )
	700 m	RL	1.61 ( $\pm 0.16$ )	0.19 ( $\pm 0.07$ )	0.22 ( $\pm 0.05$ )
IHP5/6	100 m	Fully developed ML	1.49 ( $\pm 0.15$ )	0.14 ( $\pm 0.06$ )	0.19 ( $\pm 0.04$ )
	700 m	Fully developed ML	1.63 ( $\pm 0.16$ )	0.20 ( $\pm 0.08$ )	0.20 ( $\pm 0.04$ )
			SPC- HTDMA	SPC- HTDMA	SPC- AMS + MAAP
			GF(95%)*	$K_{HTDMA}$ *	$K_{chem}$
Size			200 nm	200 nm	PM1
IHP1/2		New ML	1.61 ( $\pm 0.22$ )	0.19 ( $\pm 0.04$ )	0.31 ( $\pm 0.08$ )
IHP5/6		Fully developed ML	1.60 ( $\pm 0.21$ )	0.18 ( $\pm 0.04$ )	0.21 ( $\pm 0.06$ )

\*HTDMA uncertainty calculated assuming 2% accuracy in the RH measurement.

- 21) *The hypothesis of an aerosol layer with special properties at 100 m AGL in presumably convective boundary layer around 12:45 seems to be far-fetched; it should be corroborated by measurements, if any available, like significant change in total aerosol concentration, scattering, extinction, etc.*

We do not have any other data supporting our hypothesis and, therefore, we decided to delete the sentence on page 9460-9461, lines 26-27 and 1.

- 22) *PP 9461 - 9465: Section 4.1.2 needs to be revised. Description of how aerosol mixing state could be inferred from the WHOPS measurements should be moved to Section 2.3.1. It is not clear what "kind" of PDF is shown in Fig. 5: total sum/area of a PDF should come to 1.0 (or 100%), neither seems to be the case with all presented GF-PDFs. Non-hygroscopic mode that is present in all and every GF-PDFs measured by the WHOPS is really surprising; it looks rather like an artefact of the instrument. Ambiguity of relationship between the "wet" scattering cross section and GF is a major limitation of the WHOPS (as it is discussed in WHOPS introductory paper, Rosati et al, 2015). It is assumed, that the WHOPS is operated within certain "safe" limits of dry sizes, effective refractive indices, and growth factors where "sigma"-GF relationship is unambiguous. The problem is that these "safe" limits were found under approximation of non-absorbing aerosol; for absorbing aerosol these "safe" limits should be different, possibly not including the whole range of effective refraction indices observed in the current work. Detailed study of this problem is obviously beyond the scope of the current work, but it should be discussed in Section 2.3.1.*

The description of the mixing state retrieval has been moved from Section 4.1.2 to the experimental Section 2.3.1.

Normalization of the GF-PDFs: the GF-PDFs do actually have unit area. Subtle deviations from unity may occur due to inaccurate graphical reproduction.

The non-hygroscopic mode is indeed surprising. However, we are confident that the non-hygroscopic mode is not an artefact. Already for the technical paper (Rosati et al., 2015a) we assessed but discarded various potential problems. Several arguments are:

- The non-hygroscopic particles never appeared when e.g. measuring laboratory generated ammonium sulfate aerosols. Therefore, it is not a problem of the optical sizing of non-absorbing particles.
- The optical sizing is a single particle measurement. Thus the optical sizing of the non-absorbing particles will not be affected by the presence of absorbing particles.
- Light-absorbing particles, which would also have a different index of refraction than that applied in the data analysis are a potential problem. Candidates are e.g. black carbon containing particles. We performed a sensitivity analyses to estimate at which GF such BC containing particles would show up in the WHOPS (also considering bias between mobility diameter and volume equivalent diameter for fractal-like particles). We came to the conclusion that most BC-containing particles would not show up exactly at GF=1, except for a minor fraction with exactly matching “compactness” and coating thickness.
- The optical properties and shape of light-absorbing particles do vary from particle to particle and with time and in space. Therefore it is not expected that such BC-containing particles, or some other issue with inappropriate assumption for the optical calculations, would always produce an artefact non-hygroscopic mode that always appears at the same GF. However, the non-hygroscopic mode observed in this study consistently appears at GFs very close to unity.

23) P 9464 L 29 - PP 9465 L 2: *“Influence of Saharan dust intrusion . . . can be expected for the day of the Zeppelin flight” – so what is exactly HYSPLIT show? This is the only ground for a rather far-reaching conclusion of dust presence and its effect on aerosol hygroscopicity.*

**Revised text: Page: 9464; line: 29:**

**The HYSPLIT model for Saharan Dust Intrusions (specific analysis by “Spain HYSPLIT”; <http://www.ciecem.uhu.es/hysplit/>; not presented here) predicted Saharan dust all the way down to the lowest atmospheric layer (100 m AGL) near the SPC site. However, we do not have additional data to support these calculations.**

24) P 9465 L 19-21: *Direct comparison of the airborne measurements with MTC ground site seems to be not very relevant here due to (a) horizontal separation of 100 km (over 5 hours’ travel time with 5 m/s winds), (b) “MTC is situated at a much higher elevation than the Zeppelin NT was flying”, and (c) ground site measurements are always affected by local ground layer/sources (e. g. see current manuscript P 9660 L 26-28).*

We agree with this statement and removed the part describing any MTC data from the revised manuscript and Figs. 1, 7 and 9 as well as Table 2.

25) P 9465 L 24-26: *This limitation of the WHOPS should be described earlier, in Section 2.3.1 and reflected in the abstract.*

This limitation was on purpose mentioned along with the results rather than buried in Sect. 2.3.1 because it is relevant for correct interpretation of Fig. 7. We did not move it in the revised manuscript.

Due to this limitation we did not include any results from the 300 nm particles in the abstract. Accordingly, we consider it unnecessary to add a statement about this limitation in the abstract.

26) P 9467, L 4-6: Please elaborate how “differences . . . are influenced by data inversion algorithms”.

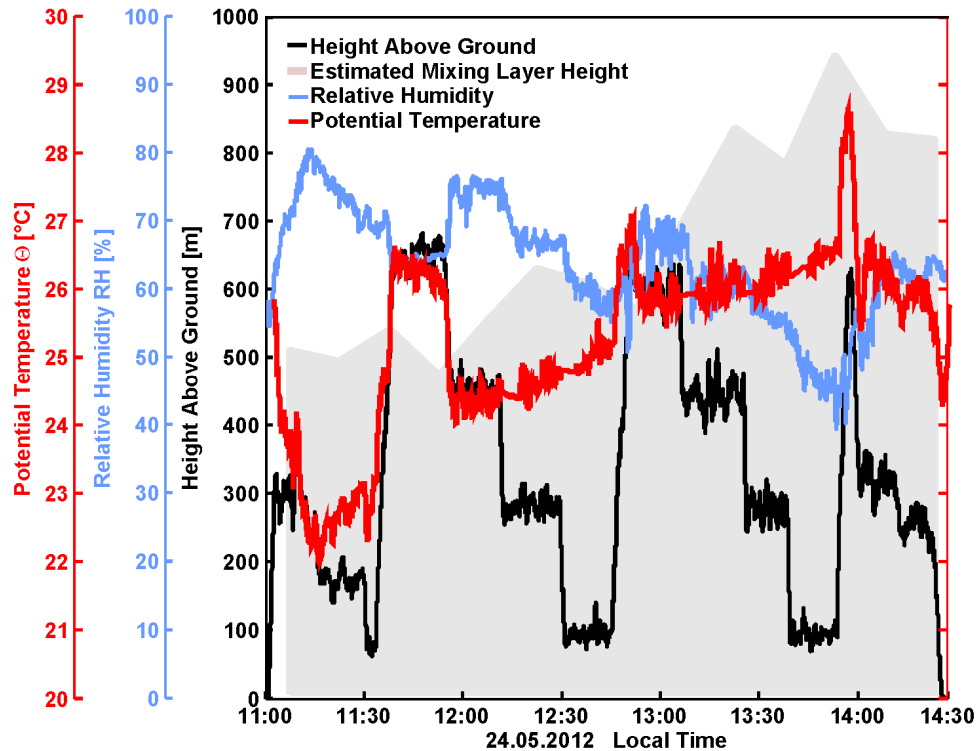
This was in a paragraph about data from the MTC site and has been removed from the manuscript. (An extensive discussion about the potential and limitations of HTDMA inversion algorithms is given in Gysel et al., 2009).

Gysel, M., McFiggans, G. B., and Coe, H.: Inversion of tandem differential mobility analyser (TDMA) measurements. *J. Aerosol Sci.*, **40**, 134-151, doi:10.1016/j.jaerosci.2008.07.013, 2009

27) P 9471, L 17-21: It might be beneficial to present vertical profiles of  $Th$  and  $RH$ ; see comment to P 9459, L 23-25. Trace for  $Th$  in Figure 10 looks like the time series was smoothed or filtered, if so, please explain why, and, if possible, present un-filtered version.

In contrast to the flights in Italy, the conditions in the Netherlands did not vary substantially throughout the day and therefore we propose to omit profiles of  $\Theta$ .

We revised Figure 10 (see below) using un-filtered data. Small adjustments had to be done for rapid altitude changes but instead of smoothing the whole-data set the few instances were corrected and the rest of the data is presented as measured on board the Zeppelin.



28) P 9471, L 21-24: see also comment to P 9453, L 4-6 and 17-18.

**Added text: Page: 9453; line: 18:**

The retrieval of the mixing layer height from the LD40 ceilometer backscatter profiles is based on a wavelet algorithm (Hay et al., 2007). The algorithm determines the height of the maximum in the gradient in the backscatter profile. The difference in backscatter in a small range below and above the retrieved height is used as an estimator for the quality of the retrieved height. Retrieved mixing heights with the highest quality index have comparable accuracy to radiosonde retrieved heights and have an estimated accuracy on the order of 50 m.

29) P 9472, L 22-24: *“GF-PDFs between a GF of 0.9 up to 3.2 are visible . . .”* – please change wording in this and subsequent phrases.

**Revised text: Page: 9472; line: 22-24:**

The GF-PDFs range between values of 0.9 until 3.2, which can be attributed to the presence of particles with very different hygroscopic behaviour.

30) PP 9475-9477, Conclusion: *the Conclusion needs to be revised in a similar manner as the Abstract (see comment to PP 9447-9448).*

We revised the conclusion.

### Reply to Referee #3:

*This manuscript describes interesting and unique results from measurements of aerosol hygroscopicity, supplemented by particle composition measurements of non-refractory and black carbon components. The measurements were made from an airship, which allowed careful evaluation of particle properties with respect to the dynamically changing planetary boundary layer. The data are really unique and of broad interest. There are no other measurements that enable both the spatial and temporal variation of aerosol hygroscopic properties in a growing PBL to be explored at these resolutions. The manuscript is unnecessarily difficult to follow, however, and needs revision for brevity and clarity. In particular, it needs to focus on specific elements of the data—the variation in hygroscopicity with evolving particle composition as a function of PBL development—and ignore speculative side-topics such as dust contributions. The manuscript now reads like "these are all the interesting things that we saw", rather than "this is an interesting and important phenomenon that we found in two locations and quantified". These data are really fascinating, and much very good analysis has been done. But the manuscript is unnecessarily disorganized, and needs focus and restructuring to be more concise and precise, and to focus on a few key conclusions rather than trying to explain every detail of the data. Some suggestions, which are not comprehensive, follow.*

We rewrote and restructured sections 4 and 2.3 to make the discussion clearer and more compact (see answers below for more details) as well as the abstract and the conclusion. We also decided to exclude data from the Monte Cimone mountain site in Italy and shortened the discussion on possible contributors to the non-hygroscopic mode.

#### Comments:

- 1) *The manuscript is peppered with imprecise language. For example, on p. 9454, line 15, the OPC technique allows for "mostly unambiguous" attribution of particle diameter to scattering cross-section. Does this mean the method is "somewhat ambiguous"? Can this ambiguity be quantified?*

A detailed description on the possible ambiguities can be found in Rosati et al. (2015).

#### **Added text: Page: 9454; line: 16:**

**Residual uncertainties with regard to the Mie oscillations amount to less than 7% in the GF (for more details see Rosati et al., 2015).**

- 2) *What are the uncertainties in the hygroscopicity method? Can a numeric value be placed on them? For example, what are the uncertainties associated with interpolating diameters from the look-up table? In situations involving Mie theory, it is not possible to propagate uncertainties from first principles. In these cases, it is appropriate to use a Monte Carlo simulation with a range of input values to determine how the various uncertainties in these parameters propagate through to the final value. I suggest this method be applied, summarized in the main text, and detailed in the supporting material. Use calculated uncertainties for every number in every table and on every graph. Without uncertainties data are meaningless.*

In the technical paper about the WHOPS (Rosati et al. 2015) all relevant uncertainties influencing the WHOPS data analysis are presented, and a final uncertainty for the GF is stated.

**Added text: Section 2.3.1:**

**As described in Rosati et al. (2015) the GF uncertainty for dry particle diameters of 500 nm is approximately  $\pm 10\%$  below GF=3.**

- 3) *The acronym "WHOPS" is unfortunate. In the U.S., this is a pejorative term for the descendants of Italian immigrants. While it might be too late to change the acronym from an earlier publication, the authors should be aware of this and minimize its use in the U.S.*

We were unaware of the similarity to the term "wop" (singular) or "wops" (plural) that you refer to. While we regret this coincidence, we introduced the term already for the technical paper (Rosati et al. 2015) and, therefore, it will be hard to change it now. However, we thank the reviewer for mentioning this fact.

- 4) *More language imprecision (p. 9457 line 10): the AMS "roughly measures particles smaller than 1  $\mu\text{m}$ ". Use the actual transmission efficiency of the inlet, and say, "the AMS detects particles with diameters  $< 0.7 \mu\text{m}$  vacuum aerodynamic diameter" or whatever the number is.*

**Revised text: Page: 9457; line: 10-13:**

**As the AMS has a transmission of close to one for particles with aerodynamic diameters between 50 nm and 600 nm, and most of eBC is assumed to be present in the size range below 1  $\mu\text{m}$ , we refer to the chemical composition as of PM<sub>1</sub> (particulate mass with an aerodynamic diameter smaller than 1  $\mu\text{m}$ ) in the following.**

- 5) *P. 9458, line 20, "pairing", not "paring".*

We corrected this mistake in the revised manuscript.

- 6) *P. 9461, lines 9-10, "less spread" relative to what? What "discrepancy" is being discussed? It's very hard to follow the logic of this paragraph.*

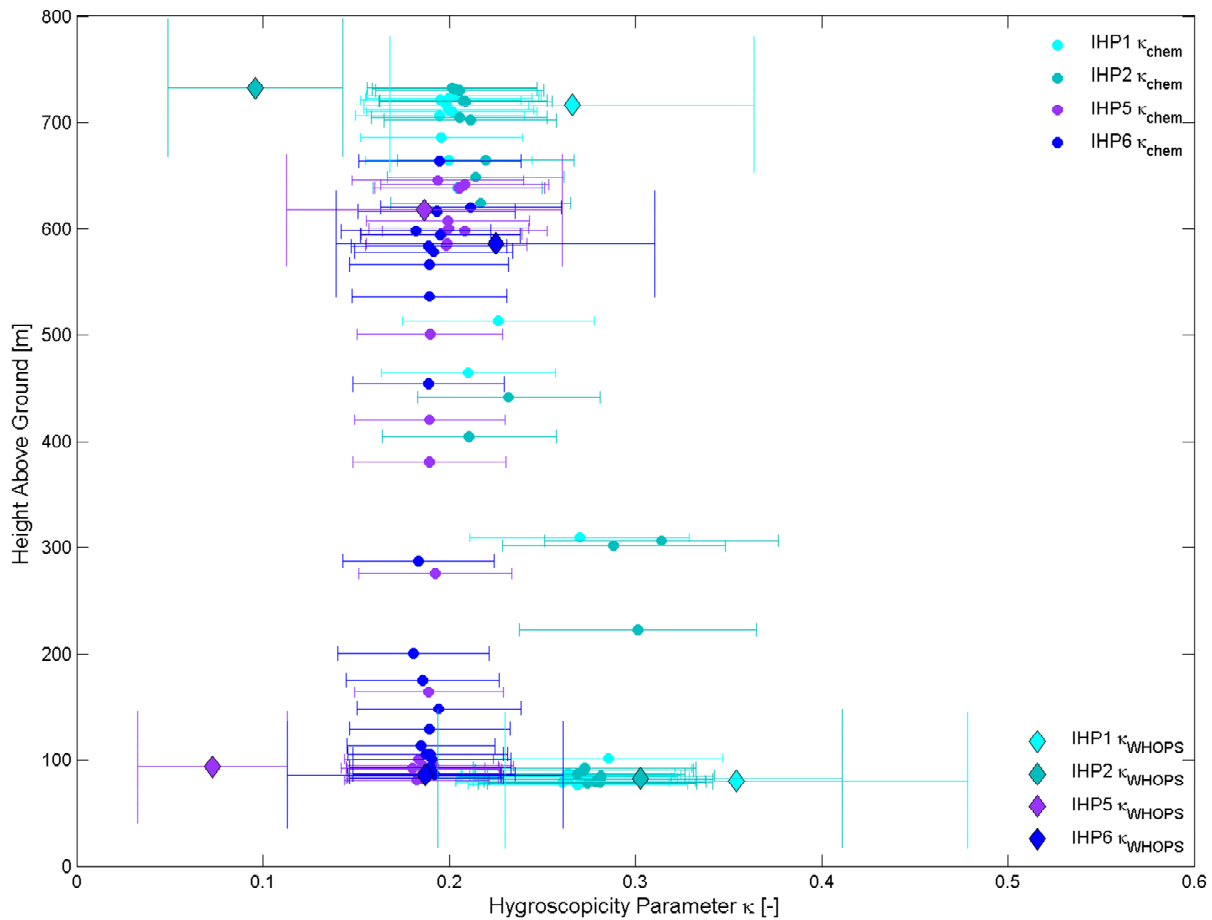
**Revised text: Page: 9461; line: 9-10:**

**In the fully developed ML, hygroscopicity results show less variability with no clear pattern between the altitudes. The values amount to  $\kappa_{\text{WHOPS}}=0.14\pm 0.06$  and  $\kappa_{\text{chem}}=0.19\pm 0.04$  at 100 m AGL and  $\kappa_{\text{WHOPS}}=0.20\pm 0.08$  and  $\kappa_{\text{chem}}=0.20\pm 0.04$  at 700 m AGL.**

- 7) *In section 4, the results are described with extreme detail. Can one example be shown from each measurement area (the Netherlands and the Po Valley), and then the remaining data compiled into different types of plots? I would find vertical profiles of the parameters, with different lines showing the evolution of the profiles, to be more informative than the time plots for which I have to estimate altitude from the altitude plot, then go to the parameter of interest and try to get a value. Since the evolution of the particle hygroscopicity with vertical growth of the PBL is of most interest, it would make sense to use altitude as the independent parameter for the plots.*

Section 4 has been revised for the new manuscript focusing on the main interesting points. Figure 4 contains both, the hygroscopicity results and the altitude (as dashed black line) in order to facilitate the attribution of the measured results to a certain layer and therefore altitude. Presenting the WHOPS data by using the altitude as the independent parameter does not seem the best solution for us as the resolution of the instrument is rather low.

In the figure below we present a possible plot illustrating the hygroscopicity results as height profiles, but we are of the opinion that Fig. 4 from the ACPD paper shows a better representation of the data and we propose not to change the plot.



8) p. 9465, line 4. Mineral dust is brought in as an explanation for large, non-hygroscopic particles. This needs more support. Are there ground or LIDAR measurements showing a dust contribution? In the next paragraph, biological material is discussed. This is all speculation. These paragraphs could be condensed to read, "the non-hygroscopic fraction of 500 nm particles may be attributable to dust, plant materials, or other components commonly found extending into the accumulation mode from the coarse mode." The digression to speculative discussion detracts from the main points of the paper.

We shortened the discussion on possible contributors to the non-hygroscopic mode as, like you mentioned, these are only assumptions.

9) p. 9465, lines 24-25. Here we learn that growth factors < 1.5 for particles with diameters < 300 nm are not detected "reliably". Why is this not detailed in the instrument description, and why are "unreliable" data being shown and discussed?

The full measurement of the 300 nm particles is, as you mention, not reliable. However, this refers only to the fraction GF<1.5. The measurements above this limit are reliable and are therefore shown in Fig. 7 and discussed. In this way, we can provide another size-dependent information of the hygroscopic fraction (GF>1.5).

Revised text: Page: 9465; line: 24-25:

Note that the WHOPS cannot reliably detect particles with  $GF < 1.5$  and  $D_{dry} = 300$  nm, as described in Rosati et al. (2015). Thus, only the reliable number fraction describing  $GF > 1.5$  for this diameter is presented in Fig. 7.

10) p. 9469, lines 25-28. *More speculation without conclusion.*

We bring up two hypotheses for the discrepancy between the HTDMA observation and other results. One is from the literature; one is our own. Unfortunately, we cannot prove or discard one or the other.

11) Section 4.2. *This section does not contribute much to the story of the evolution of particle hygroscopicity with the growing PBL. The conditions are quite different from the Po Valley, and no firm conclusions are drawn from the measurements. It might be wise to exclude these observations from the manuscript and focus on the more comprehensive and interesting Po Valley analysis, from a region with much larger air quality problems and radiative forcing implications.*

We kept the results from the Netherlands as only few data on the hygroscopicity of atmospheric particles in the 500 nm size range are available. Furthermore, while we could not probe both the developing mixing layer and the residual layer, we could still show the homogeneity of the aerosol properties within the developing PBL. However, we shortened this section substantially for the revised manuscript.

12) *There are many typographic errors and a revised manuscript would benefit from thorough editing by a native English speaker.*

We did a thorough revision for the new manuscript.

# Vertical profiling of aerosol hygroscopic properties in the planetary boundary layer during the PEGASOS campaigns

**B. Rosati<sup>1,\*</sup>, M. Gysel<sup>1</sup>, F. Rubach<sup>2,3,\*\*</sup>, T. F. Mentel<sup>2</sup>, B. Goger<sup>1,\*\*\*</sup>, L. Poulain<sup>3</sup>, P. Schlag<sup>2</sup>, P. Miettinen<sup>4</sup>, A. Pajunoja<sup>4</sup>, A. Virtanen<sup>4</sup>, H. Klein Baltink<sup>5</sup>, J. S. Henzing<sup>6</sup>, J. Gröb<sup>3</sup>, G. P. Gobbi<sup>7</sup>, A. Wiedensohler<sup>3</sup>, A. Kiendler-Scharr<sup>2</sup>, S. Decesari<sup>8</sup>, M. C. Facchini<sup>8</sup>, E. Weingartner<sup>1,\*\*\*\*</sup>, and U. Baltensperger<sup>1</sup>**

<sup>1</sup>Laboratory of Atmospheric Chemistry, Paul Scherrer Institute (PSI),  
5232 Villigen, Switzerland

<sup>2</sup>Institute for Energy and Climate Research (IEK-8), Forschungszentrum Jülich,  
52428 Jülich, Germany

<sup>3</sup>Leibniz Institute for Tropospheric Research, 04318 Leipzig, Germany

<sup>4</sup>Department of Applied Physics, University of Eastern Finland, 1627 Kuopio, Finland

<sup>5</sup>Royal Netherlands Meteorological Institute (KNMI), 3730 De Bilt, the Netherlands

<sup>6</sup>Netherlands Organization for Applied Scientific Research (TNO),  
80015 Utrecht, the Netherlands

<sup>7</sup>Institute of Atmospheric Sciences and Climate (ISAC-CNR), National Research Council, 00133  
Rome, Italy

<sup>8</sup>Institute of Atmospheric Sciences and Climate (ISAC-CNR), National Research Council, 40129  
Bologna, Italy

\*now at: Institute for Aerosol Physics and Environmental Physics, University of Vienna, 1090  
Vienna, Austria

\*\*now at: Max Planck Institute for Chemistry, 55128 Mainz, Germany

\*\*\* now at: Institute of Meteorology and Geophysics, University of Innsbruck,  
6020 Innsbruck, Austria

\*\*\*\* now at: Institute for Aerosol and Sensor Technology, University of Applied Science Northwestern  
Switzerland, 5210 Windisch, Switzerland

Correspondence to: M. Gysel (martin.gysel@psi.ch)

## Abstract

### Airborne measurements

Vertical profiles of the aerosol hygroscopic and optical properties, particles hygroscopic properties, their mixing state as well as chemical composition were performed in the Netherlands and northern Italy on board of a Zeppelin NT airship measured above northern Italy and the Netherlands. An aerosol mass spectrometer (AMS; for chemical composition) and a white-light humidified optical particle spectrometer (WHOPS; for hygroscopic growth) were deployed on a Zeppelin NT airship during the PEGASOS field campaigns in 2012. The vertical changes in aerosol properties during within the PEGASOS project. This allowed to investigate the development of the mixing layer were studied. Hygroscopic growth factors (GF) at 95 relative humidity were determined using the white-light humidified optical particles spectrometer (WHOPS) for dry diameters of 300 and 500 particles. These measurements were supplemented by an aerosol mass spectrometer (AMS) and an aethalometer providing information on the aerosol chemical composition.

Several vertical profiles between 100 and 700 a.g. were flown just after sunrise close to the San Pietro Capofiume ground station different layers within the planetary boundary layer (PBL), providing a unique in-situ data set for airborne aerosol particles properties in the first kilometre of the atmosphere. Profiles measured during the morning hours on June 20<sup>th</sup> 2012 in the Po Valley, Italy. During the early morning hours the lowest layer (newly developing mixing layer) contained a high nitrate fraction (20, showed an increased nitrate fraction at  $\sim 100$ ) which was m above ground level (AGL) coupled with enhanced hygroscopic growth. In the layer above (residual layer) small nitrate fractions of  $\sim 2$  compared to  $\sim 700$  were measured as well as low GFs. After full mixing of the layers, typically around noon and with increased temperature, the nitrate fraction decreased to 2 at all altitudes and led to similar hygroscopicity values as found in the residual layer. These distinct vertical and temporal changes underline the importance of airborne campaigns to study aerosol properties during the development of the mixed layer. The aerosol was externally mixed with 22 and 67 of the m AGL. This result was derived from both, measurements of the

aerosol composition and direct measurements of the hygroscopicity, yielding hygroscopicity parameters ( $\kappa$ ) of  $0.34 \pm 0.12$  and  $0.19 \pm 0.07$  for 500 nm particles in the range GF, at  $\sim 100$  and  $\sim 700 < 1.1$  and  $\text{GF} > 1.5$  m AGL, respectively. Contributors to the non-hygroscopic mode in the observed size range are most likely mineral dust and biological material. Mean hygroscopicity parameters ( $\kappa$ ) were 0.34, 0.19 and 0.18 for particles in the newly forming mixing layer, residual layer and fully mixed layer, respectively. These results agree well with those from chemical analysis which found values of  $\kappa = 0.27$ , 0.21 and 0.19 for the three layers. The highest  $\kappa$  values in the new mixed layer and lower values. The difference is attributed to the structure of the PBL at this time of day which featured several independent sub-layers with different types of aerosols. Later in the day the vertical structures disappeared due to the mixing of the layers and similar aerosol particle properties were found at all probed altitudes (mean  $\kappa \approx 0.18 \pm 0.07$ ). The aerosol properties observed at the lowest flight level (100 m AGL) were consistent with parallel measurements at a ground site, both in the morning and afternoon. Overall, the aerosol particles were found to be externally mixed, with a prevailing hygroscopic fraction. The flights near Cabauw in the Netherlands in the fully developed mixed layer were additionally confirmed by ground measurements.

The aerosol sampled in the Netherlands did not show any mixed PBL, did not feature altitude dependent characteristics because only the fully mixed layer or the entrainment zone between mixed and the residual layer were probed. The airborne hygroscopicity measurements agreed well with ground based composition measurements. However, the fraction of the hygroscopic particles ( $\text{GF} > 1.5$ ) was enhanced. Particles were also externally mixed and had an even larger hygroscopic fraction compared to the results from Italy amounting to 82, while 12 showed low hygroscopicity ( $\text{GF} < 1.1$ ) in Italy. The mean  $\kappa$  value measured by the WHOPS was 0.28 and therefore from direct measurements was  $0.28 \pm 0.10$ , thus considerably higher than the value measured in  $\kappa$  values measured in Italy in the fully mixed layer in Italy PBL.

~~The effective index of refraction reached values of 1.43 and 1.42 for the 500 particles in Italy and the Netherlands, respectively. This coincides well with literature data for air masses with predominant organic contribution as was the case during our flights.~~

## 1 Introduction

5 Aerosol particles ~~can~~ directly have an impact on climate by absorbing or scattering the solar radiation. The optical properties depend on the particles' size as well as their chemical composition and both can be altered at elevated relative humidities (RH) if the particles are hygroscopic (Boucher et al. IPCC, 2013).

10 Most particles are emitted or formed in the planetary boundary layer (PBL), ~~which describes~~ the lowermost layer of the troposphere. The PBL is subject to ~~many~~ changes depending on the strength of the incident solar radiation (~~see Stull, 1988 for more information on the PBL compare Stull, 1988~~): Under clear sky conditions heating of the Earth's surface by solar radiation induces convective turbulence and therefore a well-mixed PBL builds up after midday ranging up to an altitude of approximately 2 km. During night when the sur-  
15 face cools down, several sub-layers are present in the PBL where the upper most part is defined as the residual layer (RL). The RL contains a mixture of emissions and background aerosol from the day before and is decoupled from the surface. Close to the ground a stable nocturnal layer (NL) develops where local and/or regional emissions ~~can~~ accumulate. Once the sun rises a new mixing layer (ML) is formed which is separated from the other layers  
20 through a temperature inversion. Throughout the day this ML evolves until it reaches up to the free troposphere and extends across the whole PBL. The dynamics of the sub-layers in the PBL and its effect on the properties of the aerosol particles in these layers are still poorly understood.

25 Airborne studies were previously performed to investigate the aerosol chemical composition as a function of altitude utilizing an aerosol mass spectrometer (AMS), and showing that chemical composition varies with height (Morgan et al., 2009, 2010a, b; Pratt and Prather, 2010). ~~This variation should influence the particles' hygroscopic growth~~ Accordingly,

aerosol hygroscopicity, which depends on chemical composition and can also be inferred from it, is also expected to be height dependent. Morgan et al. (2010a) conducted flights over north-western Europe, ~~concentrating however focusing~~ on changes between 0 and 10 km ~~a. g. above ground level (AGL).~~ In general aircraft campaigns commonly stretch over large ~~horizontal and vertical ranges, areas and altitudes, often above the PBL,~~ therefore providing only limited information on the PBL itself. On the other hand, ~~ground-based studies have directly investigated the hygroscopic properties of particles~~ extensive data sets studying the variability of aerosol composition and hygroscopic properties are available from ground-based studies. However, surface measurements are not always representative for aerosol properties at elevated altitudes. ~~In addition, hygroscopic properties of particles are studied in reaction chambers under controlled conditions (e.g. Duplissy et al., 2011, or Tritscher et al., 2011).~~

One way to explore the hygroscopic properties of aerosols is to measure the so called hygroscopic growth factor (GF) defined as the ratio of the particle diameter  $D_{\text{wet}}$  at a certain relative humidity (RH;  $D_{\text{wet}}$ ) divided by its dry diameter ( $D_{\text{dry}}$ ):

$$\text{GF}(\text{RH}) = \frac{D_{\text{wet}}(\text{RH})}{D_{\text{dry}}} \quad (1)$$

The most common instrument for ground-based hygroscopicity measurements of atmospheric aerosol particles is the hygroscopicity tandem differential mobility analyzer (HTDMA; see e.g. Liu et al., 1978, or McMurry and Stolzenburg, 1989, for details). It explores ~~particles~~ particle growth in the sub-saturated RH range and was employed successfully in several ~~ground-based campaigns (a review is presented in~~ ground-based campaigns (compare the review by Swietlicki et al., 2008). This method investigates GFs at high precision but needs several minutes for a full measurement cycle which makes it rather unsuited for airborne measurements. Besides, its detection range is limited to a maximal dry mobility diameter of approximately 250 nm.

HTDMA and chemical composition hygroscopicity closures were performed at various sites including urban (see e.g. Kamilli et al., 2014) ~~but also and~~ rural regions (see e.g. Wu

et al., 2013). ~~Altitude dependent hygroscopic properties were investigated by employing HTDMAs at, as well as~~ elevated mountain sites, like the Jungfraujoeh (e.g. Kammermann et al., 2010) ~~or Puy de Dôme (e. g. ?), however these measurements may be influenced by surface emissions and cannot provide a detailed analysis of particles at different elevations:~~

To our knowledge, only few campaigns report airborne hygroscopicity results due to the lack of ~~available instruments suited~~ suitable instruments for this kind of measurements. The first instrument built for this special task is the aerosol hydration spectrometer (AHS; Hegg et al., 2007). The set-up comprises two optical instruments, to measure the properties of the dry and humidified aerosol particles. However, quantifying hygroscopic growth with the AHS is difficult as the measurement is performed for poly-disperse rather than size-selected aerosol samples. The differential aerosol sizing and hygroscopicity spectrometer probe (DASH-SP; Sorooshian et al., 2008) ~~.It is constructed using a~~ is using a combination of differential mobility analysis (DMA) and optical particle spectrometry (OPS) and has successfully been applied for airborne GF measurements at sub-saturated RH. This instrument ~~focuses on~~ is limited to small sizes in the range of 150–225 nm dry diameters. ~~Results are reported for aircraft campaigns in Hersey et al. (2009) and Hersey et al. (2013).~~ In the aircraft campaigns an attempt was made to reconcile simultaneously measured chemical composition and hygroscopic growth using an AMS and GF results. DASH-SP. Herein, Hersey et al. (2009, 2013) focused their studies on the free troposphere in the marine atmosphere off the coast of California.

~~All measurement techniques mentioned so far~~ Most measurement techniques to study hygroscopicity ~~focus on~~ select particles smaller than  $\sim 300$  nm, which implies that species that are more abundant at larger sizes (e.g. sea salt, mineral dust) cannot be fully easily investigated. This may induce ~~an underestimation of the scattering potential of the overall aerosol particles but also an underestimation of the overall hygroscopic properties of atmospheric aerosol particles.~~ a bias in estimates of the humidity effects on hygroscopic growth and light scattering efficiency of particles in the upper accumulation mode size range. Indeed, Zieger et al. (2011) presented a comparison between HTDMA measure-

ments for dry diameters of 165 nm and calculated GFs using size distributions, scattering enhancement factors (based on ~~polydisperse aerosol particles~~ poly-disperse aerosol particles in the  $PM_{10}$  range) and Mie theory. The comparison revealed that indeed in the presence of sea salt the HTDMA ~~results~~ hygroscopicity results for particle diameters of 165 nm were not representative for the atmospheric accumulation mode particles, finding too small GF values. Based on these findings we concluded that ~~studies-of-understanding the~~ hygroscopic properties of larger sizes-are-needed-in-order-to-get-a-more-complete picture-of-the-ambient-aerosol-particles particles is important as well to understand the RH effects on aerosol optical properties. Hence, we developed the white-light humidified optical particle spectrometer (WHOPS; ~~?~~ Rosati et al., 2015a) to perform vertical profiles of the particles' hygroscopic properties of optically more relevant sizes ( $D_{dry} = 300, 500$  nm).

Within the Pan-European Gas–AeroSOI-climate interaction Study (PEGASOS) ~~airmasses~~ air-masses over Europe were explored in order to understand feedbacks between atmospheric chemistry and a ~~-~~ changing climate. ~~A-~~ Our interest here focusses on the vertical changes in aerosol properties and particularly on changes occurring due to the dynamics of the PBL. For this purpose a Zeppelin NT ("New Technology") was chosen. "New Technology" was utilized as measurement platform to ~~specifically probe changes in probe~~ different layers present in the evolving convective PBL. The WHOPS, together in various European regions. The Zeppelin NT airship was equipped with an aethalometer ~~and an AMS~~ were mounted in the Zeppelin NT airship to investigate GFs and chemical composition, an HR-ToF-AMS and the WHOPS to investigate the chemical composition, the hygroscopic properties as well as the mixing state of the aerosol particles. In the current study, data from vertical profiles ~~measured above central (Cabauw, Netherlands) and southern Europe~~ (recorded above southern (Po Valley, Italy) and central Europe (Cabauw, Netherlands)) are presented (Fig. ~~??~~ 1 shows the campaign locations). ~~Flight data is further compared to results from ground measurements to get a complete picture of the dynamics and altitude dependent aerosol properties. Additionally, the hygroscopic mixing state and the effective index of refraction of the particles are explored~~ Comparison with co-located ground-based

in-situ measurements made it possible to assess under which conditions the ground data are representative of the column above.

## 2 Experimental

### 2.1 The Zeppelin NT airship

5 The Zeppelin NT airship, which served as a platform for the airborne measurements, flew with an average speed of  $50 \text{ km h}^{-1}$  ~~a.g.~~ AGL and reached altitudes between 80 and ~~approximately~~ 1000 m ~~a.g.~~ AGL, depending on the ~~payload~~ payload and ambient temperature. Therefore, a good spatial and temporal resolution of the gas-phase and aerosol properties could be obtained. ~~Additionally, the Zeppelin characteristics allowed for a distinct~~ This made it possible to focus on the evolution of the mixed layer forming at low altitudes in the first hours of sunlight ~~and finally expanding across the whole PBL. In order to do so, circles at selected constant heights were flown with straight ascends and descends.~~ For flight safety reasons, the Zeppelin could only be deployed on days with low wind speeds ~~and~~ and low cloud coverage or clear sky.

15 The Zeppelin NT airship could be equipped with different instrumental layouts for focusing on certain research questions. For this study the so called secondary organic aerosol (SOA) layout was utilized. This layout ~~focuses on the measurement~~ includes measurements of aerosol properties like aerosol hygroscopicity, size distribution, particle number concentration, chemical composition and volatile organic compounds (VOC). The specific instruments used to measure these properties are described in the following subsections. In addition, nitrogen oxides ( $\text{NO}_x$ ), ozone ( $\text{O}_3$ ), carbon monoxide (CO), radiative flux, hydroxy as well as peroxy radicals (OH,  $\text{HO}_2$ ) were monitored continuously on board of the airship. Each instrument had a separate inlet system and a separate sampling position.

## 2.2 Flight and ~~ground-based~~ ground-based measurement locations

### 2.2.1 Po Valley site

The Italy campaign ~~, within the PEGASOS project, was located~~ took place in the Po Valley, a region known for its remarkably high air pollution levels, compared to other places in Europe (see e.g. Putaud et al., 2010). The Po Valley hosts several industrial, urban and agricultural areas allowing for detailed anthropogenic pollution studies, however ~~also long-range~~ , also long range transport and aged aerosol from other sites can be investigated. The Zeppelin NT airship was stationed at Ozzano Airport (located at 44°28' N, 11°32' E, ~ 30 km ~~southeast~~ south-east of Bologna) and performed flights during June and July 2012 in the greater Po Valley region. The vertical profiles were ~~focused above~~ mostly taken near the San Pietro Capofiume (SPC) ground station (located at 44°39' N, 11°38' E), a ~~rural~~ background site which lies approximately 40 km north-east of Bologna. ~~Additionally, data from Monte Gimone (MTC), a mountain site located at 2165 a.s.l. approximately 100 south-west of SPC is included in the analysis presented here to complement the airborne data with results measured at an elevated site.~~ Throughout the PEGASOS campaign the SPC ~~and MTC station were~~ station was equipped with a ~~set of instruments equivalent to those on the Zeppelin NT airship in order to compare flight and~~ ground level data. In order to ground-level data. To get estimates of the mixing layer height a ~~Jenoptik CHM15K "Nimbus" automated Lidar ceilometer~~ lidar ceilometer was employed at SPC. ~~In the present analysis we used an operator-driven approach which avoids the major drawbacks of automated mixing layer height (MLH) retrievals~~ (e.g., Angelini et al., 2009, Haeffelin et al., 2012 and Di Giuseppe et al., 2012). This is performed by manually evaluating the MLH by a skilled operator's visual analysis. The trained operator manually marks a number of points (at least one per hour) matching the requirements of showing maximum signal gradients, maximum signal variance, continuity between sunrise until sunset and separation from the residual layer's gradient maxima. A spline curve is then fitted to these points to provide a continuous MLH over time. Naturally, the MLH is not retrieved when it descends below the minimum height observed by the ceilometer (about 200 m AGL). The typical uncertainty due to this approach

amounts to 3 pixels, i.e.  $\pm 45$  m. Additionally, we compared the ceilometer retrieval to the MLH found by analysing T and RH gradients from a co-located radio sounding performed at 11 UTC. Note, that the radio sounding was carried out only once every 12 hours, while ceilometer retrievals of MLH have a time resolution of minutes. The 11 UTC MLH retrieved from the radio sounding yielded a value of 753 m AGL, while an altitude of 772 m AGL was found from the ceilometer data at this time of day. The two retrievals agree within the  $\pm 45$  m we commonly use as uncertainty of our MLH retrievals. The findings of the ceilometer are additionally supported by height profiles of the potential temperature ( $\Theta$ ) measured aboard the Zeppelin NT, which can be found in the supplement.

## 2.2.2 Netherlands site

The campaign in the Netherlands was located in the South Holland and Utrecht region. This region is representative for north-west Europe and is influenced by continental and maritime airmasses, depending on the wind direction. The Zeppelin NT airship was stationed at Rotterdam – the Hague Airport and conducted several flights in May 2012. The vertical profiles were performed near the Cabauw Experimental Site for Atmospheric Research (CESAR, located at  $51^{\circ}97' N$ ,  $4^{\circ}93' E$ ). The CESAR station hosts a number of instruments to characterize radiative properties, climate monitoring and atmospheric processes ([www.cesar-observatory.nl](http://www.cesar-observatory.nl)). During the PEGASOS campaign an aerosol mass spectrometer was added to the permanently installed aerosol measurements. Also at this station, a ceilometer system (Vaisala LD40) was utilized to get an estimated mixing layer height (Hajj et al., 2007). The retrieval of the mixing layer height from the LD40 ceilometer backscatter profiles is based on a wavelet algorithm (Hajj et al., 2007). The algorithm determines the height of the maximum in the gradient in the backscatter profile. The difference in backscatter in a small range below and above the retrieved height is used as an estimator for the quality of the retrieved height. Retrieved mixing heights with the highest quality index have comparable accuracy to radiosonde retrieved heights and have an estimated accuracy on the order of  $\pm 50$  m.

## 2.3 Instrumentation for aerosol measurements

### 2.3.1 Hygroscopic and optical aerosol properties

On the Zeppelin the ~~hygroscopic and optical properties were measured using the~~ white-light humidified optical particle spectrometer (WHOPS) ~~. The WHOPS and was~~ used to determine hygroscopic GF. All instrument specifications, as well as associated calibration and data analysis procedures ~~are described~~, are presented in detail in ~~?~~Rosati et al. (2015a). Briefly, particles ~~are collected through an isokinetic inlet, developed for an average flight velocity of 50 km h<sup>-1</sup>, before they reach the WHOPS and are dried in a diffusion drier and then size selected in a~~. Then the particles are dried (RH < 10%) and ~~size selected in a~~ differential mobility analyzer (DMA). In ~~the next step these particles are either a next step, the dry particles are~~ guided directly to a WELAS 2300 optical particle spectrometer (WELAS; Palas GmbH, Karlsruhe, Germany) ~~for a measurement of the particle size distribution (~300–10 to measure the dry optical response. Alternatively, the size-selected dry particles are humidified before being directed to the WELAS to measure the wet optical response (residence time at high RH: ~20 000) or humidified in-between.~~s). Multiply charged particles appear as a distinctly separated mode in the optical size distribution measured by the WELAS and are discarded from the further data analysis. Hygroscopicity measurements are typically performed at RH = 95 %, where the uncertainty in the humidity measurement is ~~assumed to be ±2~~ estimated to be ±2%. Since the RH to which particles were exposed to varied only between ~~~94–96~~94–96 % during both flight days, no further RH corrections were applied to the results. ~~By measuring at both conditions~~ Using the WHOPS set-up, an optically measured size distribution ~~for can be achieved by stepwise recording~~ the size-selected particles ~~can be recorded~~ in their dry and humidified state.

To be able to link the measured partial scattering cross sections ( $\sigma$ ; from now on referred to as simply scattering cross section) of the WELAS to specific geometric diameters, several factors have to be known: the index of refraction ( $m$ ) as well as the optical ~~setup~~ set-up of

the instrument, the spectrum of the light source and sensitivity of the detector. ~~This specific optical instrument~~

The WELAS was chosen because ~~it uses a of its~~ white-light source (OSRAM XBO-75 Xenon short arc lamp) which minimizes Mie oscillations ~~for the light scattering which in turn of the scattering cross section as a function of particle size~~. This allows for mostly unambiguous attribution of particle diameter to measured scattering cross section. ~~Once a Residual uncertainties with regard to the Mie oscillations amount to less than 7% in the GF (for more details see Rosati et al., 2015a). Since~~ specific dry mobility ~~diameter is diameters were~~ selected, the optically measured  $\sigma$  can be converted to optical diameters ( $D$ ) using a  $\sigma$ - $D$ - $m$  table for a ~~series of different indices of refraction calculated with the Mie code based on Mie theory~~ (Mie, 1908; Bohren and Huffman, 2007). The index of refraction ~~where for which~~ the optical diameter of the dry particles coincides with the selected mobility diameter is then defined as the effective index of refraction ( $m_{dry}$ ) of the dry particles. The ~~term qualifier~~ “effective” ~~refers to the fact that only the real part can be derived and that particles are assumed to be spherical for all calculations. During the measurement campaigns the instrument was periodically checked and calibrated with well defined aerosols with known optical properties and hygroscopicity, e. g. ammonium sulfate particles. is used because the true index of refraction can be slightly different due to required approximations such as assuming an imaginary part of zero, only spherical and homogeneously internally mixed particles (see Rosati et al., 2015a, for more details).~~

~~Figure 3 illustrates the temporal variability of the observed effective~~ ~~The index of refraction of the grown particles approaches the~~ index of refraction  $m$  ~~for the described flights on 20 June 2012 in the Po Valley and 24 May 2012 in the Netherlands. It has to be noted that only the results for a dry selected mobility diameter of of pure water ( $m_{H_2O} = 1.333$ ) with increasing hygroscopic GF. Including this effect is crucial for the data analysis and the approach was done as detailed in Rosati et al. (2015a). The effective indices of refraction for 500 nm are shown. In Italy a mean  $m_{dry}$  of particles and a wavelength range of 380-600 nm (see Rosati et al., 2015a for the light spectrum of the WELAS) were found to be  $1.43 \pm 0.02$  (mean  $\pm$  SD) ~~and in Italy and  $1.42 \pm 0.02$  (mean  $\pm$  SD)~~~~

in the Netherlands  $m_{dry} = 1.42 \pm 0.02$  were found. However, an absolute uncertainty of  $\pm 0.04$  has to be attributed to considered for all index of refraction retrievals (see ?). This range compares well to former laboratory studies for SOA from biogenic sources which present values between 1.44–1.45 (?; ?). ? performed ambient aerosol measurements in Rosati et al., 2015a and supplement). During the measurement campaigns, the instrument was regularly checked and calibrated with well-defined aerosols with known optical properties and hygroscopicity, e.g. ammonium sulphate particles. Particles with a dry mobility diameter of 300 or 500 nm were alternately probed during 250 s per size, whereof 150 s were used for the Amazon background atmosphere and found also similar values of 1.42 (at  $\lambda = 545$  nm wet-mode and 100 s for the dry-mode. The results were averaged for each probed layer at a constant flight altitude. This ensured that each GF-probability density function (GF-PDF) shown in Figs. 3, 4, 11 and 12 is based on more than 90 detected particles. As described in Rosati et al. (2015a) the GF uncertainty for dry particle diameters of 500 nm ) for airmasses dominated by organics. In contrast airmasses with predominant anthropogenic pollution would reach higher indices of refraction of approximately 1.50–1.55 (?; ?). The low indices of refraction found in this study from the WHOPS results fit well to is approximately  $\pm 10\%$  in the range  $1 < GF < 3$ .

The distribution of GF can provide information on the mixing state of aerosol particles with respect to components that differ in hygroscopicity. Commonly the mixing state of aerosol particles is classified as follows: if all particles of a certain size have almost the same chemical composition, they are described as internally mixed, whereas if particles of equal size have different chemical composition, they are referred to as externally mixed. Depending on the mixture, the hygroscopic behaviour will change: internally mixed aerosols will grow uniformly with increasing RH, while external mixtures of substances with differing hygroscopic properties will result in multi-modal and/or broadened GF distributions. We chose GF-PDFs as graphical representation of WHOPS data to investigate the mixing state of the strong contribution of organics to the total aerosol mass concentration measured by the AMS as will be discussed in more detail later aerosol particles during the flight days.

The SPC ~~and MTC sites were equipped with~~ site was equipped with a hygroscopicity tandem differential mobility ~~analyzers (HTDMA; see e.g. Swietlicki et al., 2008) where analyzer~~ (HTDMA) in order to determine the hygroscopic properties of particles with 4 different dry diameters between 35 and ~~230200 nm were measured. The setup.~~ Each scan to record a GF-PDF at a fixed dry size lasted 500 s in total, thus providing a time resolution of 1.8 measurements per hour for each dry size. The set-up comprises two DMAs connected in series combined with a ~~condensation particle counter (CPC). First a monodisperse, a dry~~ mono-disperse aerosol is selected in the first DMA ( $RH < 30\%$ ), then exposed to elevated relative humidity (typically 90 %) and the resulting size distribution is then measured using a ~~second~~ DMA coupled to a ~~CPC providing a GF distribution. The inversion of the HTDMA results was done with the algorithm proposed by Gysel et al. (2009). For a direct comparison to the WHOPS measurements~~ the HTDMA GF-probability density functions (, the HTDMA GF-PDF ) were recalculated for  $RH = 95\%$  using Eq. (5) in Gysel et al. (2009). Note that the dry sizes selected by the WHOPS are larger compared to those selected by the ~~HTDMAs, which focus on HTDMA, which is built for the investigation of~~ smaller particles.

### 2.3.2 Aerosol chemical composition

A high resolution time-of-flight aerosol mass spectrometer (HR-ToF-AMS; DeCarlo et al., 2006) was employed to characterize the non-refractory chemical composition of aerosol particles. The term non-refractory refers to all species that flash vaporize at  $600^{\circ}\text{C}$  and  $\sim 10^{-7}$  Torr. ~~Aerosols pass a~~ The particles were sampled through a 1500 mm long tube (4 mm ID), ending about 200 mm below the bottom hatch of the Zeppelin. A constant pressure inlet, consisting of an orifice that is pumped with variable flow and installed between the aerosol inlet and the AMS, was used to regulate the downstream pressure to 800 hPa independent of upstream pressure. This ensured constant sampling conditions for the AMS. Within the AMS, the particles pass a critical orifice and an aerodynamic lens ~~which focuses, which collimates~~ particles of sizes between 100 and 700 nm into a ~~narrow beam. The particle beam is impinging on a hot surface (600 °C), where the non-refractory components flash vaporize. The resulting vapors vapours~~ are ionized by electron impact ionization

and measured with a time-of-flight mass spectrometer. The ~~high-mass spectral resolution of the employed mass spectrometer~~ AMS allows for identification and quantification of peaks corresponding to classes of chemical species (e.g. nitrates, sulphates, chloride, ammonia and organics). Where mass resolution is not sufficient or more than one chemical species fragments to the same ion in the ionization process, known relationships between peaks at different mass to charge ratios are used to improve quantification (fragmentation table, Allan et al., 2004). Two operational modes of the ToF-MS (V- and W-Mode) were used during the flights. Specifications of the adaptation of the HR-ToF-AMS for the Zeppelin requirements can be found in Rubach (2013). A collection efficiency (CE) of 1 was applied to the AMS measurements, based on a comparison between mass concentrations derived from particle size distributions measured by scanning mobility particle sizers (SMPS; TSI Inc., DMA Model 3081 and water – CPC Model 3786) and WELAS, and the combined results of AMS and aethalometer measurements on the Zeppelin. Because a CE of 1 is higher than observed in other field studies and we cannot explain ~~the differences, we must~~ this difference, we attribute an uncertainty of  $\sim 50\%$  for the Zeppelin AMS mass concentrations. The same procedure was applied to the ground measurements at SPC yielding the same conclusion that a CE of 1 has to be used. In Cabauw the CE was ~~corrected~~ estimated using the algorithm proposed by Middlebrook et al. (2012). The mass fractions of the compounds are independent of this uncertainty.

At the ground stations, both in Italy and the Netherlands, equivalent black carbon (eBC) mass concentrations were measured with a multi-angle absorption photometer (MAAP Thermo Scientific Model 5012; Petzold et al., 2005) with a resolution of five minutes and an uncertainty of 12% (Petzold and Schönlinner, 2004). A mass absorption cross section (MAC) of  $6.6 \text{ m}^2 \text{ g}^{-1}$  for a wavelength of 637 nm (Müller et al., 2011) was chosen to convert the ~~signal into~~ measured particle absorption coefficient to eBC mass concentrations. A portable aethalometer (AE42, MAGEE Scientific; Berkeley, USA) was mounted on the Zeppelin NT to monitor the eBC mass concentrations. The aerosol was collected through the same isokinetic inlet and sampling line as for the WHOPS. eBC concentrations were logged with a time resolution of 2 min and averaged for the time

needed to probe a certain layer. Results at a wavelength of 880 nm were used. During the flights a maximal attenuation of 70 % and a  $4 \text{ L min}^{-1}$  flow were chosen. The data was used as retrieved by the manufacturers' firmware using an apparent MAC of  $16.6 \text{ m}^2 \text{ g}^{-1}$  at a wavelength of 880 nm, which, however, contains already a correction for the multiple scattering for the BC deposited in the filter matrix. In order to get comparable eBC values This value already accounts for the additional absorption within the filter matrix due to multi-scattering effects (Weingartner et al., 2003). Furthermore, using this value provides consistent eBC mass concentrations from MAAP and aethalometer, both instruments should use the same MAC value. A comparison to the MAAP shows that the aethalometer multiple scattering correction factor if the multi-scattering enhancement factor ( $C$  (Weingartner et al., 2003) -value) of the aethalometer is 3.48 (assuming to be wavelength independent). This value fits relatively well to previous results found at the rural background site of Cabauw of 4.09 by Collaud Coen et al. (2010). As the AMS roughly measures particles smaller than 1  $\mu\text{m}$  and if the absorption Ångström exponent (AAE) of BC between 637 and 880 nm and most of eBC is assumed to be present in the size range below 1  $\mu\text{m}$  we refer to the chemical composition as of nm wavelength is 1.0. Both should be fulfilled in good approximation (WMO/GAW, 2016; Collaud Coen et al., 2010; Sandradewi, 2008).

The chemical composition obtained from the bulk measurements of AMS and aethalometer is considered to be representative of  $PM_{10}$  (particulate mass with an aerodynamic diameter smaller than 1  $\mu\text{m}$ ) in the following, as the AMS has a transmission efficiency of close to unity for particles with vacuum aerodynamic diameters between 50 nm and 600 nm and as most eBC is expected to be present in the size range below 1  $\mu\text{m}$ .

### 3 $\kappa$ -Köhler theory

In order to link hygroscopicity measurements made at different RH using different instruments, it is common to use the semi-empirical  $\kappa$ -Köhler theory introduced by Petters and

Kreidenweis (2007):

$$\text{RH}_{\text{eq}}(D_{\text{dry}}, \text{GF}, \kappa) = a_{\text{w}}(\text{GF}, \kappa) \cdot S_{\text{k}}(\text{GF}, D_{\text{dry}}) = \frac{\text{GF}^3 - 1}{\text{GF}^3 - (1 - \kappa)} \cdot \exp\left(\frac{4\sigma_{\text{s/a}}M_{\text{w}}}{RT\rho_{\text{w}}D_{\text{dry}}\text{GF}}\right) \quad (2)$$

Köhler theory relates the equilibrium RH ( $\text{RH}_{\text{eq}}$ ) over a solution droplet to the product of the water activity  $a_{\text{w}}$  representing the Raoult term, and factor  $S_{\text{k}}$  representing the Kelvin term.  $D_{\text{dry}}$  describes the dry diameter, GF the growth factor (see Eq. 1),  $\sigma_{\text{s/a}}$  is the surface tension of the solution/air interface,  $M_{\text{w}}$  the molecular mass of water,  $R$  the ideal gas constant,  $T$  the absolute temperature and  $\rho_{\text{w}}$  the density of water.  $\kappa$  is the semi-empirical hygroscopicity parameter introduced by Petters and Kreidenweis (2007), which captures the composition dependence of the Raoult term.

To derive  $\kappa$  values from GF measurements at specific RHs, the relation between  $a_{\text{w}}$  and GF is used as described by Petters and Kreidenweis (2007) ~~is used~~:

$$\kappa_{\text{meas}} = \frac{(\text{GF}(\text{RH})^3 - 1) \cdot (1 - a_{\text{w}})}{a_{\text{w}}} \quad (3)$$

The subscript “meas” refers to the fact that this  $\kappa$  value is based on the measured GF. The water activity ~~can be was~~ inferred from the RH and equilibrium droplet diameter ( $D_{\text{wet}}$ ):

$$a_{\text{w}} = \frac{\text{RH}}{\exp\left(\frac{4\sigma_{\text{s/a}}M_{\text{w}}}{RT\rho_{\text{w}}D_{\text{wet}}}\right)} \quad (4)$$

In our calculations the surface tension of water is assumed. For a ~~composition-~~hygroscopicity closure, the  $\kappa$  values derived from the GF measurements (WHOPS) ~~as described above are compared with the  $\kappa$  values are compared to those~~ derived from the chemical composition measurements (AMS and aethalometer). The composition based  $\kappa$  ~~values of a mixed particle value~~,  $\kappa_{\text{mix}}$ , ~~can be of a mixture was~~ estimated from the ~~pure component behavior using the Zdanovskii, Stokes and Robinson (ZSR; Stokes and Robinson, 1966) mixing rule. According to the ZSR mixing~~

rule,  $\kappa_{\text{mix}}$  is simply the volume fraction weighted mean of the  $\kappa$  values,  $\kappa_i$ , of all components in pure form (Petters and Kreidenweis, 2007), of the pure components and the respective volume fractions,  $\epsilon_i$ , using the Zdanovskii-Stokes-Robinson (ZSR) mixing rule (Stokes and Robinson, 1966; Petters and Kreidenweis, 2007):

$$\kappa_{\text{mix}} = \sum_i \epsilon_i \kappa_i \quad (5)$$

Where  $\epsilon_i$  is the volume fraction of component  $i$  in the mixed particle.

The mass concentrations of nitrate, sulfate sulphate, ammonia, organics and chloride ions as measured by the AMS were converted to neutral salts in order to apply Eq. (5) to calculate hygroscopic properties of the aerosol particles. To do so the ion pairing pairing mechanism described by Gysel et al. (2007) in their Eq. (2) was used. The corresponding densities as well as  $\kappa$  values for the corresponding pure compounds for the prediction of the hygroscopicity parameter are summarized in Table 1. For the inorganic salts, the bulk densities were taken from literature and the  $\kappa$  values were derived from ADDEM predictions (Topping et al., 2005) which is a detailed model capable of calculating growth factors of inorganic aerosols with high accuracy. The final  $\kappa$  values were calculated for 95 RH and a dry diameter of 500. For the organics a equilibrium solution concentrations at  $a_w=95$ . The  $\kappa$  value of 0.11 was used. This was values for the organics were inferred from the median measured O : C ratio of 0.5 measured during the flights and Fig. 7 in Duplissy et al. (2011), assuming that the organics measured in our studies behaved like organics in previous measurement campaigns and like secondary organic aerosol derived from the oxidation of  $\alpha$ -pinene. To determine the organic's density using the relationship between O : C and  $\kappa$  value reported in Duplissy et al. (2011) for organics in atmospheric aerosols. The O:C ratio was deduced from the HR-ToF-AMS measurements using the method presented by Aiken et al. (2007). During the flight in Italy, O:C differed slightly between the three probed layers with values of  $0.45 \pm 0.03$ ,  $0.55 \pm 0.03$  and  $0.50 \pm 0.05$  for the newly forming ML, the RL and the fully developed ML, respectively. The corresponding  $\kappa$  values were estimated to be 0.09, 0.14 and 0.12 accordingly. The mean O:C ratio of the organics measured at the SPC ground

site was  $0.60 \pm 0.03$ , which translates to a  $\kappa$  value of 0.17 for the organic fraction. In the Netherlands, the mean O:C ratio of the organic matter measured by the HR-ToF-AMS at the ground station of Cabauw was  $0.48 \pm 0.02$  and the corresponding  $\kappa$  value of the organic matter was estimated to be 0.11.

Calculations of the density of organic matter were based on a parametrization based on O:C and H:C ratios introduced by Kuwata et al. (2012) was used. The mean organics' density and SD was found to be  $1233 \pm 35 \text{ kg m}^{-3}$ . eBC was assumed to have  $\kappa = 0$  and a bulk density of  $2000 \text{ kg m}^{-3}$ .

## 4 Results and discussion

### 4.1 Po Valley campaign

Here in the following we present hygroscopicity results recorded with the WHOPS aboard the Zeppelin NT airship. The vertical flight pattern performed on the 20 June 2012 is shown in Fig. 1. During this day vertical profiles were measured near within 5 km horizontal distance from the SPC site from  $\sim 08:30$  LT until approximately 14:00 LT with a refuel break in-between ( $\sim 10:00$ – $11:00$  LT). Two different height levels were covered at approximately 100 and 700 m AGL. On this day westerly winds and wind speeds around  $2$ – $3 \text{ m s}^{-1}$  prevailed. Therefore the air masses originated from the Po Valley plain and due to the low wind speeds the influence of local pollution was highest. Figure 1 depicts the temporal evolution of potential temperature ( $\Theta$ ) and RH profiles observed during the flight together with at different altitudes. The shaded area denotes the estimated mixing layer height provided by Ceilometer-Lidar inferred from ceilometer-Lidar data. The RH ranges from 30 % to a maximum of 60 % and shows a clear altitude dependence: during the first part of the flight the RH was always higher near the ground, while later in the day the opposite trend is visible. The evolution of  $\Theta$  and RH elucidates a clear layering during the beginning of the flight (seen as abrupt change in  $\Theta$  between 100 and 700 m AGL), which slowly disappears towards the last pro-

files. ~~This development~~ Detailed height profiles of  $\Theta$  as well as mean values of RH and  $\Theta$  for each height profile can be found in the supplement. The development of  $\Theta$  is also consistent with the evolution of the estimated mixing layer height, which indicates that during the morning hours ( $\sim 08:30$ – $10:00$  LT) we were able to ascend into the RL and investigate the new ML at the lower altitudes. During the second half of the flight ( $\sim 12:00$ –~~14:30~~–14:00 LT) the fully developed ML was probed at both altitudes.

#### ~~4.1.1 Hygroscopic GF measured with the WHOPS~~ Mixing state inferred from hygroscopicity measurements

Figure 4 gives an overview of the flight day complemented by the time series of the hygroscopicity parameters deduced from the WHOPS measurements (colored in violet). The shaded area describes the accuracy of the WHOPS of 10 (see ? for more details). Variations of the particles' hygroscopic properties can be observed as a function of altitude and time: The first two height profiles ( $\sim 08:30$ – $10:00$ ; from now on referred to as IHP1/2), depict higher hygroscopicity values close to the ground ( $\sim 100$ ) compared to those at elevated altitudes of  $\sim 700$ . This altitude dependence implies different layers with distinct aerosol properties, consistent with the vertical layering of the PBL suggested by  $\Theta$  and the estimated mixing layer height illustrated in Fig. 1. Table 2 contains the mean GF(95) and  $\kappa$  values for both layers, averaged over both profiles. In the new ML the mean GF(95) is 1.88 which is equivalent to  $\kappa = 0.34$ . These values considerably exceed the results in the RL (GF(95%) = 1.61 and  $\kappa = 0.19$ ). After 11:00 a second set of profiles was performed. To study particles in the fully developed ML the results from IHP4/5/6 ( $\sim 12:00$ – $14:00$ ) are considered, while IHP3 is excluded since the ML was not fully developed before noon (see Fig. 4). In the fully developed ML, hygroscopicity results show less variability with no clear pattern for results at different altitudes. We observed one event at around 12:45 and 100, when the mean  $\kappa$  was considerably lower. This could be explained by the presence of an aerosol layer which contained particles with a much lower hygroscopicity compared to particles measured before and after. With exception of this instance, the particle hygroscopic properties were homogeneous across all altitudes in the afternoon.

This is in concordance with the findings from  $\Theta$  and the estimated mixing layer height displayed in Fig. 1 which indicate the presence of only one layer below  $\sim 700$ . Once the fully developed ML is present vertical differences in aerosol properties are expected to disappear. Only altitudedependent changes in temperature and RH could potentially lead to alterations of the particles e. g. through phase partitioning effects. Mean 3 illustrates the GF-PDFs measured by the WHOPS for different altitudes and times of day and therefore specific layers within the PBL. Each GF-PDF represents an average over the chosen time interval and altitude. The mean GF and  $\kappa$  values at different altitudes in the fully developed ML, for each panel are presented in Table 2, show less spread with values of 0.14 and 0.21 at 100 and 700, respectively. The discrepancy can be attributed to the outlier described above which causes a decreased mean value at an altitude of  $\sim 100$ , however the results still agree within the measurement accuracy. In addition, the hygroscopic properties in the fully developed ML appear very similar to those measured in the RL.

#### 4.1.2 Mixing state inferred from WHOPS measurements

The GF-PDFs of the humidified particles can provide information on the mixing state of particles with respect to aerosol components of different hygroscopicity. Commonly the mixing state of aerosol particles is classified as follows: if all particles of a certain size have almost the same chemical composition, they are described as internally mixed, whereas if particles of equal size have different chemical composition, they are referred to as externally mixed. Depending on the mixture the hygroscopic behavior will change: internally mixed aerosols will grow uniformly with increasing RH, while external mixtures of substances with differing hygroscopic properties will result in multimodal and/or broadened GF-PDFs.

In order to further explore differences in hygroscopic properties between the different layers, Fig. 5 illustrates the GF-PDFs averaged for the same layers, i.e. the same times and altitudes, as the mean values shown in Table 2. In general broad GF(95%) distributions with values particles exhibiting GFs between 0.9 and  $\sim 2.5$  were observed independently of flightaltitude or time of day, hence in all four panels of Fig. 5. Vertical differences can be observed for the PDFs can be observed throughout the flight. Vertical differences appear

during IHP1/2 (Fig. 53a and c). ~~The~~, with a more pronounced fraction of more hygroscopic particles (GF > 1.5) ~~is more pronounced~~ in the new ML, ~~while the~~ compared to the RL. ~~On the other hand, the~~ fraction of particles with GF < 1.1 is ~~higher~~ more prominent in the RL. ~~This explains the higher mean particle~~ As a result, the mean hygroscopicity in the new ML ~~compared to the RL~~ is higher than in the RL reaching GF(95 %) values of  $1.88 \pm 0.19$  in the former compared to  $1.61 \pm 0.16$  in the latter.

~~In the early afternoon, the~~ The GF-PDFs measured ~~during IHP4~~ after approximately 12:30 LT (IHP5/5/6) do not exhibit any clear vertical differences (Fig. 53b and d), ~~supporting the above finding of being~~ indicating that in this period the Zeppelin NT flew within the fully developed ML at both altitudes. ~~Subtle differences are a slightly higher fraction of particles with GF~~ The mean GF(95 < 1.1 and a slightly lower fraction of particles with GF > 1.5 %) values amount to  $1.49 \pm 0.15$  and  $1.63 \pm 0.16$  at 100 ~~compared to and~~ 700 m AGL, respectively. This difference in mean GF(95 %) is for the most part caused by the outlier at ~ 12:45 LT, as will be shown below with Fig. 6-4. ~~It leads to subtle differences between the two altitudes with a slightly higher fraction of particles with GF < 1.1 and a slightly lower fraction of particles with GF > 1.5 at 100 m AGL compared to 700 m AGL.~~ When comparing the results at fixed elevation ~~at but~~ different times (Fig. 5a-3a vs. b and c vs. ~~as well as~~ Fig. 4) distinct changes ~~were are~~ only observed at the lower altitude in the transition from the new ML to the fully developed ML, while little changed at the higher altitude in the transition from the RL to the fully developed ML. This ~~indicates that local aerosol sources have a stronger influence in the shallow new ML, while can be explained by the differing chemical composition of the particles in these layers, with a very strong nitrate fraction in the new ML which decreases in the fully developed ML is dominated by background aerosol, as will be discussed in more detail in Sect. 4.1.2.~~

~~Figure 5 illustrates qualitative differences for distributions which were averaged over a certain time period.~~ Even though the GF-PDFs in Fig. 3 imply externally mixed aerosol particles, this is not necessarily the case ~~at all times~~ as the average of an internally mixed aerosol with variable composition could potentially yield the same result. Due to low counting statistics highly ~~time resolved~~ time-resolved GF-PDFs are not available. For this reason,

we divide the particles in ~~different hygroscopic fractions in order~~ three hygroscopic fractions to further investigate the ~~time dependent~~ time-dependent mixing state characteristics. Measurements for  $D_{\text{dry}} = 500$  nm are classified ~~in three hygroscopicity categories: as~~ GF  $< 1.1$  (“non-hygroscopic”),  $1.1 < \text{GF} < 1.5$  (“moderately hygroscopic”) and  $\text{GF} > 1.5$  (“most hygroscopic”), which correspond to ranges of  $\kappa < 0.02$ ,  $0.02 < \kappa < 0.13$  and  $\kappa > 0.13$ , respectively. Figure 6-4 presents the temporal evolution of the number fractions of particles in these three categories together with the flight altitude. At all times, particles are simultaneously present in at least two, mostly all three hygroscopicity ranges, ~~which~~. This indicates an externally mixed aerosol throughout the flight. The moderately hygroscopic ~~particles are almost always the smallest fraction, constantly~~ fraction is mostly the smallest one, accounting for less than 20 % of all particles (light blue dots in Fig. 64). The most hygroscopic ~~particles are almost always the largest fraction~~ fraction is predominantly the largest one, accounting for  $\sim 45\text{--}85\%$  of all particles, while the non-hygroscopic ~~particles contribute~~ fraction contributes to  $\sim 9\text{--}34\%$ , whereby these values do not include the outlier. It is important to note that part of the temporal variability of the number fractions shown in Fig. 64 is caused by limited counting statistics rather than true variability of aerosol properties. However, the outlier in the fully developed ML at  $\sim 12:45$  ~~with a~~ LT with a non-hygroscopic fraction as high as 50 %, reflects truly different aerosol properties rather than just statistical noise.

Previous mixing state studies, based on hygroscopic growth ~~behavior~~ behaviour measured with HTDMAs, found similar substantial non-hygroscopic fractions in ~~airmasses~~ air masses influenced by urban areas, where externally mixed black carbon (BC) was revealed as the major contributor (see e.g. Juranyi et al., 2013; Laborde et al., 2013; Lance et al., 2013). The number size distributions of freshly emitted BC particles typically peak in the diameter range around  $\sim 100$  nm (Rose et al., 2006). Therefore, externally mixed BC is less likely to give a ~~significant~~ contribution to ~~the total number of~~ particles with a ~~diameter of 500 nm~~, ~~which is as~~ probed by the WHOPS, ~~while substantial contributions from externally mixed BC can be expected even so a substantial contribution might be detected~~ in the lower accumulation mode size range probed by e.g. HTDMAs, ~~when being~~

close to sources. Besides, externally mixed BC particles are known to have a low effective density due to their fractal-like morphology (?), and the index of refraction of BC differs substantially from that of organic and inorganic aerosol components (?). These two effects lead to a systematic bias in the GF inferred from WHOPS measurements of externally mixed BC particles. Sensitivity analysis HDMAs. Sensitivity analyses showed that it is very unlikely that non-hygroscopic externally mixed BC ~~shows up~~ particles appear at  $GF \sim 1.0-1$  in the WHOPS, ~~despite the fact that the two effects counteract each other to some extent. BC-containing particles may potentially grow into the size range probed by the WHOPS through atmospheric aging.~~ However, atmospheric ageing processes, i.e. the acquisition of condensable ~~vapors forming a~~ vapours forming a shell around the BC core. ~~This can result in large accumulation mode particles enriched in BC as previously found in the Po Valley by ?.~~ The acquisition of coatings also increases, may lead to BC-containing particles in the size range probed by the WHOPS. These processes increase the effective density of BC-containing particles ~~and makes,~~ make their effective index of refraction more similar to that of BC-free particles (Zhang et al., 2008) ~~;~~ however, the hygroscopicity increases as well and enhance their hygroscopicity (e.g. Tritscher et al., 2011; Laborde et al., 2013). ~~Thus, internally mixed~~ A combination of these effects might result in detection of aged BC-containing particles ~~may give a significant contribution to particles with diameters of  $\sim 500$  at GF ; however, they are expected to be moderately hygroscopic and they should be detected as such by the WHOPS.~~ Based on the above arguments, we consider it unlikely that the  $\sim 1$ . Other possible contributors for the non-hygroscopic particles measured by the WHOPS ~~are for the most part BC-containing particles. Besides,~~ could be non-BC products of biomass burning, from biomass burning like tar balls (Pósfai et al., 2004; Alexander et al., 2008) ~~are also known to exist up to diameters of  $\sim 500$ . Their optical properties differ significantly from those of BC leading to scattering cross sections similar to those for particles with  $m = 1.43$  (effective index of refraction measured in this study). Therefore, also these tar balls could describe a fraction of the non-hygroscopic particles.~~

Mineral dust is another substance known to be non-hygroscopic, mineral dust (e.g. Herich et al., 2008, 2009) ~~;~~ though it can potentially become more hygroscopic through

atmospheric aging processes such as e.g. heterogeneous chemical reactions at the particle surface (?). Fresh Saharan dust sampled at Cape Verde was related to the non-hygroscopic particle mode (?). Aged Saharan dust, observed at the high-alpine site Jungfraujoch after long-range transport, was still reported to be non-hygroscopic using HTDMA and humidified nephelometry techniques (?; ?). The number size distribution of mineral dust particles is known to extend down to sub-micrometer sizes (or biological material such as virus particles, bacteria or fungal spores (e.g. ?) and therefore into the range of the WHOPS measurements. The hygroscopic growth factor of externally mixed dust particles could hypothetically explain our non-hygroscopic fraction. Dust particles have an index of refraction that is approximately  $1.53 - 0.08i$  (?), thus leading to similar scattering cross sections at  $D_{dry} = 500\text{ nm}$  as for the effective index of refraction determined for the whole aerosol population ( $m = 1.43$ ). Influence of Saharan dust intrusions all the way down to the lowest atmospheric layers near the SPC site can be expected for the day of the Zeppelin flight reported here according to the Després et al., 2012). Mineral dust is indeed a candidate as the HYSPLIT model for Saharan Dust Intrusions (specific analysis by "Spain HYSPLIT"; <http://www.ciecem.uhu.es/hysplit/>; not presented here). Thus, mineral dust is a likely explanation for the non-hygroscopic particles (at  $D_{dry} = 500\text{ nm}$ ) detected by the WHOPS in the Po Valley.

A last potential candidate for non-hygroscopic particles is biological material, which is non-hygroscopic and exists in the sub-micron size range (e.g. Després et al., 2012). Virus particles, bacteria, fungal spores and plant pollen are commonly ranked among these species. The optical properties vary considerably between different types of bio-aerosol. Values between 1.397–1.53 for the real part of the index of refraction are reported in the literature (?; ?; ?). This is close to predicted Saharan dust all the way down to the lowest atmospheric layer (100 m AGL) near the SPC site. However, we do not have adequate data to further investigate the source or chemical composition of the effective index of refraction applied in this study for the WHOPS data analysis, such that non-hygroscopic bioparticles would correctly be measured at a GF of  $\sim 1$  by the WHOPS fraction.

#### 4.1.2 ~~Hygroscopicity comparison between airborne WHOPS and ground-based HTDMA measurements~~

The ground stations were equipped with HTDMAs which measured ~~The SPC ground station was equipped with an HTDMA to measure~~ GF-PDFs at  $RH = 90\%$  in the dry diameter range below ~~230~~200 nm. ~~Since SPC is located in the valley At the location of SPC~~ only the new ML and later the fully developed ML could be measured, while MTC, situated on a mountain, probes air in the RL in the morning and the fully developed ML later in the day. The fact that the fully developed ML extends to altitudes higher than the MTC site was previously reported by ?. ~~Figure ?? provides the WHOPS and HTDMA probed. Figure 5 compares the~~ GF-PDFs measured on the Zeppelin, in SPC and MTC divided into results at the ground site (HTDMA) with the airborne data from 100 m AGL (WHOPS) separately for the new ML, the RL and the fully developed ML. Note that the WHOPS cannot reliably detect particles with  $GF < 1.5$  and  $D_{dry} = 300$  nm, as described in ?Rosati et al. (2015a). Thus, no information is available from the WHOPS ~~measurement measurements~~ on the number fraction and properties of the 300 nm particles with  $GF < 1.5$ .

Figure ??a illustrates the averaged GF-PDFs in the newly forming ML. A first comparison between the ~~Comparing the~~ two dry sizes probed by the WHOPS reveals a ~~in the newly forming ML (red line and blue bars in Fig. 5a) reveals a~~ strong resemblance of the GF-PDF shapes for  $GF > 1.5$ , except for a small shift towards larger GFs for the smaller particle size. This suggests that hygroscopic particles of these two sizes have a similar chemical composition. When, however, comparing to the ~~HTDMA<sub>SPC</sub> HTDMA (yellow line)~~ obvious differences appear: The distinct mode at  $GF \sim 1$  ~~seen by the WHOPS in the WHOPS data~~ for the 500 nm particles is much smaller ~~less pronounced~~ in the HTDMA results. ~~This might be due to the fact, that possible explanations for~~ The reason might be that possible contributors to the non-hygroscopic particles (described in Sect. ??) are more probable ~~mode are different~~ for the larger size investigated by the WHOPS compared to the HTDMA size range. In addition, the dominant hygroscopic mode is centered ~~centred~~ at smaller GFs in the HTDMA GF-PDF, which causes a smaller mean GF and  $\kappa$  value compared to the WHOPS. ~~This is seen~~

in the mean  $\kappa$  values, (listed in Table 2, which have been derived from the mean GFs using Eq. (3)). It is very unlikely that these differences solely arise from the size-dependent particle composition since upper accumulation mode particles at 200 and 300 nm are expected to be similar. The chemical analysis, which will be discussed in Sect. 4.1.2, reveals a nitrate mass fraction of  $\sim 22\%$  in the non-refractory  $PM_{10}$  composition. Ammonium nitrate is semi-volatile and prone to evaporation artifacts. Gysel et al. (2007) provided strong evidence for ammonium nitrate artifacts during HTDMA measurements, which resulted in underestimated hygroscopic GFs. The HTDMAs employed in SPC and MTC featured shorter residence times in the range between 10–15 s, which should minimize nitrate evaporation losses, however, they can still not be fully excluded. GF measurements done by the WHOPS are most likely less susceptible to ammonium nitrate evaporation, as the residence time in the dry part of the instrument is lower very short due to higher flow rates. Thus, part of the difference between the ground-based SPC-HTDMA and the airborne WHOPS in the new ML could potentially be caused by artifacts in the HTDMA, which results in a small bias of measured GFs. Another possible reason could be that the particles at the ground (measured in the surface layer) and at 100 m AGL were not exactly the same due to e.g. direct influences by local emissions.

Figure 2b depicts the averaged GF-PDFs in the RL. For  $GF > 1.5$  the WHOPS results for both sizes agree well, again indicating similar chemical composition of particles with dry diameters of 300 and 500 nm. The GF-PDFs measured by the HTDMA at the MTC site are similar to the results from the airborne WHOPS measurements. This hypothesis is also supported by measurements of the particles' optical properties on this flight day, presented in Rosati et al. (2015b). A comparison of the scattering and extinction coefficients between the airborne and ground-based measurements, shown in Fig. 4 and 8 in the stated paper, respectively, also illustrate differences between the two altitudes, which are independent of the hygroscopicity measurements and associated artefacts. Differences in the fine structure of the GF-PDFs should not be over-interpreted, as they are influenced by the data inversion algorithms for both instruments. Larger discrepancies are visible for the non-hygroscopic

fraction. The HTDMA at MTC measured the GF-PDF for particles with a diameter of 230, which could be too small to have a substantial fraction of dust or biological particles that are known to be non-hygroscopic and more abundant at larger sizes. Besides, MTC is situated at a much higher elevation than the Zeppelin NT was flying and its location is approximately 100 southeast of SPC, therefore different airmasses could be present which lead to additional discrepancies.

Figure 5b displays the results for the fully developed ML. ~~There is again little difference~~ Little variation can be seen between the results for the two sizes probed by the WHOPS, ~~as for the other two layers. The fully developed ML was probed.~~ The GF-PDF measured by the HTDMA at both sites is quite similar to the one found in the newly forming ML and therefore yields comparable mean hygroscopicity values (listed in Table 2). The number fraction of non-hygroscopic particles is again smaller compared to the WHOPS, ~~while the results.~~ The dominant hygroscopic mode is similar except for small differences in its position, which is also reflected in the mean  $\kappa$  values listed in Table 2. more alike though slightly shifted to smaller GFs in the HTDMA results. Better agreement between the ground-based and airborne data for the fully developed ML, as opposed to substantial differences within the new ML, may be caused by stronger vertical mixing, thus resulting in better vertical homogeneity.

#### 4.1.2 Composition – hygroscopicity closure

The WHOPS measurements indicate distinct differences in hygroscopic particle properties between the probed layers in the PBL. Here we examine which chemical components cause these differences and whether closure is achieved between measured particle hygroscopicity and that calculated from chemical composition. Figure 7 depicts the

#### 4.1.2 Chemical composition

Figure 6 depicts the mass fractions of carbonaceous and inorganic aerosol components in  $PM_{10}$ , as well as the mean  $PM_{10}$  mass concentrations for the SPC ground station

(Fig. 7a and b) and the altitude levels probed during the Zeppelin NT flights (Fig. 7c-f). Organic and inorganic species were always measured by an AMS, while eBC was measured by a MAAP and an aethalometer at the SPC site and on board the Zeppelin NT, respectively.

Figure 7a, c and e illustrate results for the early morning hours. At this time of day, the highest  $PM_1$  mass concentrations were measured in new ML with mean values of 22 and  $20 \mu\text{g m}^{-3}$  at the ground site and  $\sim 100$  m AGL, respectively (Figs. 6a, c and e). This is expected as most emissions from the ground, which accumulated during the night, are trapped in the new ML. The mean  $PM_1$  concentrations in the RL at  $\sim 700$  m AGL (Fig. 6c), which is decoupled from the emissions at the ground, were substantially lower ( $15 \mu\text{g m}^{-3}$ ). These vertical gradients in aerosol concentration disappeared and aerosol loadings within the ML dropped as the new ML evolved to a fully developed ML in the course of the day, which resulted in stronger dilution and better vertical mixing of fresh emissions from the ground. This is confirmed by the results of the afternoon flights, when consistently  $12-13-14 \mu\text{g m}^{-3}$  were measured at both flight levels and the ground station (Fig. 7b, d and f).

Overall, organic compounds were with 43 to 62 % by mass the largest fraction of  $PM_1$ , while the sum of inorganic species contributed between 29 and 48 % (Fig. 7). The eBC mass fraction remained constantly below 12 % and chloride was always negligible with less than 1 %. During IHP1/2 a clear difference between the mass fractions in the new ML with a high nitrate fraction of 20-22 % (Fig. 7a-6a and c), and the RL with a nitrate contribution of only 5 % (Fig. 7e) were observed. This increased nitrate fraction in the new ML can be explained by the accumulation of nitrate species over night, which are formed in the nocturnal surface layer and are then entrained into the new ML after sunrise. The drop of the nitrate mass fraction in the fully developed ML is due to volatilization of nitrate species as a result of both, increased temperature and dilution. The eBC fraction was slightly higher in the new ML compared to the RL, whereas the organics and sulfate fractions were substantially lower. During the afternoon flights (IHP4/5/6; Fig. 7b, d and f) in the fully developed ML, the differences in chemical

composition ~~between-at~~ different altitudes disappeared as they did for the aerosol loading. The mass fractions of all species were comparable at the ground and the two flight altitudes and also very similar to those in the RL probed in the morning.

Several AMS campaigns at SPC previously determined the chemical composition at ~~ground level. A~~ ground-level. A springtime campaign presented in Saarikoski et al. (2012) revealed a ~~-nitrate~~ peak during the break-up of the nocturnal boundary layer, consistent with our observations, suggesting local sources of nitrate. In contrast, ~~sulfate~~ sulphate concentrations stayed constant throughout the day, thus indicating small local influence, again consistent with our results. Previous airborne AMS measurements showed high ammonium nitrate concentrations in the Po Valley plume, thus indicating large nitrogen oxide and ~~ammonium~~ ammonia sources in the Po Valley region (Crosier et al., 2007).

A

#### 4.1.3 Hygroscopicity results from airborne and ground-based measurements

A quantitative closure study between measured chemical composition and hygroscopic ~~properties was done with the approach~~ growth was performed as described in Sect. 3. ~~For this purpose, Eq. Figure 7 illustrates the time series of the hygroscopicity parameter as deduced from the WHOPS measurements (violet points) and the chemical composition data (blue diamonds) on board the Zeppelin NT. During IHP1/2 (5) was used to calculated the~~ ~ 08:30–10:00 LT) a clear vertical trend is seen by both techniques: Higher hygroscopicity values are found close to the ground (~100 m AGL) compared to those at elevated altitudes of ~ 700 m AGL. This altitude dependence implies different layers with distinct aerosol properties, consistent with the vertical layering of the PBL indicated by  $\Theta$  and the mixing layer height illustrated in Fig. 2. In the new ML the mean  $\kappa_{\text{WHOPS}}$  is found to be  $0.34 \pm 0.12$ , while  $\kappa_{\text{chem}}$  amounts to  $0.26 \pm 0.06$ . These values exceed considerably the values in the RL where a  $\kappa$  value corresponding to the measured chemical composition from AMS and aethalometer. Resulting  $\kappa$  values averaged for the different layers are listed in Table 2. of  $0.19 \pm 0.07$  and  $0.22 \pm 0.05$  was found by the WHOPS and chemical composition, respectively. Closure is achieved between  $\kappa_{\text{WHOPS}}$  and  $\kappa_{\text{chem}}$ , which agree

within uncertainty. Inorganic species are strongly hygroscopic, while organics and BC are only weakly hygroscopic and non-hygroscopic, respectively (Table 1). Consequently As a consequence, the hygroscopicity of a ~~mixture increases~~ mixture is expected to increase with increasing inorganic fraction. ~~This explains why the highest composition-derived  $\kappa$  values are obtained for~~ Indeed, the higher GF in the new ML (44–48 inorganic mass fraction); both for the ground-based and airborne measurements at 100, while those for the RL (35 compared to the RL can be attributed to a higher inorganic mass fraction ) and the fully developed ML (29–30 inorganic mass fraction) are distinctly lower. The differences in (45% compared to 30%; Fig. 6). The variation of the inorganic fraction between the different layers are mainly caused itself is driven by the variability of the nitrate mass fraction. Thus, the high nitrate mass fraction in the new ML is responsible for the increased particle hygroscopicity in this layer. Figure 4 (time-resolved data)

After ~11:00 LT further profiles were performed. During IHP3 and IHP4 the ML had not reached its maximum height and could, therefore, be influenced by the RL or by the entrainment zone between the layers. Therefore, we discuss only the results from IHP5 and IHP6 (~ 12:30–14:00 LT), when the ML was fully developed and reached above the upper flight level. In the fully developed ML, hygroscopicity results show less variability with no clear dependence on altitude. The observed hygroscopicity values amount to  $\kappa_{\text{WHOPS}} = 0.14 \pm 0.06$  and  $\kappa_{\text{chem}} = 0.19 \pm 0.04$  at 100 m AGL and  $\kappa_{\text{WHOPS}} = 0.20 \pm 0.08$  and  $\kappa_{\text{chem}} = 0.20 \pm 0.04$  at 700 m AGL, which is again closure within uncertainty (Fig. 7 and Table 2 (mean values for layers) further show that closure between composition-derived  $\kappa$  values–). These values appear well comparable to those measured in the RL and were characterized by a similar inorganic mass fraction of 30–34%. An exception is the measurement taken at around 12:45 LT and WHOPS-derived 100 m AGL, when the mean  $\kappa$  values is achieved within experimental uncertainty was considerably lower due to a strongly increased fraction of non-hygroscopic particles likely originating from a local source (see Fig. 4). Apart from this singular observation, the particle hygroscopic properties were homogeneous across all altitudes in the afternoon. This is in concordance with the analysis of  $\Theta$  and the mixing layer height displayed in Fig. 2 which indicate the presence of a

single layer below  $\sim 700$  m AGL. Once the fully developed ML is present vertical differences in aerosol properties are expected to disappear. Only altitude dependent changes in temperature and RH can lead to alterations of the particles e.g. through phase partitioning effects.

The  $\kappa$  values derived from the HTDMA measurement hygroscopicity parameters inferred from the chemical composition measurements at the SPC site are significantly lower than the corresponding composition-derived  $\kappa$  values for the measurements in the new ML ground site.  $\kappa_{\text{chem-SPC}}$  are  $0.31 \pm 0.08$  and  $0.21 \pm 0.06$  for the new ML and the fully developed ML, respectively (Table 2). This disagreement might be caused as the result of ammonium nitrate evaporation artifacts in the HTDMA, as already speculated in Sect. ???. During previous measurements decrease of hygroscopicity is caused by the decreased nitrate and with that also total inorganic mass fraction, as also seen from the airborne measurements. However, the HTDMA at the SPC site, Bialek et al. (2014) observed peaks of the nitrate mass fraction without a concurrent peak in particle hygroscopicity. It was suggested that this might have been due to the presence of organo-nitrates or organic coating on particles, which both lead to low hygroscopic growth. However, also evaporation artifacts could potentially play a role. did not observe this decrease in hygroscopicity and the HTDMA-derived  $\kappa$  value was significantly lower than the airborne and ground-based  $\kappa_{\text{chem}}$  in the new ML. This disagreement might be a result of ammonium nitrate evaporation artefacts in the dry section of the HTDMA as already mentioned above.

#### 4.1.4 Comparison of hygroscopicity results with previous campaigns

The aerosol hygroscopic properties reported in this study were measured on 20 June 2012, a near SPC during a predominately cloudless summer day with low wind speeds. To better understand whether this case study is representative of typical conditions in the Po Valley in the summer season, a comparison is made with literature data from previous campaigns that covered longer time periods. Mean  $\kappa$  values determined with different methods and at different sites are shown in Fig. 8. Only measurements taken in the fully developed ML are included in the averages (for the literature data, the time

of day between 12:00 and 17:00 is assumed to be representative of the fully developed ML. Vertical gradients of aerosol properties are minimal in the fully developed ML. This ensures comparability between the measurements taken at different altitudes. Previous hygroscopicity measurements in the summer season were carried out with HTDMAs at MTC (?), at The Po Valley has already been investigated with regard to hygroscopicity at ground-level and literature data is reported for SPC (Bialek et al., 2014) and Ispra (Adam et al., 2012). Ispra is (Adam et al., 2012; located at 45°49' N, 8°38' E at 209 m a.s.l. approximately 60 km north of Milan at the north-end of the Po Valley). In both locations measurements were carried out with HTDMAs. To compare our case study with these previous results only data recorded in the fully developed ML is chosen, where vertical gradients of aerosol properties are minimal. For the literature data, the time of day between 12:00 and 17:00 LT is assumed to be representative of the fully developed ML.

Mean  $\kappa$  values from the different campaigns are shown in Fig. 8. All mean  $\kappa$  values in SPC, shown in Fig. 8 fall into the rather, fall into a very narrow range between 0.18 and 0.28; independent of location, 0.18 and 0.20, independent on method and dry sizes. The value of  $\kappa$  in Ispra is somewhat higher but still commensurable with the SPC results. These medium-low  $\kappa$  values can be explained with are typical for mixtures of ammonium salts and organic fractions of 50% or larger (see e.g. Fig. 7). Additionally, the 6). The temporal variability is small, such that the range  $\kappa = 0.11 - 0.33$  and the range  $\kappa = 0.11 - 0.33$  includes all data points within  $\pm 1SD$   $\pm 1SD$  of the mean values. This means that a We conclude that a  $\kappa$  value of  $\sim 0.22$  is a good approximation for the aerosol hygroscopic properties in the fully developed ML in the Po Valley in summertime. Such approximations can for example be useful, A value of  $\kappa = 0.22$  should be used when estimating the cloud condensation nuclei activity at times or sites without concurrent in absence of hygroscopicity or composition measurements. A closer look into the spatial pattern reveals Note, that the summertime aerosol at Ispra and MTC, at the northern edge of the Po Valley, seems to be slightly more hygroscopic than in the SPC area.

The close agreement between aerosol hygroscopic properties observed in this study with available literature data from previous studies suggests that our case study is indeed

representative of the Po Valley summertime aerosol. Combined with the results shown in Figs. 4–?? follows that ground-based measurements taken in the afternoon at sites in the valley plain are representative of aerosol properties over the whole vertical extent of the fully developed ML, whereas they may be representative of only a shallow layer at other times of day.

## 4.2 Netherlands campaign

Here we present the findings of a Zeppelin flight on 24 May 2012 near the CESAR ground station in the Netherlands (Fig. ??1). We performed a set of height profiles between approximately 11:00 and 14:00 LT, including longer legs at the following ~~for four~~ altitudes:  $\sim 100$ , 300, 500 and 700 m AGL. The first height profile (NHP1) was performed from  $\sim 11:30$ –12:45 LT and the second height profile (NHP2) from  $\sim 12:45$ –13:50 LT. The wind direction was predominately from north-east and the wind speed on average between  $\sim 3$  and  $\sim 4.5 \text{ m s}^{-1}$ . Therefore, the probed ~~airmasses were most probably air masses were most likely~~ originating from the continent ~~and likely~~ with some local/regional influence due to low wind speeds. Figure 2–9 displays the time series of the flight altitude, estimated mixing layer height, ~~relative humidity RH~~ and potential temperature ( $\Theta$ ). During the whole flight relatively high RH dominated (40–80 %). The pattern of  $\Theta$  reveals a vertical layering during ~~the first profile NHP1~~, showing a clear difference at  $\sim 700 \text{ m AGL}$  compared to the lower altitudes. ~~A similar but less pronounced vertical structure in the potential temperature can also be seen at the beginning of the second profile. A very similar development of the~~ This layering is consistent with the estimated mixing layer height ~~is captured by data calculated from a Ceilometer. This indicates that indeed inferred from the ceilometer data (grey shading in Fig. 9), indicating that~~ we managed to fly above the new ML during ~~the first profile NHP1~~ at 700 m AGL. However, since the change in  $\Theta$  and the vertical distance to the ~~ML estimated mixing layer~~ height are rather small, it is not clear whether the RL or the entrainment zone between the new ML and the RL were probed. ~~The second profile~~ A similar but less pronounced vertical structure in  $\Theta$  can also be seen during NHP2 at 700 ~~was most likely in~~ m AGL. Again, most likely the threshold range between ~~the~~ new ML, entrainment

zone and RL were probed at this altitude. In contrast to the flights in Italy, the ~~ones~~ flights in the Netherlands started later in the day and therefore the ML had more time to develop. This is one reason why most measurements during this flight were within the new ML while none of them was for certain in the RL.

#### 4.2.1 ~~Hygroscopicity and mixing state inferred from WHOPS measurements~~ Chemical composition

~~Figure ?? shows particle hygroscopicity measured by the WHOPS. The same flight pattern was repeated once. No substantial differences can be observed neither as a function of altitude nor of time. Absence of vertical gradients is expected for all measurements at altitudes of 500~~ Unfortunately, the airborne HR-ToF-AMS data is not available for this Zeppelin flight due to an instrument failure. At the Cabauw ground site an HR-ToF-AMS and MAAP were successfully deployed to measure the composition of  $PM_{10}$ . A mean  $PM_{10}$  concentration of 15 or lower, which have been shown to be within the almost fully to fully developed ML. The fact that the first measurement at  $700 \mu\text{g m}^{-3}$  was measured during NHP1, which decreased to 12 is also similar to all others indicates either that the entrainment zone between the new ML and RL was probed or that the aerosol properties in the RL were similar to those in the new ML. As no temporal trend was observed, Table 3 presents directly mean values averaged over both profiles for each flight altitude separately. ~~GF values between 1.84 and 1.93 at RH~~  $\mu\text{g m}^{-3}$  during NHP2 (Fig. 10). This small variation is consistent with the findings from  $\Theta$  and the ceilometer indicating that the mixing layer was almost fully developed already during NHP1. Likewise, the composition also varied only little in time. Organic matter was the dominant mass fraction describing 47 and 51 % of the aerosol, during NHP1 and NHP2, respectively. During both profiles nitrate constituted the second most abundant fraction accounting for 24 and 17 95%, while sulphate made up 10 and 13 % ~~were measured, which corresponds to~~ and eBC 7 and 9 % of the total mass, during NHP1 and NHP2, respectively.

## 4.2.2 Hygroscopicity results and mixing state

The airborne hygroscopicity results from the WHOPS instrument are presented as GF-PDFs (Fig. 11), number fractions in different hygroscopicity classes (Fig. 12) and hygroscopicity parameters ( $\kappa$  values between 0.25–0.29). It seems that particle hygroscopicity increases slightly but systematically with increasing altitude. One possible explanation for this could be temperature dependent partitioning of ammonium nitrate (which is hygroscopic; Fig. 13). All three figures show little variability of the aerosol hygroscopic properties with altitude. This is expected given the previously discussed layering of the PBL, which indicates that mainly the fully developed ML was probed. Small changes in aerosol hygroscopicity are also in agreement with almost constant chemical composition at the ground site (Fig. 10). Furthermore, composition-hygroscopicity closure is achieved, i.e. the composition derived  $\kappa$  ( $\kappa_{\text{chem}} = 0.28 \pm 0.06$ ) agrees well with the GF-derived  $\kappa$  ( $\kappa_{\text{WHOPS}} = 0.25 - 0.29$ ; see Table 1). Morgan et al. (2010a) previously reported an increasing nitrate fraction with increasing altitude (3). This good agreement should be taken with some care, as for example sea salt can potentially play a role in the Cabauw area, which was observed between measurements at the ground site and  $\sim 2000$  is not quantitatively detected by the HR-ToF-AMS. However, in the next section we will show that the sea salt influence was likely low during the flight presented in this study.

The appearance of particles with GF(95%) across the whole range from around 0.9 to 3.2 in the GF-PDFs for a dry particle diameter of 500 nm averaged for each altitude are presented in Fig. 9. GF-PDFs between a GF of 0.9 up to 3.2 are visible. This implies the presence of particles that differ substantially in their hygroscopic properties between each other. The GF-PDFs measured at the four altitudes are very similar. This shows that also the aerosol mixing state is equal within the ML, indicates that the aerosol was externally mixed (Fig. 11). In order to further investigate the time evolution of the mixing state, the GF-PDFs were split into three hygroscopicity classes, and the corresponding number fractions of particles are shown in Fig. 11 (the hygroscopicity classes were equally chosen as equivalent to the ranges chosen for the flight data from Italy shown in Fig. 6 in

the Po Valley). The aerosol was externally mixed during the whole flight with very stable number fractions in each hygroscopicity class at any time and altitude. The dominant fraction of particles was more hygroscopic ( $GF > 1.5$ ) making up 82 % (72–89 %) of the particles, while 12 % (7–18 %) were non-hygroscopic ( $GF < 1.1$ ) and only 6 % (1–9 %) of the particles fell into the range  $1.1 < GF < 1.5$ . As many as 12 (Fig. 12). The number fraction of non-hygroscopic particles on average is, despite being only observed in Cabauw was about half of the corresponding fraction observed in the Po Valley, higher than expected. Potential candidates for these particles are dust, biological material or tar balls as already discussed in Sect. ???. The influence of dust should be smaller in the Netherlands compared. Despite being only half, it was still larger than expected as no evidence for Saharan dust influence was observed in contrast to the Po Valley. We do not have any evidence of specific influence from potential sources of tar balls. This would leave biological material as an important contributor to the non-hygroscopic particles at  $D_{dry} = 500$  nm. However, we do not have any supporting data to corroborate or discard this speculation.

### 4.2.3 Composition – hygroscopicity closure

Unfortunately, the AMS data is not available for this Zeppelin flight due to an instrument failure. However, at the ground site an AMS measurement was successfully performed. The chemical composition results at the ground station in Cabauw (see Fig. 12) indicate organics as the major fraction describing 47 and 51 further assess whether it was dust or whether other candidates such as biological material, tar balls or BC containing particles contributed to the non-hygroscopic fraction (see also Sect. 4.1.1). The variability of aerosol hygroscopicity with altitude was found to be small but consistently decreasing from  $GF(95\%)$  values of  $1.93 \pm 0.19$  at 700 of the aerosol, during NHP1 and NHP2, respectively. During both profiles nitrate constitutes the second most abundant fraction accounting for 24 and 17, while sulfate makes up 10 and 13 of the total mass. The eBC fraction measured at the ground contributes to 7–9 of the total mass.

The approach described in Sect. 3 is used to compare the ground based composition measurements with the airborne hygroscopicity measurements in a quantitative manner.

For this purpose, Eq. (5) is used to calculate the  $\kappa$  value corresponding to the measured chemical composition. The resulting  $\kappa$  value is 0.28, which agrees well within uncertainty with the WHOPS-derived  $\kappa$  value of 0.25 in the lowermost flight level at  $\sim 100$  m AGL to  $1.84 \pm 0.18$  at  $\sim 100$  m AGL (see also Table 3). Such good agreement cannot necessarily be expected, as for example fresh and aged sea salt components are not quantitatively detected by the AMS. However, in the next section we show that Figure 13 shows that this trend applies for every flight altitude change after  $\sim 12:15$  LT. One possible explanation for this could be temperature dependent partitioning of ammonium nitrate (which is strongly hygroscopic; see Table 1). Morgan et al. (2010a) previously reported an increasing nitrate fraction with increasing altitude in the Cabauw area, which was observed between measurements at the ground site and  $\sim 2000$  m AGL.

In summary, the sea salt influence was likely low during the flight presented in this study. Convective mixing within the fully developed ML leads to almost constant aerosol hygroscopicity as a function of altitude except for small effects from potential repartitioning of semi-volatile species. This shows that ground-based measurements provide valid information about the aerosol properties for the well-mixed part of the column aloft.

### 4.2.3 Comparison of hygroscopicity results with previous campaigns

Airborne hygroscopicity measurements from a different Zeppelin flight in on 22 May 2012 close to Cabauw have previously been reported in (?) as a first example of airborne operation of the WHOPS Rosati et al. (2015a). This flight was characterized by sampling two distinct air mass types with and without substantial influence of sea salt aerosol. Figure ?? provides a comparison of the results from (?) with those of this study. The general features of the three 14 illustrates a GF-PDF comparison from results from 22 and 24 May 2012 (Rosati et al., 2015a). Generally speaking, the GF-PDFs are comparable, all featuring a similar in that all feature a minor peak at  $GF \sim 1$  and a dominant broad mode peaking dominant peak in the range  $GF = 1.9\text{--}2.5$ . A clear increase of particles with  $GF > 2.5$  was observed by (?) for the air mass on May 22 for the air mass with sea salt (SS) influence, as opposed to the air mass without sea salt (non-SS)

influence. The results of this study more closely resemble the latter airmass from this flight on 24 May 2012 resemble more closely the non-SS case, thus indicating that this flight was not substantially influenced by sea salt.

The aerosol hygroscopic properties reported in this study were measured in a continental airmass with likely some local/regional influence due to low wind speeds. To better understand whether this case study is representative of typical conditions in Zieger et al. (2011) presented hygroscopicity data for the Cabauw region, a comparison is made with literature data from previous campaigns. Mean  $\kappa$  values determined with different methods and for different airmass types are shown in Fig. 10. Only measurements taken in the fully developed ML are included in the averages (for the literature data, the time of day in 2009 achieved by a humidified nephelometer (“Wet-Neph”) and an HTDMA. From this campaign we selected two representative dates for SS (8 July 2009) and non-SS (14 July 2009 conditions. In order to ensure comparability only data between 12:00 and 17:00 LT is assumed to be representative of the fully developed ML). Vertical gradients of aerosol properties are minimal are included as they were all recorded in the fully developed ML. This ensures comparability between the airborne and ground based measurements. Zieger et al. (2011) determined the hygroscopic properties with both, a HTDMA and a humidified nephelometer (“Wet-Neph”). To assess differences between days with and without influence from sea salt aerosol, two days were selected here from their comprehensive data set: 8 July 2009 is representative for SS and 14 July 2009 for non-SS conditions. The airborne WHOPS measurements from (?) are also separately shown for SS and non-SS influence. The Figure 15 presents mean  $\kappa$  values determined with different methods on different days, all in the Cabauw region in the fully developed ML. The literature data in Fig. 10-15 clearly show that the aerosol at Cabauw is more hygroscopic under the influence of sea salt aerosol, with mean  $\kappa$  values between 0.33 and 0.5. The spread variability between the three methods (WHOPS, Wet-Neph and HTDMA) is partially related to the increasing sea salt fraction with increasing particle size, as shown by Zieger et al. (2011) (Zieger et al., 2011). For conditions without SS influence, literature reports lower  $\kappa$  values between 0.23 and 0.31, which matches the results of this study

well. Thus, the flight of this study can be considered to be representative of the ML in the Cabauw area when ~~airmasses~~ air masses without substantial SS influence prevail. ~~When~~ The  $\kappa$  values ~~from the overview presented~~ in Fig. ?? ~~are~~ 15 ~~can be~~ used as estimates for aerosol hygroscopicity at the Cabauw site ~~for times when no direct or indirect~~ when no hygroscopicity measurement is available, ~~then the~~. The uncertainty of the estimate can be reduced by distinguishing between air masses with and without SS influence ~~if possible~~.

## 5 Conclusions

~~The night time and the morning~~ During morning hours, the PBL is often separated ~~in layers~~ into sub-layers, which contain particles of different age and chemical history. ~~Vertical profiles of chemical composition and hygroscopic growth factors were performed to relate particle properties to the layering of the atmosphere during the development of the mixing layer. The campaigns were performed~~ Within the PEGASOS project a Zeppelin NT was deployed in the Po Valley ~~in Italy, near the ground station of San Pietro Capofiume (SPC), Italy, and~~ in the Netherlands close to Cabauw.

, permitting to investigate the evolving layers inside the PBL with regard to the aerosol particles' chemical composition, hygroscopic growth and mixing state. This unique airborne data set was further combined with concurrent ground-based measurements to get a more complete picture of the particles' properties throughout the flights. During the flight on 20 ~~June 2012 close to SPC different layers in the Po Valley, different layers in the PBL~~ could be explored: the residual layer (RL), the new mixed layer (ML) and the ~~ML when it was fully developed~~ fully developed ML. Major differences in chemical composition and hygroscopicity were found in the first hours of the day when the new ML ~~entrains~~ entrained air from the nocturnal boundary layer. During this time ~~nitrate concentrations amount to~~ nitrate concentrations represent 20% of the total aerosol mass leading to hygroscopicity parameters ( $\kappa$ ) of ~~0.34 and 0.27~~  $0.34 \pm 0.12$  and  $0.26 \pm 0.06$  measured by the WHOPS (at  $D_{\text{dry}} = 500$  nm) and retrieved from the  $PM_{10}$  chemical composition, respectively. This nitrate peak can be explained by the accumulation of nitrate species during the night which

are diluted decreases during the day by partitioning to the gas-phase and dilution in the new ML during the day.  $\kappa$  values in the RL and fully developed ML are comparable for the physical and chemical analysis approach. Both measurements yield lower values compared to the new ML around 0.19. During the last flight hours only the yielding lower values around 0.19. The fully developed ML could be probed where, which was probed during the last flight hours, showed no characteristic altitude dependence was found. Ground-based. Ground-based observations compare well to low-altitude, airborne results. Therefore, during the early development of the ML it is not possible to infer, confirming the higher  $\kappa$  values early in the morning compared to later in the day. This underlines the problematic estimation of altitude specific data from surface measurements during the development of the ML, which could not take into account different aerosol particle properties in the RL. In contrast, ground-based data can yield reasonable results for the fully developed ML. The mixing state of the aerosols was investigated using the WHOPS, revealing an external mixture over the whole day at all altitudes. The major fraction (67 %) experienced GF(95%) > 1.5, while 22 % were non-hygroscopic (GF(95%) < 1.1). There is evidence that the fraction of non-hygroscopic aerosols is associated with mineral dust and biological particles.

Airmasses in the Netherlands probed on 24 May 2012 did not feature altitude dependent aerosol properties which can be explained by the fact that in the Netherlands only the fully developed ML or the entrainment zone between ML and RL were sampled. Therefore, air masses did not feature altitude dependent aerosol properties. The hygroscopic fraction (GF(95%) > 1.5) was more pronounced than in the Po Valley amounting to 82 % of the total aerosol. Again an externally mixed aerosol was found, where 12 % of the particles showed GF(95%) < 1.1 when exposed to high RH. The mean  $\kappa$  value found by the WHOPS measurements was of 0.28, while ground based measurements yielded lower values of 0.24. These results coincided within the errors and the higher values found with the WHOPS could possibly be explained by a higher fractional contribution of semi-volatile and more hygroscopic aerosol species at higher altitudes values deduced from the WHOPS and the

ground-based chemical composition data are very similar amounting to  $0.28 \pm 0.10$  and  $0.28 \pm 0.06$ , respectively.

~~Comparing the two different sites it seems~~ When comparing results from Italy and the Netherlands it appears that the non-hygroscopic aerosol fraction ( $GF(95\%) < 1.1$ ) plays a more important role is more dominant in the Po Valley, which could be explained by enhanced Saharan dust intrusions which affect the bigger size range. ~~Hysplit are more likely to occur in Italy.~~ HYSPLIT calculations support this hypothesis observing dust intrusions even in the lowest layer of 100 m AGL on this specific flight day. On the other hand, the fraction of particles with  $GF(95\%) > 1.5$  in the fully developed ML is considerably higher in ~~Gabauw compared to the Po Valley.~~

the Netherlands. Overall chemical composition measurements feature the organics fraction as the most dominant one both in Italy and the Netherlands, describing approximately 50 % of the total aerosol mass. ~~The effective index of refraction reached values of 1.43 and 1.42 for the 500 particles in Italy and the Netherlands, respectively. This coincides well with literature data for air masses with predominant organic contribution.~~

**The Supplement related to this article is available online at [doi:10.5194/acpd-0-1-2016-supplement](https://doi.org/10.5194/acpd-0-1-2016-supplement).**

*Acknowledgements.* This work was supported by the EC project PEGASOS, funded by the European Commission under the Framework Programme 7 (FP7-ENV-2010-265148). We thank all PEGASOS participants for the excellent team work during the campaigns. Additionally we thank F. Holland for the analysis and maintenance of all meteorological and GPS data on the Zeppelin ~~and~~. ~~We also thank~~ R. Tillmann ~~for his~~, J. Bialek and C. O'Dowd for their contributions to the paper. ~~Also, Then~~ we thank I. Pap and K. Weinhold for their help in maintaining the MAAP instrument at the SPC ground site. M. Gysel was supported by the ERC under grant 615922-BLACARAT. The field work at the ground-based stations was partly funded by Regione Emilia Romagna as part of the SUPERSITO project (DRG no. 428/10). The research leading to these results has also received funding from the European Union's Seventh Framework Programme's (FP7/2007-2013) BACCHUS

project (grant agreement no. 603445). Part of the in-situ aerosol observations used in this study have received funding from the European Union Seventh Framework Programme (FP7/2007-2013) ACTRIS under grant agreement no. 262254.

## References

- 5 Adam, M., Putaud, J. P., Martins dos Santos, S., Dell'Acqua, A., and Gruening, C.: Aerosol hygroscopicity at a regional background site (Ispra) in Northern Italy, *Atmos. Chem. Phys.*, 12, 5703–5717, doi:10.5194/acp-12-5703-2012, 2012.
- Alexander, D. T. L., Crozier, P. A., and Anderson, J. R.: Brown carbon spheres in east asian outflow and their optical properties, *Science*, 321, 833–836, doi:10.1126/science.1155296, 2008.
- 10 Allan, J. D., Delia, A. E., Coe, H., Bower, K. N., Alfarra, M., Jimenez, J. L., Middlebrook, A. M., Drewnick, F., Onasch, T. B., Canagaratna, M. R., Jayne, J. T., and Worsnop, D. R.: A generalised method for the extraction of chemically resolved mass spectra from Aerodyne aerosol mass spectrometer data, *J. Aerosol Sci.*, 35, 909–922, doi:10.1016/j.jaerosci.2004.02.007, 2004.
- Angelini, F., Barnaba, F., Landi, T., Caporaso, L., and Gobbi, G.: Study of atmospheric aerosols and mixing layer by LIDAR, *Radiat. Prot. Dosim.*, 137, 275–279, 2009.
- 15 ~~Balaev, A. E., Dvoretzki, K. N., and Doubrovski, V. A.: Determination of refractive index of rod-shaped bacteria from spectral extinction measurements, *Proceedings of the SPIE*, 5068, 375–380, doi:, 2003.~~
- Bialek, J., Dall'Osto, M., Vaattovaara, P., Decesari, S., Ovadnevaite, J., Laaksonen, A., and O'Dowd, C.: Hygroscopic and chemical characterisation of Po Valley aerosol, *Atmos. Chem. Phys.*, 14, 1557–1570, doi:10.5194/acp-14-1557-2014, 2014.
- 20 Bohren, C. F. and Huffman, D. R.: *Absorption and Scattering of Light by Small Particles*, Wiley-VCH Verlag GmbH, New York, NY, USA, doi:10.1002/9783527618156.fmatter, 2007.
- ~~Bond, T. C. and Bergstrom, R. W.: Light absorption by carbonaceous particles: an investigative review, *Aerosol Sci. Tech.*, 40, 27–67, doi:, 2006.~~
- ~~Gharière, F., Cuche, E., Marquet,~~
- Boucher, O., Randall, D., Artaxo, P., Bretherton, C., Feingold, G., Forster, P., Kerminen, V.-M., Kondo, Y., Liao, H., Lohmann, U., Rasch, P., and Depeursinge, C.: Biological cell (pollen grain) refractive index tomography with digital holographic microscopy, *Proceedings of the SPIE*, 6090, p. 9008;

~~doi:;2006-Satheesh, S.K., Sherwood, S., Stevens, B. and Zhang, X.Y.: Clouds and Aerosols. In: Climate Change 2013: The Physical Science Basis. Contribution of Working Group I to the Fifth Assessment Report of the Intergovernmental Panel on Climate Change [Stocker, T.F., D. Qin, G.-K. Plattner, M. Tignor, S.K. Allen, J. Boschung, A. Nauels, Y. Xia, V. Bex and P.M. Midgley (eds.)]. Cambridge University Press, Cambridge, United Kingdom and New York, NY, USA, Chapter 7, 571–658, doi:10.1017/CBO9781107415324.016, url:www.climatechange2013.org, 2013.~~

Collaud Coen, M., Weingartner, E., Apituley, A., Ceburnis, D., Fierz-Schmidhauser, R., Flentje, H., Henzing, J. S., Jennings, S. G., Moerman, M., Petzold, A., Schmid, O., and Baltensperger, U.: Minimizing light absorption measurement artifacts of the Aethalometer: evaluation of five correction algorithms, *Atmos. Meas. Tech.*, 3, 457–474, doi:10.5194/amt-3-457-2010, 2010.

Crosier, J., Allan, J. D., Coe, H., Bower, K. N., Formenti, P., and Williams, P. I.: Chemical composition of summertime aerosol in the Po Valley (Italy), northern Adriatic and Black Sea, *Q. J. Roy. Meteor. Soc.*, 133, 61–75, doi:10.1002/qj.88, 2007.

DeCarlo, P. F., Kimmel, J. R., Trimborn, A., Northway, M. J., Jayne, J. T., Aiken, A. C., Gonin, M., Fuhrer, K., Horvath, T., Docherty, K. S., Worsnop, D. R., and Jimenez, J. L.: Field-deployable, high-resolution, time-of-flight aerosol mass spectrometer, *Anal. Chem.*, 78, 8281–8289, doi:10.1021/ac061249n, 2006.

~~Decesari, S., Allan, J., Plass-Duelmer, C., Williams, B. J., Paglione, M., Facchini, M. G., O'Dowd, C., Harrison, R. M., Gietl, J. K., Coe, H., Giulianelli, L., Gobbi, G. P., Lanconelli, C., Carbone, C., Worsnop, D., Lambe, A. T., Ahern, A. T., Moretti, F., Tagliavini, E., Elste, T., Gilge, S., Zhang, Y., and Dall'Osto, M.: Measurements of the aerosol chemical composition and mixing state in the Po Valley using multiple spectroscopic techniques, *Atmos. Chem. Phys.*, 14, 12109–12132, doi:;2014.~~

Després, V., Huffman, J., Burrows, S., Hoose, C., Safatov, A., Buryak, G., Fröhlich-Nowoisky, J., Elbert, W., Andreae, M., Pöschl, U., and Jaenicke, R.: Primary biological aerosol particles in the atmosphere: a review, *Tellus B*, 64, 15598, doi:10.3402/tellusb.v64i0.15598, 2012.

Di Giuseppe, F., Riccio, A., Caporaso, L., Bonafé, G., Gobbi, G., and Angelini, F.: Automatic detection of atmospheric boundary layer height using ceilometer backscatter data assisted by a boundary layer model, *Q. J. Roy. Meteor. Soc.*, 138, 649–663, 2012.

Duplissy, J., DeCarlo, P. F., Dommen, J., Alfarra, M. R., Metzger, A., Barmapadimos, I., Prevot, A. S. H., Weingartner, E., Tritscher, T., Gysel, M., Aiken, A. C., Jimenez, J. L., Canagaratna, M. R., Worsnop, D. R., Collins, D. R., Tomlinson, J., and Baltensperger, U.: Relating

hygroscopicity and composition of organic aerosol particulate matter, *Atmos. Chem. Phys.*, 11, 1155–1165, doi:10.5194/acp-11-1155-2011, 2011.

Ferrero, L., Castelli, M., Ferrini, B. S., Moscatelli, M., Perrone, M. G., Sangiorgi, G., D'Angelo, L., Rovelli, G., Moroni, B., Scardazza, F., Močnik, G., Bolzacchini, E., Petitta, M., and Cappelletti, D.: Impact of black carbon aerosol over Italian basin valleys: high-resolution measurements along vertical profiles, radiative forcing and heating rate, *Atmos. Chem. Phys.*, 14, 9641–9664, doi: 2014.

Fierz-Schmidhauser, R., Zieger, P., Gysel, M., Kammermann, L., DeCarlo, P. F., Baltensperger, U., and Weingartner, E.: Measured and predicted aerosol light scattering enhancement factors at the high alpine site Jungfraujoch, *Atmos. Chem. Phys.*, 10, 2319–2333, doi: 2010.

Guyon, P., Boucher, O., Graham, B., Beck, J., Mayol-Bracero, O., Roberts, G., Maenhaut, W., Artaxo, P., and Andreae, M.: Refractive index of aerosol particles over the Amazon tropical forest during LBA-EUSTACH 1999, *J. Aerosol Sci.*, 34, 883–907, doi: 2003.

Gysel, M., Crosier, J., Topping, D. O., Whitehead, J. D., Bower, K. N., Cubison, M. J., Williams, P. I., Flynn, M. J., McFiggans, G. B., and Coe, H.: Closure study between chemical composition and hygroscopic growth of aerosol particles during TORCH2, *Atmos. Chem. Phys.*, 7, 6131–6144, doi:10.5194/acp-7-6131-2007, 2007.

Gysel, M., McFiggans, G., and Coe, H.: Inversion of tandem differential mobility analyser (TDMA) measurements, *J. Aerosol Sci.*, 40, 134–151, doi:10.1016/j.jaerosci.2008.07.013, 2009.

Haefelin, M., Angelini, F., Morille, Y., Martucci, G., Frey, S., Gobbi, G., Lolli, S., O'Dowd, C., Sauvage, L., Xueref-Rémy, I., Wastine, B., and Feist, D.: Evaluation of mixing-height retrievals from automatic profiling lidars and ceilometers in view of future integrated networks in Europe, *Bound.-Lay. Meteorol.*, 143, 49–75, doi:10.1007/s10546-011-9643-z, 2012.

Hajj, M., Wauben, W., and Klein-Baltink, H.: Continuous mixing layer height determination using the LD-40 ceilometer: a feasibility study, KNMI Scientific Report 07-01, available at: [http://www.knmi.nl/publications/fulltexts/200701\\_bsikmlh\\_wr200701.pdf](http://www.knmi.nl/publications/fulltexts/200701_bsikmlh_wr200701.pdf), 2007.

[Hegg, D.A., Covert, D.S., Jonsson, H., and Covert, P.A.: An instrument for measuring size-resolved aerosol hygroscopicity at both sub- and super-micron sizes, \*Aerosol Science and Technology\*, 41, 873–883, doi:10.1080/02786820701506955, 2007.](#)

Herich, H., Kammermann, L., Gysel, M., Weingartner, E., Baltensperger, U., Lohmann, U., and Cziczo, D. J.: In situ determination of atmospheric aerosol composition as a function of hygroscopic growth, *J. Geophys. Res.-Atmos.*, 113, D16213, doi:10.1029/2008JD009954, 2008.

- Herich, H., Tritscher, T., Wiacek, A., Gysel, M., Weingartner, E., Lohmann, U., Baltensperger, U., and Cziczo, D. J.: Water uptake of clay and desert dust aerosol particles at sub- and supersaturated water vapor conditions, *Phys. Chem. Chem. Phys.*, 11, 7804–7809, doi:10.1039/b901585j, 2009.
- 5 Hersey, S. P., Sorooshian, A., Murphy, S. M., Flagan, R. C., and Seinfeld, J. H.: Aerosol hygroscopicity in the marine atmosphere: a closure study using high-time-resolution, multiple-RH DASH-SP and size-resolved C-ToF-AMS data, *Atmos. Chem. Phys.*, 9, 2543–2554, doi:10.5194/acp-9-2543-2009, 2009.
- Hersey, S. P., Craven, J. S., Metcalf, A. R., Lin, J., Latham, T., Suski, K. J., Cahill, J. F., Duong, H. T., Sorooshian, A., Jonsson, H. H., Shiraiwa, M., Zuend, A., Nenes, A., Prather, K. A., Flagan, R. C., and Seinfeld, J. H.: Composition and hygroscopicity of the Los Angeles Aerosol: CalNex, *J. Geophys. Res.-Atmos.*, 118, 3016–3036, doi:10.1002/jgrd.50307, 2013.
- ~~Holmgren, H., Sellegri, K., Hervo, M., Rose, C., Freney, E., Villani, P., and Laj, P.: Hygroscopic properties and mixing state of aerosol measured at the high-altitude site Puy de Dôme (1465 m a.s.l.), France, *Atmos. Chem. Phys.*, 14, 9537–9554, doi:, 2014.~~
- ~~IPCC: The Physical Science Basis. Contribution of Working Group I to the Fifth Assessment Report of the Intergovernmental Panel on Climate Change, Cambridge University Press, Cambridge, UK and New York, NY, USA, 2013.~~
- 15 Jurányi, Z., Tritscher, T., Gysel, M., Laborde, M., Gomes, L., Roberts, G., Baltensperger, U., and Weingartner, E.: Hygroscopic mixing state of urban aerosol derived from size-resolved cloud condensation nuclei measurements during the MEGAPOLI campaign in Paris, *Atmos. Chem. Phys.*, 13, 6431–6446, doi:10.5194/acp-13-6431-2013, 2013.
- Kamilli, K. A., Poulain, L., Held, A., Nowak, A., Birmili, W., and Wiedensohler, A.: Hygroscopic properties of the Paris urban aerosol in relation to its chemical composition, *Atmos. Chem. Phys.*, 14, 737–749, doi:10.5194/acp-14-737-2014, 2014.
- 25 Kammermann, L., Gysel, M., Weingartner, E., and Baltensperger, U.: 13-month climatology of the aerosol hygroscopicity at the free tropospheric site Jungfraujoch (3580 m a.s.l.), *Atmos. Chem. Phys.*, 10, 10717–10732, doi:10.5194/acp-10-10717-2010, 2010.
- ~~Kim, H. and Paulson, S. E.: Real refractive indices and volatility of secondary organic aerosol generated from photooxidation and ozonolysis of limonene,  $\alpha$ -pinene and toluene, *Atmos. Chem. Phys.*, 13, 7711–7723, doi:, 2013.~~
- 30 Kuwata, M., Zorn, S. R., and Martin, S. T.: Using elemental ratios to predict the density of organic material composed of carbon, hydrogen, and oxygen, *Environ. Sci. Technol.*, 46, 787–794, doi:10.1021/es202525q, 2012.

- Laborde, M., Crippa, M., Tritscher, T., Jurányi, Z., Decarlo, P. F., Temime-Roussel, B., Marchand, N., Eckhardt, S., Stohl, A., Baltensperger, U., Prévôt, A. S. H., Weingartner, E., and Gysel, M.: Black carbon physical properties and mixing state in the European megacity Paris, *Atmos. Chem. Phys.*, 13, 5831–5856, doi:10.5194/acp-13-5831-2013, 2013.
- 5 Lance, S., Raatikainen, T., Onasch, T. B., Worsnop, D. R., Yu, X.-Y., Alexander, M. L., Stolzenburg, M. R., McMurry, P. H., Smith, J. N., and Nenes, A.: Aerosol mixing state, hygroscopic growth and cloud activation efficiency during MIRAGE 2006, *Atmos. Chem. Phys.*, 13, 5049–5062, doi:10.5194/acp-13-5049-2013, 2013.
- ~~Limsui, D., Carr, A. K., Thomas, M. E., Boggs, N. T., and Joseph, R. I.: Refractive index measurement of biological particles in visible region, *Proceedings of the SPIE*, 6954, 69540X-69540X-7, doi:, 2008.~~
- 10 Liu, B. Y. H., Pui, D. Y. H., Whitby, K. T., Kittelson, D. B., Kousaka, Y., and McKenzie, R. L.: Aerosol mobility chromatograph – new detector for sulfuric – acid aerosols, *Atmos. Environ.*, 12, 99–104, doi:10.1016/0004-6981(78)90192-0, 1978.
- ~~Mahowald, N., Albani, S., Kok, J. F., Engelstaeder, S., Scanza, R., Ward, D. S., and Flanner, M. G.: The size distribution of desert dust aerosols and its impact on the Earth system, *Aeolian Research*, 15, 53–71, doi:, 2014.~~
- 15 McMurry, P. H. and Stolzenburg, M. R.: On the sensitivity of particle-size to relative humidity for los angeles aerosols, *Atmos. Environ.*, 23, 497–507, doi:10.1016/0004-6981(89)90593-3, 1989.
- 20 Middlebrook, A. M., Bahreini, R., Jimenez, J. L., and Canagaratna, M. R.: Evaluation of composition-dependent collection efficiencies for the Aerodyne aerosol mass spectrometer using field data, *Aerosol Sci. Tech.*, 46, 258–271, doi:10.1080/02786826.2011.620041, 2012.
- Mie, G.: Beiträge zur Optik trüber Medien, speziell kolloidaler Metallösungen, *Annalen der Physik*, 330, 377–445, doi:10.1002/andp.19083300302, 1908.
- 25 Morgan, W. T., Allan, J. D., Bower, K. N., Capes, G., Crosier, J., Williams, P. I., and Coe, H.: Vertical distribution of sub-micron aerosol chemical composition from North-Western Europe and the North-East Atlantic, *Atmos. Chem. Phys.*, 9, 5389–5401, doi:10.5194/acp-9-5389-2009, 2009.
- Morgan, W. T., Allan, J. D., Bower, K. N., Esselborn, M., Harris, B., Henzing, J. S., Highwood, E. J., Kiendler-Scharr, A., McMeeking, G. R., Mensah, A. A., Northway, M. J., Osborne, S., Williams, P. I., Krejci, R., and Coe, H.: Enhancement of the aerosol direct radiative effect by semi-volatile aerosol components: airborne measurements in North-Western Europe, *Atmos. Chem. Phys.*, 10, 8151–8171, doi:10.5194/acp-10-8151-2010, 2010a.
- 30

- Morgan, W. T., Allan, J. D., Bower, K. N., Highwood, E. J., Liu, D., McMeeking, G. R., Northway, M. J., Williams, P. I., Krejci, R., and Coe, H.: Airborne measurements of the spatial distribution of aerosol chemical composition across Europe and evolution of the organic fraction, *Atmos. Chem. Phys.*, 10, 4065–4083, doi:10.5194/acp-10-4065-2010, 2010b.
- 5 Müller, T., Henzing, J. S., de Leeuw, G., Wiedensohler, A., Alastuey, A., Angelov, H., Bizjak, M., Collaud Coen, M., Engström, J. E., Gruening, C., Hillamo, R., Hoffer, A., Imre, K., Ivanow, P., Jennings, G., Sun, J. Y., Kalivitis, N., Karlsson, H., Komppula, M., Laj, P., Li, S.-M., Lunder, C., Marinoni, A., Martins dos Santos, S., Moerman, M., Nowak, A., Ogren, J. A., Petzold, A., Pichon, J. M., Rodriguez, S., Sharma, S., Sheridan, P. J., Teinilä, K., Tuch, T., Viana, M., Virkkula, A., Weingartner, E., Wilhelm, R., and Wang, Y. Q.: Characterization and intercomparison of aerosol absorption photometers: result of two intercomparison workshops, *Atmos. Meas. Tech.*, 4, 245–268, doi:10.5194/amt-4-245-2011, 2011.
- 10 Petters, M. D. and Kreidenweis, S. M.: A single parameter representation of hygroscopic growth and cloud condensation nucleus activity, *Atmos. Chem. Phys.*, 7, 1961–1971, doi:10.5194/acp-7-1961-2007, 2007.
- 15 Petzold, A., and Schönlinner, M.: Multi-angle absorption photometry a new method for the measurement of aerosol light absorption and atmospheric black carbon, *J. Aerosol Sci.*, 35, 421–441, doi:10.1016/j.jaerosci.2003.09.005, 2004.
- Petzold, A., Schloesser, H., Sheridan, P., Arnott, W., Ogren, J., and Virkkula, A.: Evaluation of multi-angle absorption photometry for measuring aerosol light absorption, *Aerosol Sci. Tech.*, 39, 40–51, doi:10.1080/027868290901945, 2005.
- 20 Pratt, K. A. and Prather, K. A.: Aircraft measurements of vertical profiles of aerosol mixing states, *J. Geophys. Res.-Atmos.*, 115, D11305, doi:10.1029/2009JD013150, 2010.
- Pósfai, M., Gelencsér, A., Simonics, R., Arató, K., Li, J., Hobbs, P. V., and Buseck, P. R.: Atmospheric tar balls: Particles from biomass and biofuel burning, *J. Geophys. Res.-Atmos.*, 109, D06213, doi:10.1029/2003JD004169, 2004.
- 25 Putaud, J.-P., Dingenen, R. V., Alastuey, A., Bauer, H., Birmili, W., Cyrys, J., Flentje, H., Fuzzi, S., Gehrig, R., Hansson, H., Harrison, R., Herrmann, H., Hitztenberger, R., Hüglin, C., Jones, A., Kasper-Giebl, A., Kiss, G., Kousa, A., Kuhlbusch, T., Löschau, G., Maenhaut, W., Molnar, A., Moreno, T., Pekkanen, J., Perrino, C., Pitz, M., Puxbaum, H., Querol, X., Rodriguez, S., Salma, I., Schwarz, J., Smolik, J., Schneider, J., Spindler, G., ten Brink, H., Tursic, J., Viana, M., Wiedensohler, A., and Raes, F.: A European aerosol phenomenology – 3: Physical and chemical char-
- 30

- acteristics of particulate matter from 60 rural, urban, and kerbside sites across Europe, *Atmos. Environ.*, **44**, 1308–1320, doi:10.1016/j.atmosenv.2009.12.011, 2010.
- Rosati, B., Wehrle, G., Gysel, M., Zieger, P., Baltensperger, U., and Weingartner, E.: The white-light humidified optical particle spectrometer (WHOPS) – a novel airborne system to characterize aerosol hygroscopicity, *Atmos. Meas. Tech.*, **8**, 921–939, doi:10.5194/amt-8-921-2015, [2015](#), [2015a](#).
- [Rosati, B., Herrmann, E., Bucci, S., Fierli, F., Cairo, F., Gysel, M., Tillmann, R., Größ, J., Gobbi, G., P. Di Liberto, L., Di Donfrancesco, G., Wiedensohler, A., Weingartner, E., Virtanen, A., Mentel, T. F., and Baltensperger, U.: Comparison of vertical aerosol extinction coefficients from in-situ and LIDAR measurements, \*Atmos. Chem. Phys. Discuss.\*, \*\*15\*\*, 18609-18651, doi:10.5194/acpd-15-18609-2015, \[2015b\]\(#\).](#)
- Rose, D., Wehner, B., Ketzler, M., Engler, C., Voigtländer, J., Tuch, T., and Wiedensohler, A.: Atmospheric number size distributions of soot particles and estimation of emission factors, *Atmos. Chem. Phys.*, **6**, 1021–1031, doi:10.5194/acp-6-1021-2006, 2006.
- Rubach, F.: Aerosol Processes in the Planetary Boundary Layer: High resolution Aerosol Mass Spectrometry on a Zeppelin NT Airship, PhD thesis, Bergische Universität Wuppertal, Germany, 2013.
- Saarikoski, S., Carbone, S., Decesari, S., Giulianelli, L., Angelini, F., Canagaratna, M., Ng, N. L., Trimborn, A., Facchini, M. C., Fuzzi, S., Hillamo, R., and Worsnop, D.: Chemical characterization of springtime submicrometer aerosol in Po Valley, Italy, *Atmos. Chem. Phys.*, **12**, 8401–8421, doi:10.5194/acp-12-8401-2012, 2012.
- ~~Schladitz, A., Mueller, T., Nowak, A., Kandler, K., Lieke, K., Massling, A., and Wiedensohler, A.: In situ aerosol characterization at Cape Verde Part 1: Particle number size distributions, hygroscopic growth and state of mixing of the marine and Saharan dust aerosol, *Tellus B*, **63**, 531–548, doi:, 2011~~
- [Sandradewi, J., Prévôt, A.](#)
- ~~Sjogren, S., Gysel, M. H., Weingartner, E., Alfara, M., Schmidhauser, R., Duplissy, J., Cozic, J., Grosier, J., Coe, H., Gysel, M., and Baltensperger, U.: Hygroscopicity of the submicrometer aerosol at the high alpine site Jungfraujoch, 3580 m a.s.l., Switzerland, *Atmos. Chem. Phys.*, **8**, 5715–5729~~ [A study of wood burning and traffic aerosols in an Alpine valley using a multi-wavelength Aethalometer, \*Atmos. Environ.\*, \*\*42\*\*, 101-112, doi:10.1016/j.atmosenv.2007.09.034, 2008.](#)

Sorooshian, A., Hersey, S. P., Brechtel, F. J., Corless, A., Flagan, R. C., and Seinfeld, J. H.: Rapid, size-resolved aerosol hygroscopic growth measurements: differential aerosol sizing and hygroscopicity spectrometer probe (DASH-SP), *Aerosol Sci. Tech.*, 42, 445–464, doi:10.1080/02786820802178506, 2008.

5 Stokes, R. H. and Robinson, R. A.: Interactions in aqueous nonelectrolyte solutions, I. Solute – solvent equilibria, *J. Phys. Chem.-US*, 70, 2126, doi:10.1021/j100879a010, 1966.

Stull, R.: *An Introduction to Boundary Layer Meteorology*, Kluwer Academic Publisher, Dordrecht, the Netherlands, 1988.

10 Swietlicki, E., Hansson, H. C., Hameri, K., Svenningsson, B., Massling, A., McFiggans, G., McMurry, P. H., Petaja, T., Tunved, P., Gysel, M., Topping, D., Weingartner, E., Baltensperger, U., Rissler, J., Wiedensohler, A., and Kulmala, M.: Hygroscopic properties of submicrometer atmospheric aerosol particles measured with H-TDMA instruments in various environments - a review, *Tellus B*, 60, 432–469, doi:10.1111/j.1600-0889.2008.00350.x, 2008.

15 Topping, D. O., McFiggans, G. B., and Coe, H.: A curved multi-component aerosol hygroscopicity model framework: Part 1 – Inorganic compounds, *Atmos. Chem. Phys.*, 5, 1205–1222, doi:10.5194/acp-5-1205-2005, 2005.

20 Tritscher, T., Juranyi, Z., Martin, M., Chirico, R., Gysel, M., Heringa, M. F., DeCarlo, P. F., Sierau, B., Prevot, A. S. H., Weingartner, E., and Baltensperger, U.: Changes of hygroscopicity and morphology during ageing of diesel soot, *Environ. Res. Lett.*, 6, 034026, doi:10.1088/1748-9326/6/3/034026, 2011.

~~Van Dingenen, R., Putaud, J.-P., Martins-Dos Santos, S., and Raes, F.: Physical aerosol properties and their relation to air mass origin at Monte Cimone (Italy) during the first MINATROC campaign, *Atmos. Chem. Phys.*, 5, 2203–2226, doi:, 2005.~~

25 ~~Vlasenko, A., Sjogren, S., Weingartner, E., Stemmler, K., Gäggeler, H. W., and Ammann, M.: Effect of humidity on nitric acid uptake to mineral dust aerosol particles, *Atmos. Chem. Phys.*, 6, 2147–2160, doi:, 2006.~~

~~Wagner, R., Ajtai, T., Kandler, K., Lieke, K., Linke, C., Müller, T., Schnaiter, M., and Vragel, M.: Complex refractive indices of Saharan dust samples at visible and near UV wavelengths: a laboratory study, *Atmos. Chem. Phys.*, 12, 2491–2512, doi:, 2012.~~

30 ~~Weingartner, E., Burtcher, H., and Baltensperger, U.: Hygroscopic properties of carbon and diesel soot particles, *Atmos. Environ.*, 31, 2311–2327, doi:, 1997.~~

Weingartner, E., Saathoff, H., Schnaiter, M., Streit, N., Bitnar, B., and Baltensperger, U.: Absorption of light by soot particles: determination of the absorption coefficient by means of aethalometers, *J. Aerosol Sci.*, 34, 1445–1463, doi:10.1016/S0021-8502(03)00359-8, 2003.

~~Wex, H., Petters, M. D., Carrico, C. M., Hallbauer, E., Massling, A., McMeeking, G. R., Poulain, L., Wu, Z., Kreidenweis, S. M., and Stratmann, F.: Towards closing the gap between hygroscopic growth and activation for secondary organic aerosol: Part 1 – Evidence from measurements, *Atmos. Chem. Phys.*, 9, 3987–3997, doi:, 2009.~~

[WMO/GAW: Aerosol measurements procedures guidelines and recommendations, second edition, World Meteorological Organization, Geneva, Switzerland, 2016.](#)

Wu, Z. J., Poulain, L., Henning, S., Dieckmann, K., Birmili, W., Merkel, M., van Pinxteren, D., Spindler, G., Müller, K., Stratmann, F., Herrmann, H., and Wiedensohler, A.: Relating particle hygroscopicity and CCN activity to chemical composition during the HCCT-2010 field campaign, *Atmos. Chem. Phys.*, 13, 7983–7996, doi:10.5194/acp-13-7983-2013, 2013.

~~Yamasoe, M. A., Kaufman, Y. J., Dubovik, O., Remer, L. A., Holben, B. N., and Artaxo, P.: Retrieval of the real part of the refractive index of smoke particles from Sun/sky measurements during SCAR-B, *J. Geophys. Res.-Atmos.*, 103, 31893–31902, doi:, 1998.~~

Zhang, R., Khalizov, A. F., Pagels, J., Zhang, D., Xue, H., and McMurry, P. H.: Variability in morphology, hygroscopicity, and optical properties of soot aerosols during atmospheric processing, *P. Natl. Acad. Sci. USA*, 105, 10291–10296, doi:10.1073/pnas.0804860105, 2008.

Zieger, P., Weingartner, E., Henzing, J., Moerman, M., de Leeuw, G., Mikkilä, J., Ehn, M., Petäjä, T., Clémer, K., van Roozendaal, M., Yilmaz, S., Frieß, U., Irie, H., Wagner, T., Shaiganfar, R., Beirle, S., Apituley, A., Wilson, K., and Baltensperger, U.: Comparison of ambient aerosol extinction coefficients obtained from in-situ, MAX-DOAS and LIDAR measurements at Cabauw, *Atmos. Chem. Phys.*, 11, 2603–2624, doi:10.5194/acp-11-2603-2011, 2011.

**Table 1.**  $\kappa$  values and densities for pure compounds used for the prediction of aerosol hygroscopicity based on AMS and Aethalometer or MAAP measurements.

Compound	Density $\rho$ [ $\text{kg m}^{-3}$ ]	$\kappa$ (95 %, 500 nm)
$(\text{NH}_4)_2\text{SO}_4$	1769	0.458
$\text{NH}_4\text{HSO}_4$	1780	0.575
$\text{H}_2\text{SO}_4$	1830	0.687
$\text{NH}_4\text{NO}_3$	1720	0.629
eBC	2000	0.000
organics	1233*	<del>0.110</del> <u>0.08 - 0.13**</u>

\* Mean value retrieved throughout the campaign with the Kuwata et al. (2012) parametrization.

\*\* Estimated from the measured O:C ratio according to Duplissy et al. (2011). See also Sect. 3.

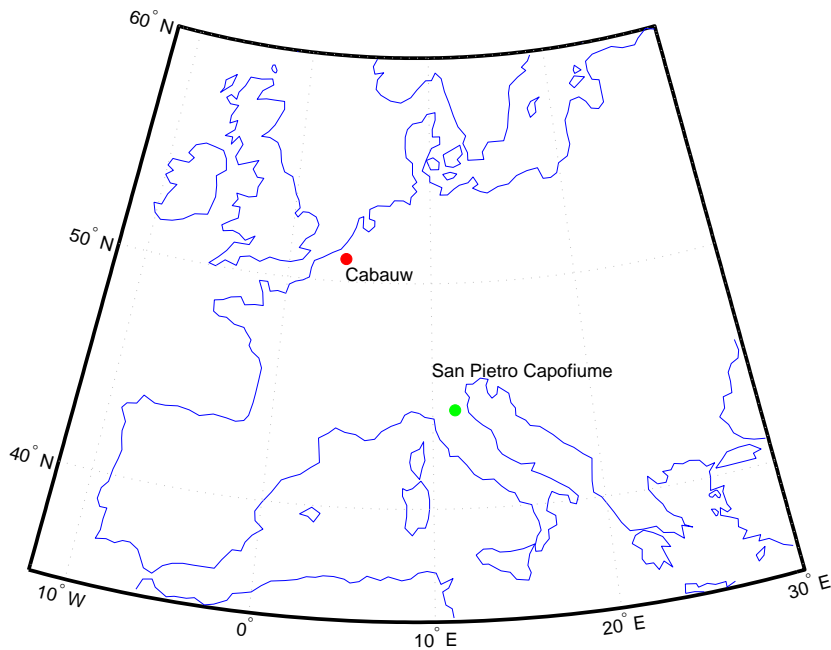
**Table 2.** Mean GF(95%) and  $\kappa$  values for IHP1/2 and ~~IHP4~~IHP5/5/6 with respective accuracies.  $\kappa^{\text{chem}}$  is the calculated  $\kappa$  using the AMS and ~~A~~aethalometer measurements on board of the Zeppelin NT or AMS/MAAP combination at the SPC ground station. Besides, results for two different altitudes and the corresponding layers probed are mentioned. Additionally, the size at which the measurements are performed is stated.

Zeppelin					
Size	Altitude	Layer	WHOPS		AMS + Aethalometer
			GF(95%) 500 nm	$\kappa^{\text{WHOPS}}$ 500 nm	$\kappa^{\text{chem}}$ PM <sub>1</sub>
IHP1/2	100 m	new ML	1.88(±0.19)	0.34(±0.12)	<del>0.27</del> 0.26(±0.06)
	700 m	RL	1.61(±0.16)	0.19(±0.07)	<del>0.21</del> 0.22(±0.05)
IHP4/5/6	100 m	fully developed ML	<del>1.48</del> 1.49(±0.15)	0.14(±0.06)	0.19(±0.04)
	700 m	fully developed ML	<del>1.65</del> (±0.17) <u>1.63</u> (±0.16)	<del>0.21</del> 0.20(±0.08)	<del>0.19</del> 0.20(±0.04)
Ground Stations			San Pietro Capofiume		Monte Cimone
Size PM <sub>1</sub>			<del>HTDMA</del> $\kappa^{\text{chem}}$ GF(95%)* PM <sub>T</sub>	<del>HTDMA</del> $\kappa^{\text{HTDMA}}$ 200 nm	AMS + MAAP <del>HTDMA</del> $\kappa^{\text{HTDMA}}$ $\kappa^{\text{chem}}$ 230200 nm
IHP1/2		new ML	<del>0.31</del> (±0.08) <u>1.61</u> (±0.22)	0.19(±0.04)* 0.23(±0.05)*	<u>0.31</u> (±0.08)
		RL			
IHP4/5/6		fully developed ML	<del>0.21</del> (±0.06) <u>1.60</u> (±0.21)	0.18(±0.04)*	<del>0.25</del> (±0.05)* <u>0.21</u> (±0.06)

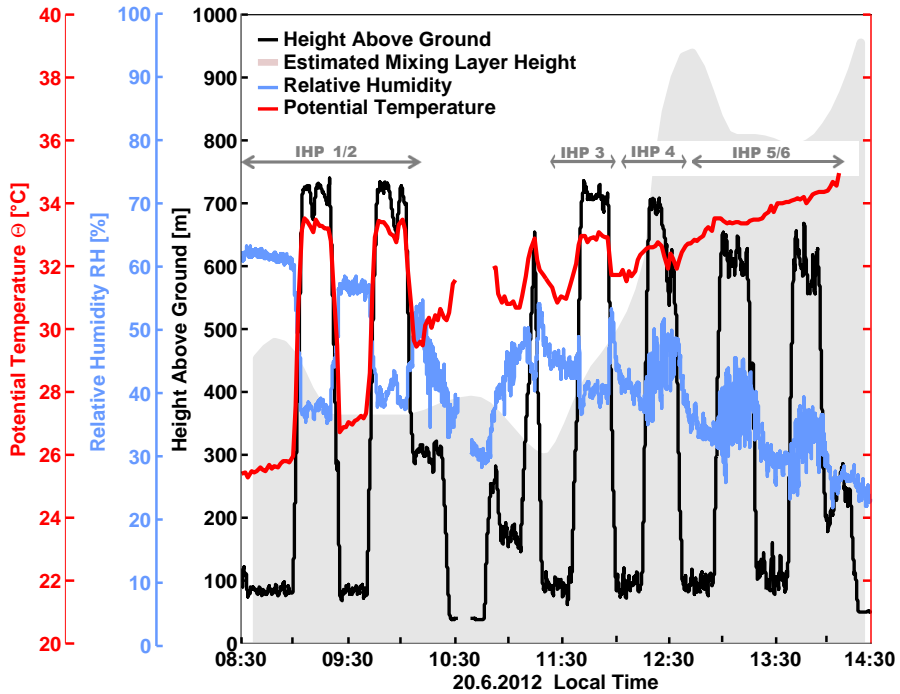
\* HTDMA uncertainty calculated assuming ±2% accuracy in the RH measurement.

**Table 3.** Mean GF and  $\kappa$  values for NHP1/2 with respective accuracies are presented. For the WHOPS measurements at four different altitudes are shown.  $\kappa_{\text{chem}}$  is calculated from the Cabauw ground site combining AMS and MAAP results.

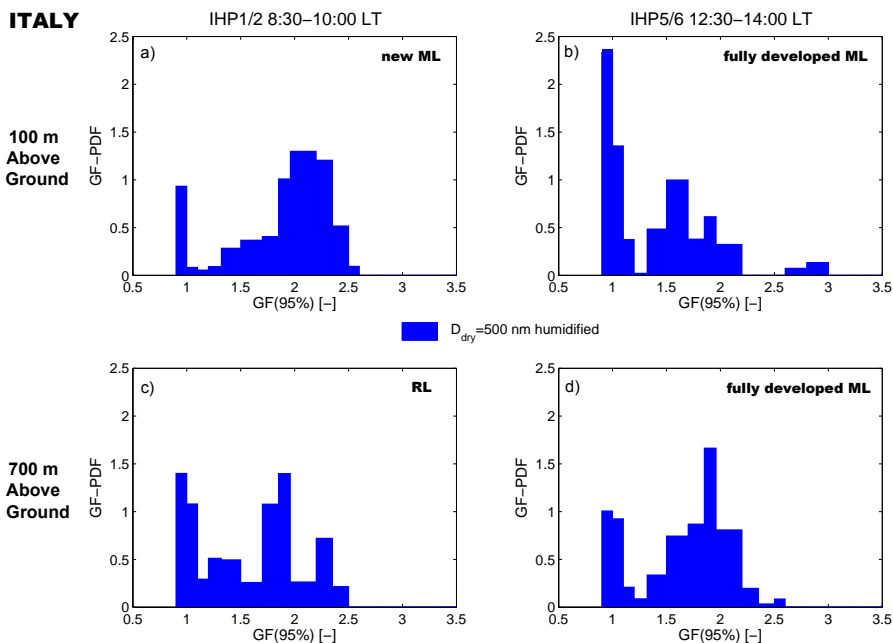
Zeppelin			
Size	Altitude	WHOPS	
		GF(95 %) 500 nm	$\kappa^{\text{WHOPS}}$ 500 nm
NHP1/2	100 m	1.84( $\pm 0.18$ )	0.25( $\pm 0.09$ )
	300 m	1.91( $\pm 0.19$ )	0.28( $\pm 0.10$ )
	500 m	1.92( $\pm 0.19$ )	0.29( $\pm 0.10$ )
	700 m	1.93( $\pm 0.19$ )	0.29( $\pm 0.10$ )
Ground Station		Cabauw	
Size	AMS + MAAP		
	$\kappa^{\text{chem}}$ PM <sub>1</sub>		
NHP1/2	0.28( $\pm 0.06$ )		



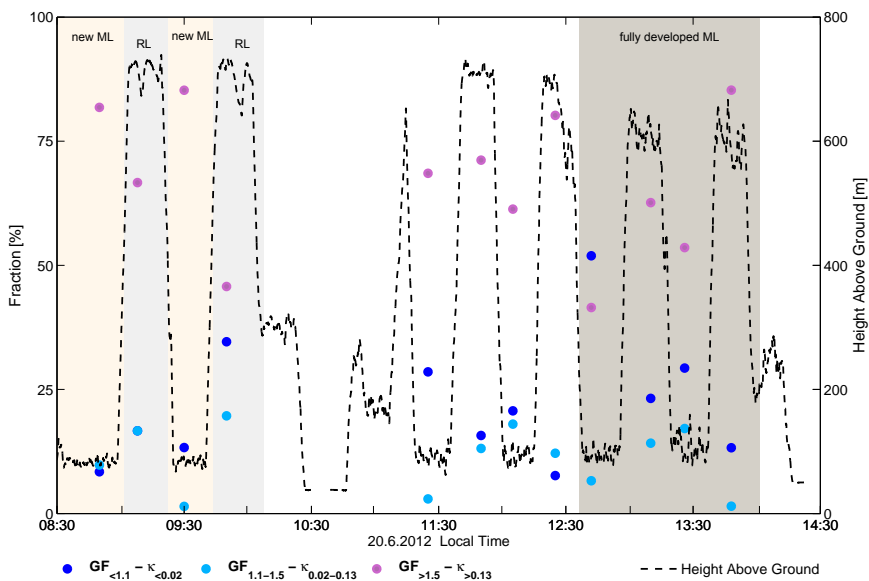
**Figure 1.** Map showing the different measurement sites in Europe: Cabauw located in the Netherlands (red dot) and San Pietro Capofiume (green dot) ~~and Monte Cimone (blue dot)~~ located in the Po Valley in Italy.



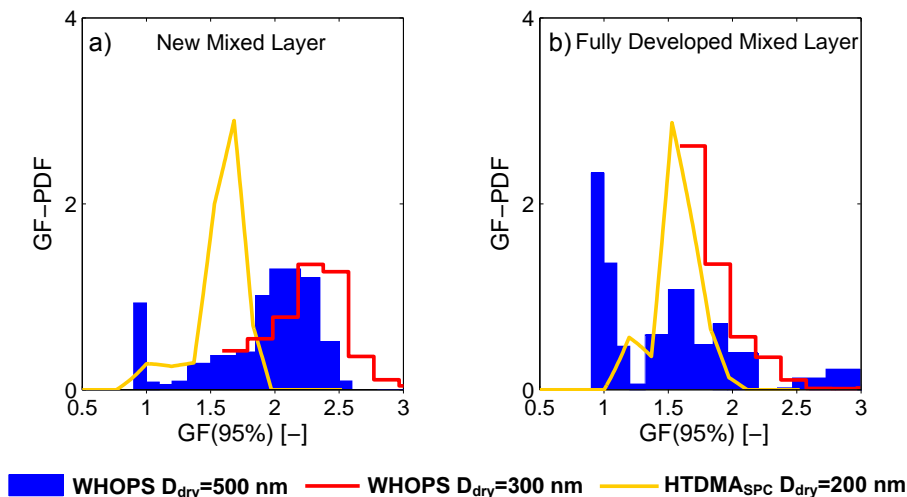
**Figure 2.** Retrieved dry effective index of refraction  $m$  for the flight in the Po Valley ( $m_{\text{IT}}$ , dark red bars) and the flight in the Netherlands ( $m_{\text{NL}}$ , violet bars) for particles with dry diameters of  $D_{\text{dry}} = 500$  nm. Additionally mean values and their temporal variability are presented for both sites. Overview of the flight on 20 June 2012 near San Pietro Capofiume ground station (Po Valley, Italy). In black the flight altitude and in gray-grey the estimated mixing layer height, determined from ceilometer – Lidar measurements, are presented. The red and blue lines show the potential temperature  $\Theta$  and RH profiles, respectively. Time series of  $\kappa$  values on the 20 June 2012 in Italy. Results from chemical composition ( $\kappa_{\text{chem}}$ ; green diamonds), and WHOPS for a dry selected diameter of 500 ( $\kappa_{\text{WHOPS}}$ ; red dots) are shown. The shaded areas depict the measurement accuracy. The dashed line shows the flight altitude, while the grey, dashed rectangle indicates the break for refuelling. In addition, the times for different height profiles IHP1/2, IHP3 and IHP4 and IHP5/6 are indicated. The coloured areas refer to the layer which was probed at that altitude.



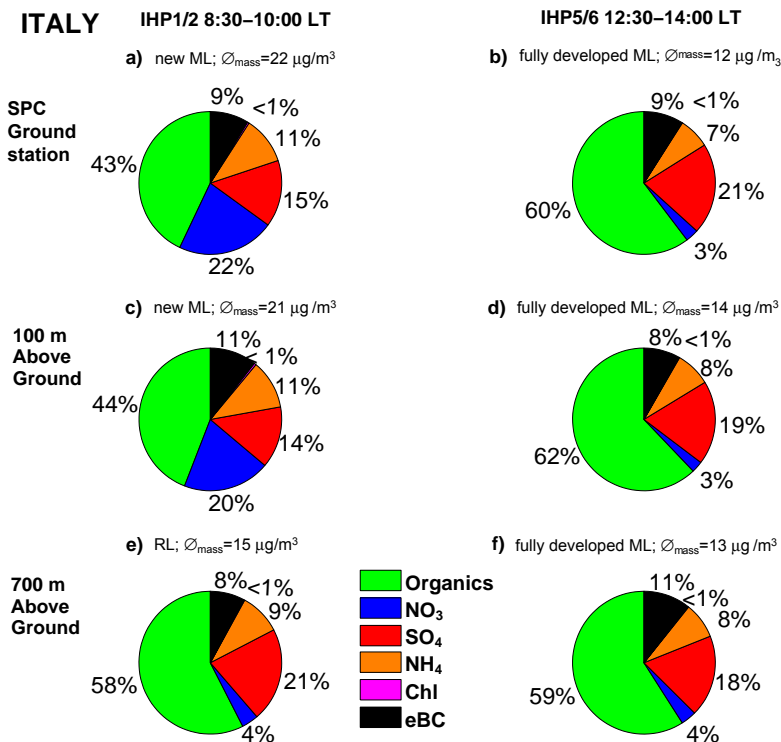
**Figure 3.** GF-PDFs during 20 June 2012 in Italy: profile IHP1/2 was flown between 08:30 and 10:00 LT and ~~IHP4~~IHP5/5/6 between ~~~12:00-30~~ and 14:00 LT; the blue area displays the GF-PDFs for a selected dry diameter of 500 nm. **(a and b)** illustrate the results at approximately 100 m AGL and **(c and d)** for approximately 700 m AGL.



**Figure 4.** Time series of the mixing state of the aerosol particles (with  $D_{\text{dry}} = 500 \text{ nm}$ ) for the height profiles in Italy on 20 June 2012. Particles are classified into three hygroscopicity categories according to their GF:  $\text{GF} < 1.1$ ,  $1.1 < \text{GF} < 1.5$ ,  $\text{GF} > 1.5$ , in blue, light blue and pink respectively; these are equivalent to  $\kappa < 0.02$ ,  $0.02 < \kappa < 0.13$  and  $\kappa > 0.13$ . The black, dashed line denotes the flight altitude and the gray rectangle illustrates the time of the refuel break. The colored labelled, coloured areas refer to the layer which was probed at that the certain altitude.

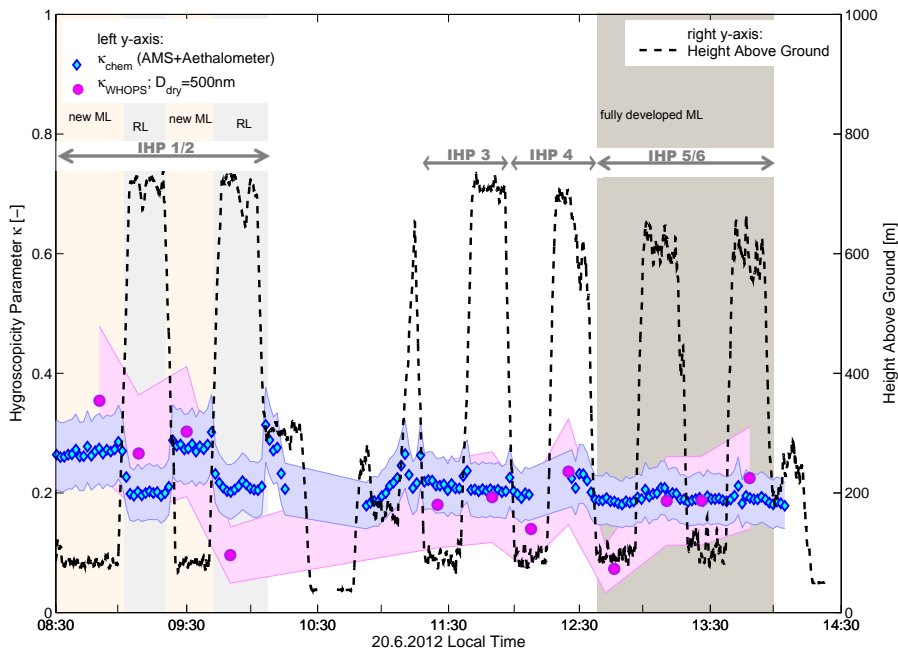


**Figure 5.** GF-PDF comparison between WHOPS (at 100 m AGL) and HTDMA subdivided for different layers in the Po Valley on 20 June 2012. The WHOPS results were averaged from 8:30 - 10:00 LT for the new mixed layer, the residual layer ML and 12:30 - 14:00 LT for the fully developed mixed ML, equivalent to results in Fig. 3a and b. The HTDMA data was averaged over the same time interval which corresponds to the mean over 3 full measurements per layer. Note that the WHOPS cannot reliably detect particles with  $GF < 1.5$  and  $D_{\text{dry}} = 300$  nm, as described in Rosati et al. (2015a). Thus, no information is available from the WHOPS measurements on the number fraction and properties of the 300 nm particles with  $GF < 1.5$ .

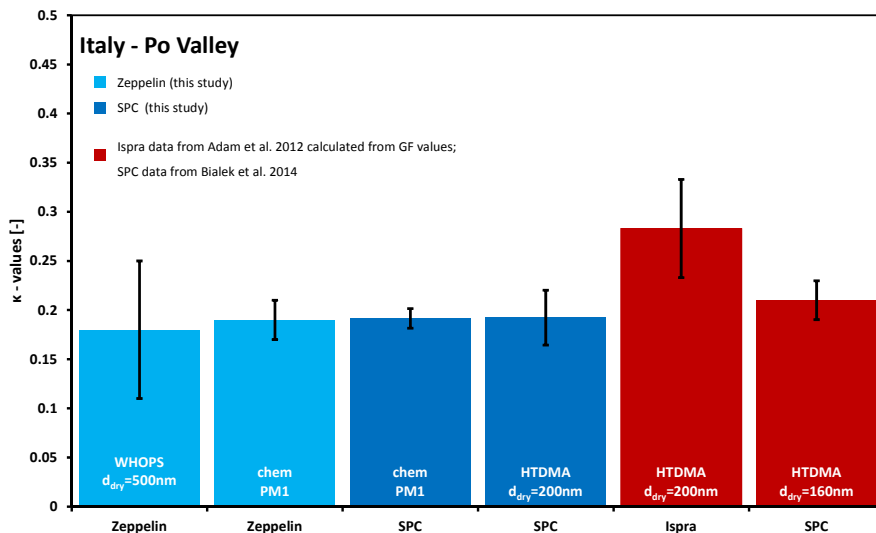


**Figure 6.**  $\text{PM}_{10}$  chemical composition results from the flight on 20 June 2012 in Italy. (a and b) show the mass fractions measured by the HR-ToF-AMS and MAAP at San Pietro Capofiume ground station; (a) was recorded during IHP1/2 whereas (b) was measured during IHP5/6. (c–f) depict the mass fractions measured by the HR-ToF-AMS and aethalometer on the Zeppelin. (c and e) illustrate the results for the first height profiles, (c) at 100 and (e) at 700 m AGL, while (d and f) show the results for IHP5/6 for 100 and 700 m AGL, respectively.

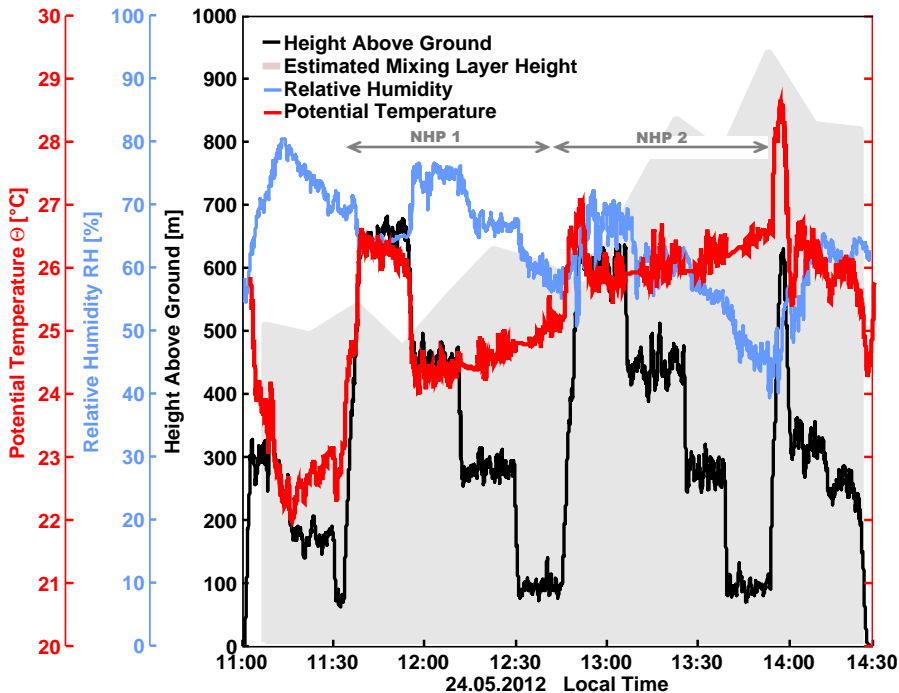
chemical composition results during the flight on 20 June 2012 in Italy. (a and b) show the mass fractions measured by AMS and MAAP at San Pietro Capofiume ground station; (a) was recorded during IHP1/2 whereas (b) was measured during IHP4/5/6. (c–f) depict the mass fractions measured by AMS and Aethalometer on the Zeppelin. (c and e) illustrate the results for the first height profiles, (c) at 100 and (e) at 700, while (d and f) show the results for IHP4/5/6 for 100 and 700, respectively.



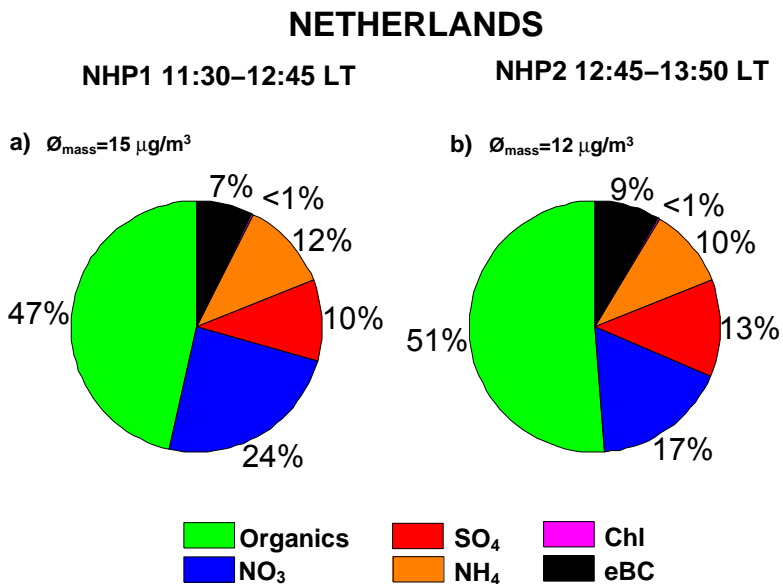
**Figure 7.** Time series of  $\kappa$  values on 20 June 2012 in Italy. Results from chemical composition ( $\kappa_{\text{chem}}$ ; violet diamonds), and WHOPS for a dry selected diameter of 500 nm ( $\kappa_{\text{WHOPS}}$ ; blue points) are shown. The shaded areas depict the measurement accuracy. The dashed line shows the flight altitude. In addition, the times for IHP1/2, IHP3, IHP4 and IHP5/6 are indicated. The coloured areas refer to the layer which was probed at a certain altitude and time.



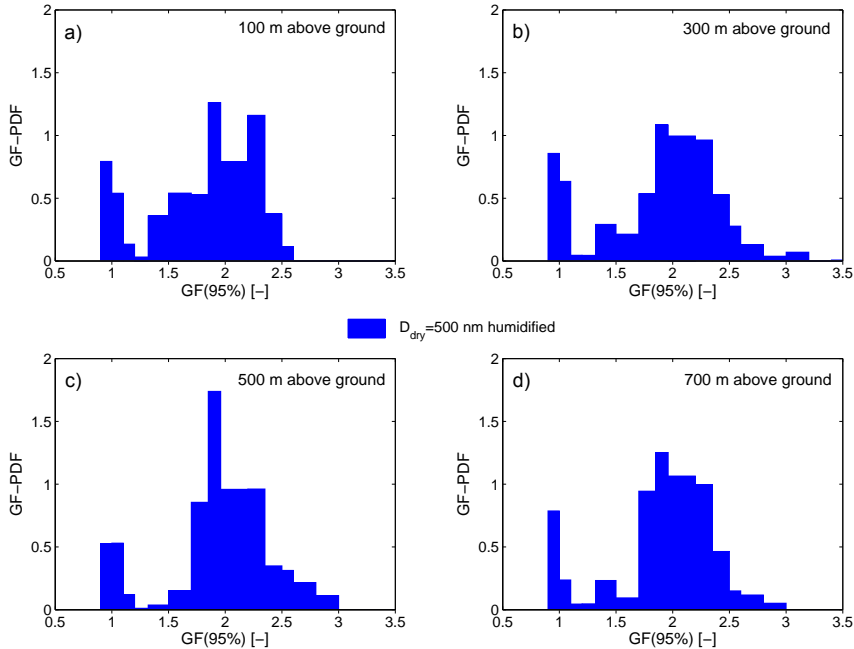
**Figure 8.** ~~Intercomparison~~ Inter-comparison of mean  $\kappa$  values measured in during this study at different locations in the Po Valley on 20 June 2012 (blue bars) compared with literature data from this area (red bars).  $\kappa$  values are either derived from measured hygroscopic growth factors or chemical composition. Only results for the fully developed ML, when vertical gradients of aerosol properties are minimal, are included in the averages. This ensures comparability between the measurements taken at different altitudes. The error bars indicate the temporal variability of the observed  $\kappa$  values (1 SD).



**Figure 9.** Overview of the flight on 24 May 2012 near [the](#) Cabauw CESAR station in the Netherlands. In black the flight altitude and in [gray grey](#) the estimated mixing layer height, inferred from [Ceilometer ceilometer](#) measurements, are presented. The red and blue lines show the potential temperature  $\Theta$  and RH profiles, respectively. [In addition, the different height profiles NHP1 and NHP2 are indicated.](#)



**Figure 10.** Time-series Ground measurements of  $\kappa$ -values retrieved during the flight aerosol particle chemical composition at the Cabauw tower during NHP1 and NHP2 on 24 May 2012. WHOPS-HR-ToF-AMS and MAAP results for a dry diameter of 500 are presented. The measurement accuracy is shown as combined for the shaded area total aerosol mass. Additionally, the flight altitude is indicated averaged mass concentrations during the profile periods are stated.

**NETHERLANDS**

**Figure 11.** GF-PDFs recorded at near Cabauw on 24 May 2012 at four different altitudes: approximately 100, 300, 500 and 700 m AGL seen in panels (a–d), respectively. Every curve is the mean over the two flown profiles NHP1 and NHP2.

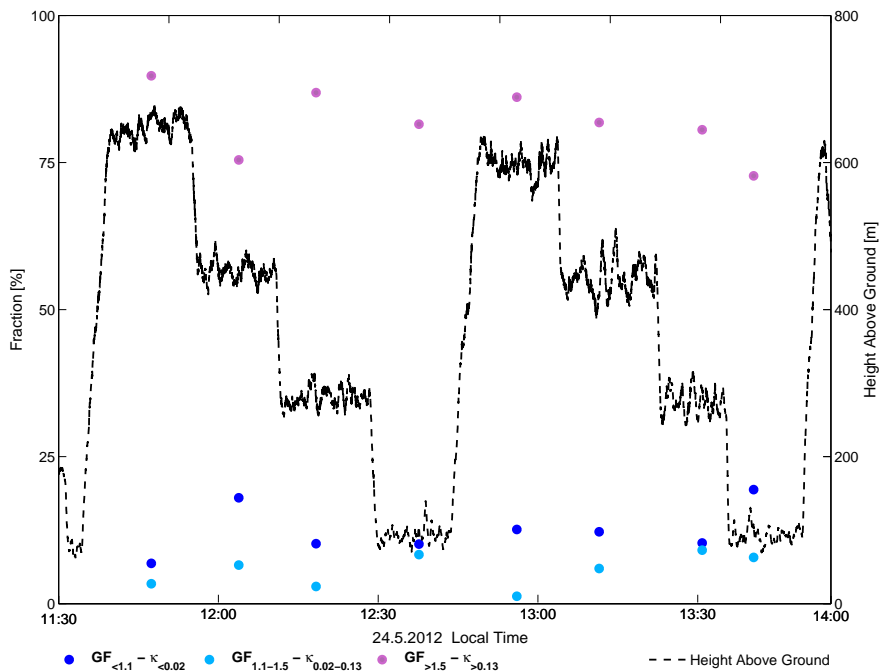


**Figure 12.** Time evolution of the mixing state of the aerosol particles (with  $D_{\text{dry}} = 500 \text{ nm}$ ) for the height profiles [at near](#) Cabauw on 24 May 2012. Particles are classified into three hygroscopicity categories according to their GF (equally defined as for Fig. 64):  $GF < 1.1$ ,  $1.1 < GF < 1.5$ ,  $GF > 1.5$ , in blue, light blue and pink respectively; these correspond to  $\kappa < 0.02$ ,  $0.02 < \kappa < 0.13$  and  $\kappa > 0.13$ .

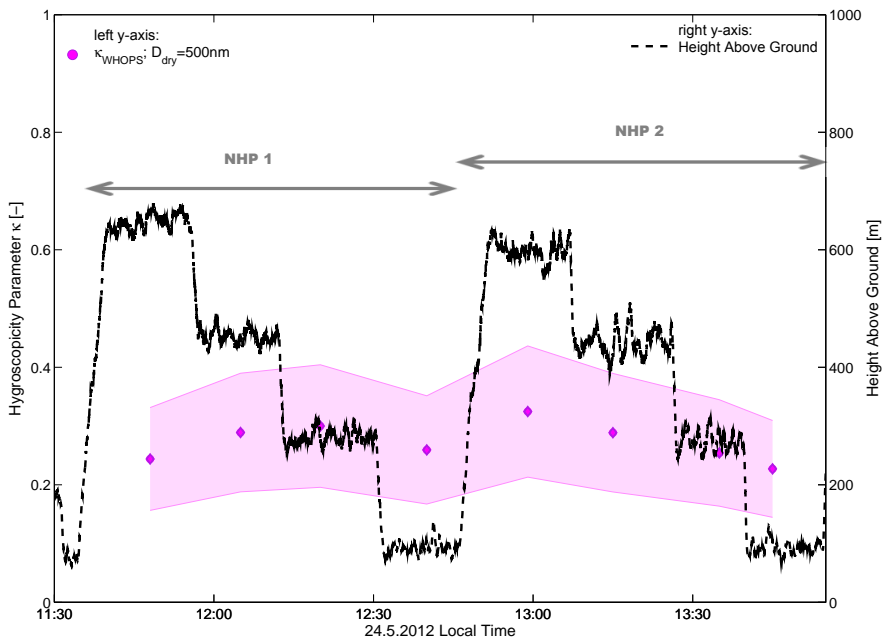


**Figure 13.** Ground measurements—Time series of the aerosol particle chemical composition at the Gabauw tower  $\kappa$  values retrieved during NHP1 and NHP2 the flight on 24 May 2012. AMS and MAAP WHOPS results are combined for a dry diameter of 500 nm are presented. The measurement accuracy is shown as the total aerosol mass shaded area. Also Additionally, the averaged mass concentrations during the profile periods are stated flight altitude is indicated.

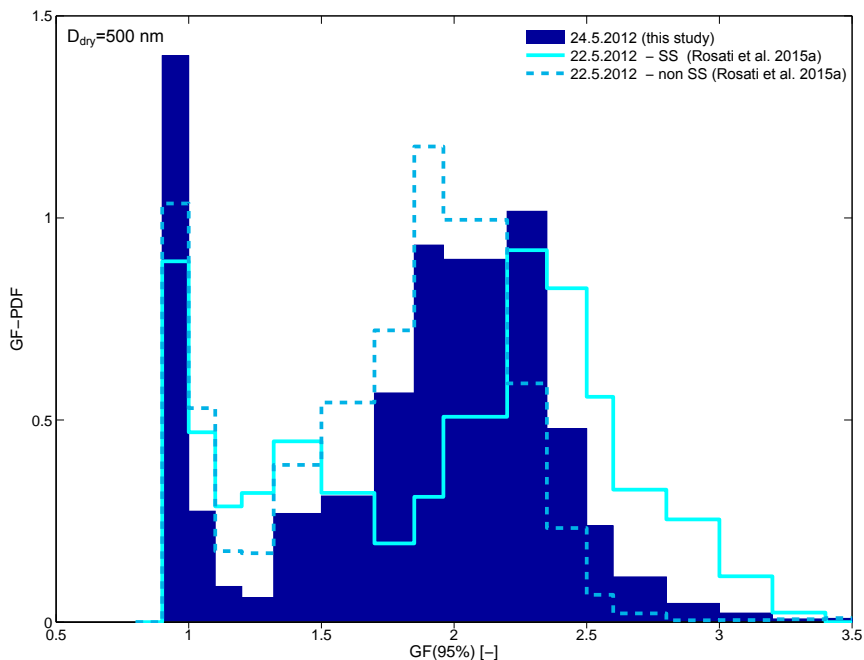


**Figure 14.** Comparison of GF-PDFs of particles with  $D_{\text{dry}} = 500 \text{ nm}$  recorded with the Zeppelin mounted-WHOPS during flights around Cabauw on board of the Zeppelin for two different flight days: 24 May 2012 (this study) and on 22 May 2012 (?) (Rosati et al., 2015a). Both flights were located close to Cabauw and results are representative for particles with  $D_{\text{dry}} = 500 \text{ nm}$ .

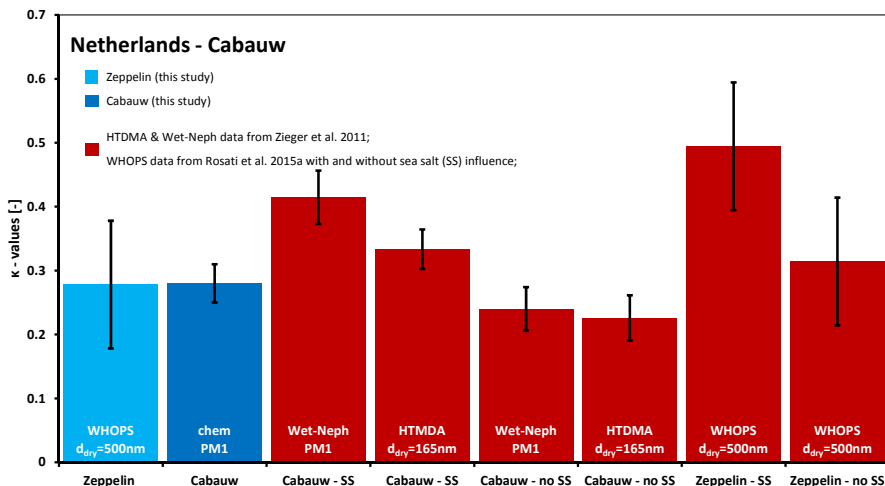


**Figure 15.** ~~Intercomparison~~ Inter-comparison of mean  $\kappa$  values and their temporal variability measured on board of the Zeppelin NT (light blue bar) and at the ground (dark blue bar) during the PEGASOS campaign on 24 May 2012 in the Netherlands. Additionally, results from two separate campaigns reported in the literature are shown (red bars). For the flight described in [Rosati et al. \(2015a\)](#) two different separate bars are presented dividing results in sea salt (SS) and non-sea salt (non-SS) influenced periods. In the same way results from Zieger et al. (2011) are split in SS and non-SS periods for measurements performed with two different techniques.

## Supplementary Material:

### Effective indices of refraction during the PEGASOS study:

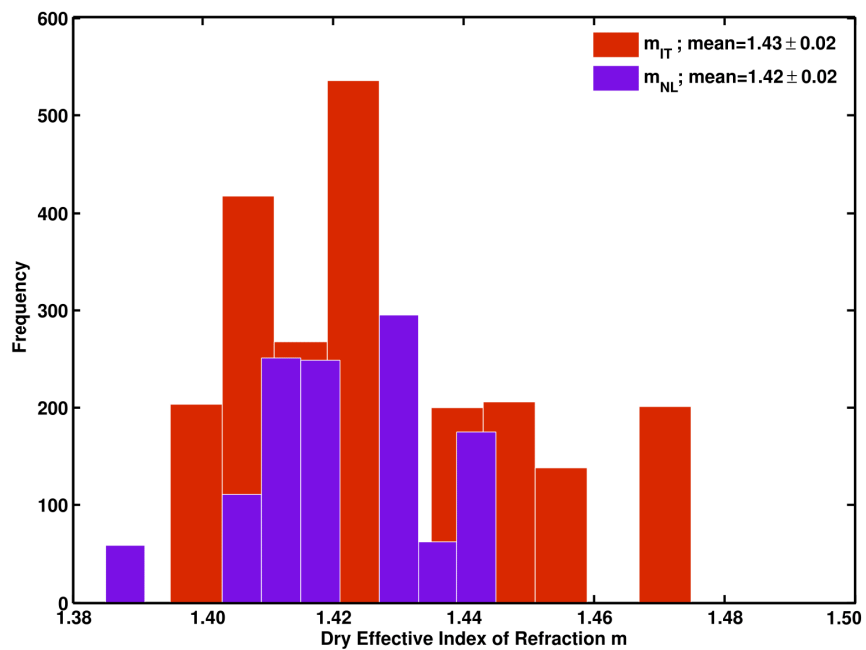


**Figure S1.** Histogram of the temporal variability of the dry effective indices of refraction ( $m$ ), observed during the flights on 20 June 2012 in the Po Valley, Italy, ( $m_{IT}$ , dark red bars) and 24 May 2012 close to Cabauw, Netherlands, ( $m_{NL}$ , violet bars). Only the results for size-selected particles with a dry mobility diameter of 500 nm are presented. On average, effective indices of refraction of  $1.43 \pm 0.02$  (mean  $\pm$  SD) and  $1.42 \pm 0.02$  were found in Italy and the Netherlands, respectively. However, an absolute uncertainty of  $\pm 0.04$  has to be attributed to all index of refraction retrievals (see Rosati et al., 2015a).

**Meteorological parameters measured during the flight on 20 June 2012 in the Po Valley, Italy:**

**Supplement Table 1.** Mean potential temperature ( $\Theta$ ) and relative humidity (RH) during IHP1/2 and IHP5/6 with respective standard deviations representing the temporal variability. Results are presented for two different altitudes, 100 m and 700 m AGL. Measurements of the temperature (Pt100-Sensor; OMEGA; 15s time respond), RH (HMP45-Sensor; Vaisala; 15s time respond), height above ground, wind-speed and direction (all three retrieved by measurement of the pressure using sensors #239 and #270; Setra) were continuously recorded on board the airship. All of these measurements were logged with a 100 Hz frequency and finally averaged over 10 data points.

<i>Profile</i>	<i>Altitude</i>	<i>Layer</i>	<i>Zeppelin</i> $\Theta$ [ $^{\circ}\text{C}$ ]	<i>Zeppelin</i> RH [%]
IHP1/2	100 m	New ML	26.0 ( $\pm 0.6$ )	60.1 ( $\pm 2.0$ )
	700 m	RL	33.0 ( $\pm 0.9$ )	39.4 ( $\pm 3.1$ )
IHP5/6	100 m	Fully developed ML	33.4 ( $\pm 0.6$ )	31.5 ( $\pm 3.1$ )
	700 m	Fully developed ML	33.6 ( $\pm 0.5$ )	36.5 ( $\pm 4.2$ )

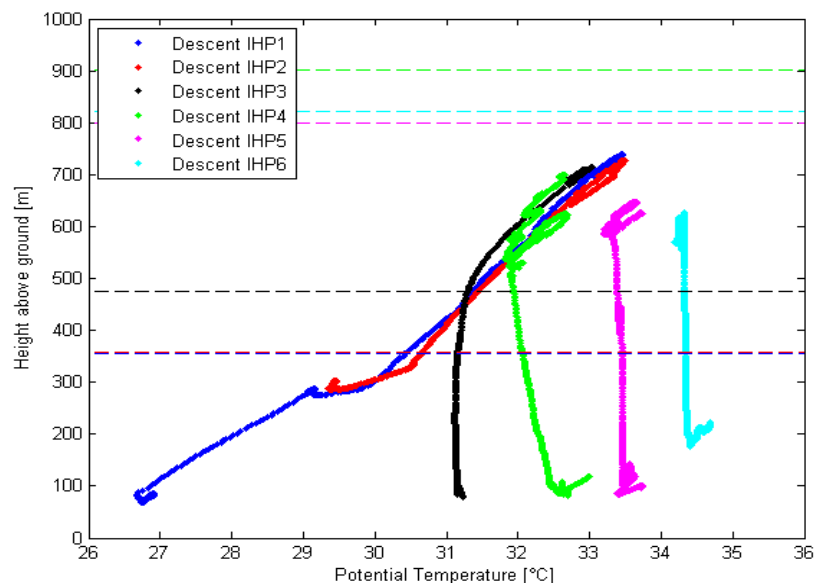


**Figure S2:** Height profiles of the potential temperature ( $\Theta$ ) measured aboard the Zeppelin NT during the flight on 20 June 2012, in Italy. Each color represents the descents of height profiles 1-6 (IHP1-6), respectively. The horizontal lines depict the estimated mixed layer height (MLH) from the ceilometer retrieval during the six height profiles. A clear vertical structure of  $\Theta$  is visible for the first two profiles, while the last four show very little or no altitude dependence at all. This indicates that the sub-layers in the PBL were still separated at the beginning of the flight and that a fully mixed layer was probed at the end. The estimated MLH retrieved from the ceilometer shows comparable results with a low MLH of approximately 350 m above ground in the morning that evolves to over 800 m above ground later during the day.